Master's thesis

NTNU
Norwegian University of Science and Technology
Faculty of Engineering
Department of Marine Technology

Shuzhou Jiang

Installation of Offshore Wind Turbine Blade Using a Semi-submersible Floating Installation Vessel

Master's thesis in Marine Technology
Supervisor: Professor Zhen Gao
June 2021

NTNU
Norwegian University of
Science and Technology

Shuzhou Jiang

Installation of Offshore Wind Turbine Blade Using a Semi-submersible Floating Installation Vessel

Master's thesis in Marine Technology
Supervisor: Professor Zhen Gao
June 2021

Norwegian University of Science and Technology
Faculty of Engineering
Department of Marine Technology

NTNU
Norwegian University of
Science and Technology

Abstract

With the development of modern technology, wind energy is used more and more frequently, especially offshore wind energy. The use of offshore wind energy has gradually become an important trend. This study simulates the installation of blades in an offshore wind turbine farm located in the North Sea and studies its movement.

This thesis mainly simulates the motion of offshore wind turbine blades during the installation process after being lifted to by a floating vessel. The software SIMA is used to carry out this simulation work. The blade is selected from DTU 10 MW offshore wind turbine model. The aerodynamic force comes from the TurbSim software. The combined environmental conditions of the complex irregular waves and turbulent wind during the installation of offshore wind turbine blades are decomposed into several simple environmental conditions for analysis.

This thesis simulates regular waves, constant winds, irregular waves and turbulent winds respectively. Different single conditions are analyzed to find the effect of different single conditions on the motion of the offshore wind turbine blade when it is being lifted. The combined situations of irregular waves and turbulent wind are also simulated. The study found that when using the floating vessel to install the offshore wind turbine blade, it is recommended to set the original blade pitch angle to around -9 degrees to reduce the wind force experienced by the offshore wind turbine blade. At the same time, it was also found that when the floating vessel is used to install the offshore wind turbine blade, the motion of the blade is related to the floating vessel affected by wave forces and the wind force affects the blade motion as well.

Sammendrag

Med utviklingen av moderne teknologi blir vindenergi brukt oftere og oftere, spesielt offshore vindkraft. Bruk av vindkraft til havs har gradvis blitt en viktig trend. Denne studien simulerer installasjon av kniver i en vindmøllepark offshore i Nordsjøen og studerer bevegelsen.

Denne oppgaven simulerer hovedsakelig bevegelse av vindturbinblader til havs under installasjonsprosessen etter å ha blitt løftet opp av et flytende fartøy. Programvaren SIMA brukes til å utføre dette simuleringsarbeidet. Bladet er valgt fra offshore vindturbinmodell DTU 10 MW. Den aerodynamiske kraften kommer fra TurbSim-programvaren. De kombinerte miljøforholdene til de komplekse uregelmessige bølgene og turbulent vinden under installasjonen av vindturbinblad til havs blir spaltet i flere enkle miljøforhold for analyse.

Denne oppgaven simulerer henholdsvis vanlige bølger, konstant vind, uregelmessige bølger og turbulente vinder. Forskjellige enkeltforhold blir analysert for å finne effekten av forskjellige enkeltforhold på bevegelsen til vindturbinbladet til havs når det løftes. De kombinerte situasjonene med uregelmessige bølger og turbulent vind er også simulert. Studien fant at når det flytende fartøyet brukes til å installere vindturbinbladet til havs, anbefales det å stille den opprinnelige bladhellingvinkelen til rundt -9 grader for å redusere vindkraften som havvindturbinbladet opplever. Samtidig ble det også funnet at når det flytende fartøyet brukes til å installere vindturbinbladet til havs, er bladets bevegelse relatert til det flytende fartøyet som påvirkes av bølgekrefter, og vindstyrken påvirker også bladets bevegelse.

Preface

This thesis is the final work written by Shuzhou Jiang in order to obtain a master's degree in marine technology from the Norwegian University of Science and Technology (NTNU). The paper was completed under the guidance of Professor Zhen Gao. Part of this paper was completed in collaboration with Taewoo Kim. The main purpose of this paper is to study the numerical analysis of the blade motion of offshore wind turbines installed by floating vessels. Kim used the jack-up vessel model for the same research work.

Acknowledgements

First of all, I would like to thank Professor Zhen Gao from the Norwegian University of Science and Technology. I am very grateful to Professor Zhen Gao for giving me such an opportunity to conduct research on this subject. During this thesis, Professor Zhen Gao gave me a great help and devoted a lot of effort. I can't forget that Professor Zhen Gao patiently explained to me many issues during the research process, which greatly expanded my knowledge about offshore wind turbines. I learned a lot from Professor Gao. I would also like to thank my best teammate and friend in the department of marine technology, Taewoo Kim. During my study in marine technology, he gave me a lot of help which means a lot to me. Without Taewoo, I cannot finish what I have done in my study. During the thesis working, Taewoo also helps me a lot especially the comparison part of this thesis, Taewoo gave me a lot of new opinions about it.

I want to thank my parents for more than 20 years of raising and supporting me to study in Norway. They gave me very rare opportunities and did their best to give me the best living and learning environment. From a small city called Yantai on the east coast of China to Trondheim in Norway, their funding gave me the opportunity to pursue a better education and understand the wider world. I want to thank all my friends for their company and support. I want to especially thank my beloved girlfriend Dr. Wenxiu Jiao. When I was studying in Norway, although we were more than 8,000 kilometers apart, her love, companionship and comfort shortened the distance between us and made me more confident to go step by step to the present and complete my studies.

Table of Contents

List of Figures

List of Tables

List of Abbreviations (or Symbols)

θ_B	Blade initial pitch angle
θ_{wd}	Wind incident angle
θ_{wv}	Wave incident angle
H_s	Significant wave height
O-XYZ	Global coordinate system
T_I	Turbulence intensity
T_p	Wave peak period
U_w	Wind speed
COG	Center of Gravity
DLL	Dynamic Link Library
DOF	Degree of Freedom
DP	Dynamic Positioning
GW	Gigawatt
HAWC2	Horizontal Axis Wind turbine simulation Code 2nd generation
IEC	International Electrotechnical Commision
JONSWAP	Joint North Sea Wave Project
MW	Megawatt
RAO	Response Amplitude Operation
STD	Standard deviation
TLP	Tension Leg Platform

1 Introduction

More than 30 years ago, the power generation of offshore wind turbines was still zero, but according to current market forecasts, in the next 30 years, more than 1,400GW of offshore wind turbines may be installed globally[1].

The European Union has set the goal of offshore wind power development to achieve 40 GW of installed capacity by 2020 and 150 GW of installed capacity by 2030. This means a lot of offshore operations related to the transportation, installation, operation and maintenance of offshore wind power systems. On average, more than one thousand turbines need to be installed each year. The increase in turbine size will help reduce the number of turbines, thereby reducing the number of offshore operations, but this trend, including the increase in water depth and distance to shore, will pose new challenges to on-site installation[2].

Currently, Jack-up vessels are widely used to install wind turbine blades. The most significant benefit of this installation method is that during the installation process, because the hull is lifted by the legs and leaves the water, it is not affected by hydrodynamic loads. Compared with floating vessels, the motion of jack-up vessels during the installation of offshore wind turbine blades is smaller, but due to their own limitations, it is more difficult to install offshore wind turbine blades in deep waters[3]. However, jack-up containers are sensitive to wave conditions during the positioning process, and therefore cannot be used for deep water installations. It is interesting to consider a floating installation vessel with efficient and weather-independent operation. This floating installation vessek can be a ship-type single-hull vessel or a semi-submersible vessel. The main challenge of this type of vessel is to limit its fluctuations to avoid impact/damage to the lifted objects. Generally, this damage is relatively small due to limited contact/impact velocity. However, this may affect the ultimate strength or fatigue strength of the blade and cause a shortened service life.

1.1 Offshore Wind Turbine

Nowadays, with the advancement of technology and the development and utilization of various renewable energy sources, offshore wind energy has received more and more attention. For now, offshore wind power still has great development potential. In theory, the global wind energy resource potential is 6000 EJ/year. Technically speaking, onshore wind energy resource potential is between 70 EJ/year

and 320 EJ/year, and offshore energy resource potential is between 15 EJ/year and 130 EJ/year.

Figure 1. 1: Offshore Wind Turbine Farm [4]

In 2019, 6.1 GW of installed capacity of offshore wind turbines was newly added worldwide, which is the best year since the offshore wind power field began to be put into practical application[5]. Among them, China installed 2.4 GW of offshore wind turbines in 2019, Britain installed 1.8 GW, and Germany installed 1.1 GW[2].

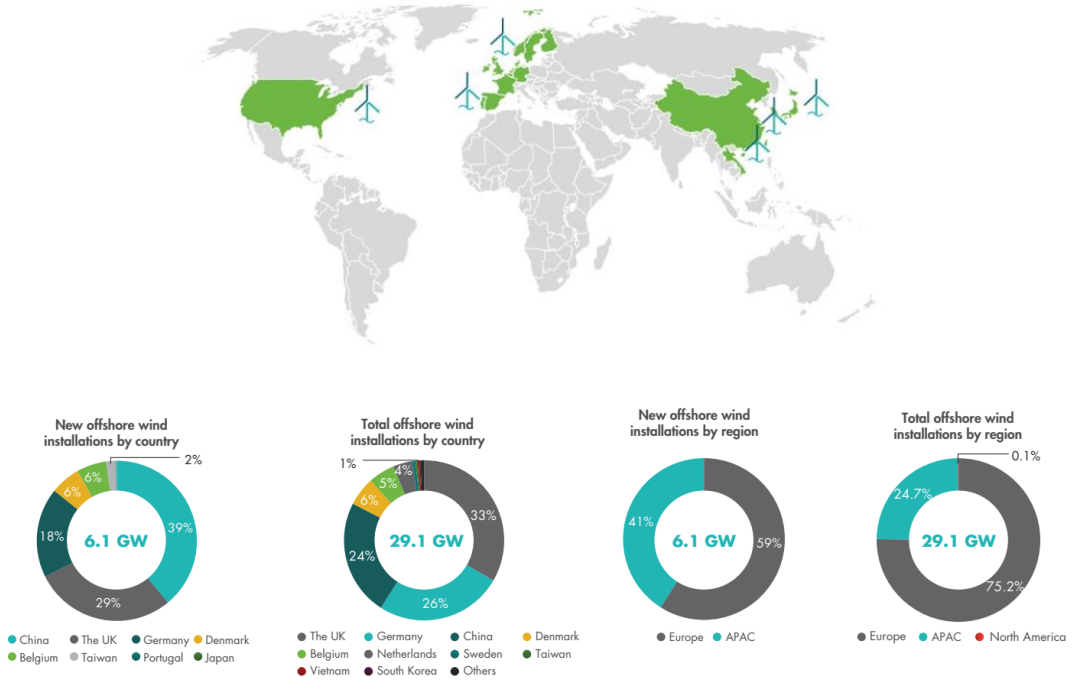

Figure 1. 2：Offshore wind turbine installation present conditions as of 2019[2]

In 2019, 6.1 GW of installed capacity of offshore wind turbines was newly added worldwide, which is the best year since the offshore wind power field began to be put into practical application as we can see from figure 1.2. According to the figure

1.3, the total installed capacity of offshore wind turbines in Europe is gradually increasing.

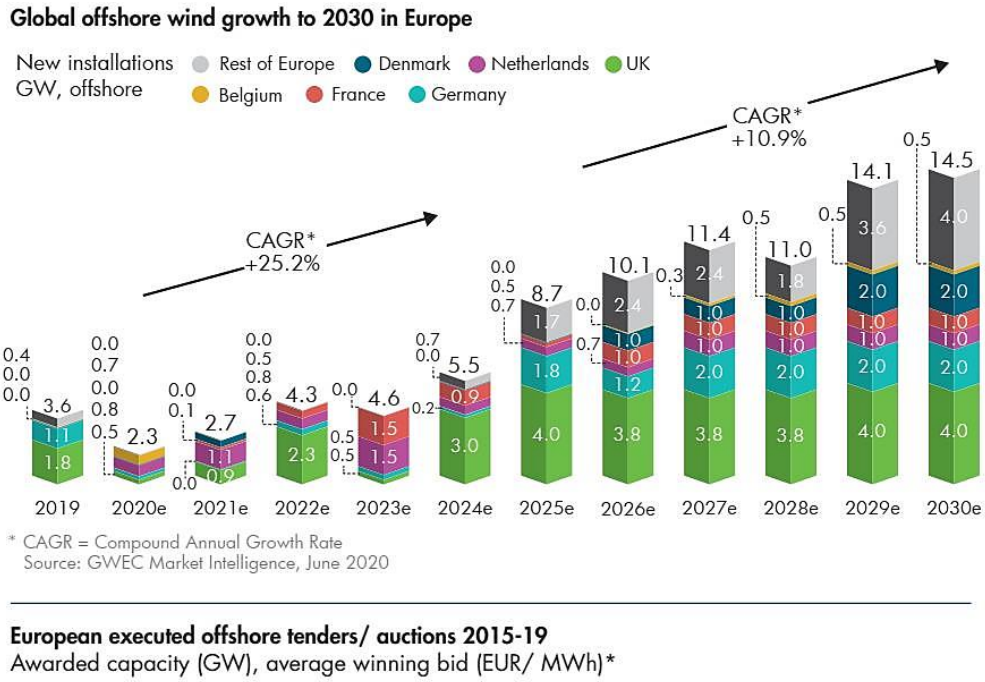

Figure 1. 3：Global offshore wind growth to 2030 in Europe[2]

1.2 Types of Offshore Wind Turbine

At this stage, there are two main types of offshore wind turbines, one is bottom fixed wind turbines, and the other is floating offshore wind turbines[6, 7]. The currently recognized technologies are gravity, monopile and tripod/jacket foundations, all of which are offshore wind turbines fixed on the seabed. The tension leg platform (TLP), semi-submersible platform (Semi-sub) and Spar Buoy (Spar) are mainly used in floating offshore wind turbines, which are based on oil and gas industry regulations [7, 8].

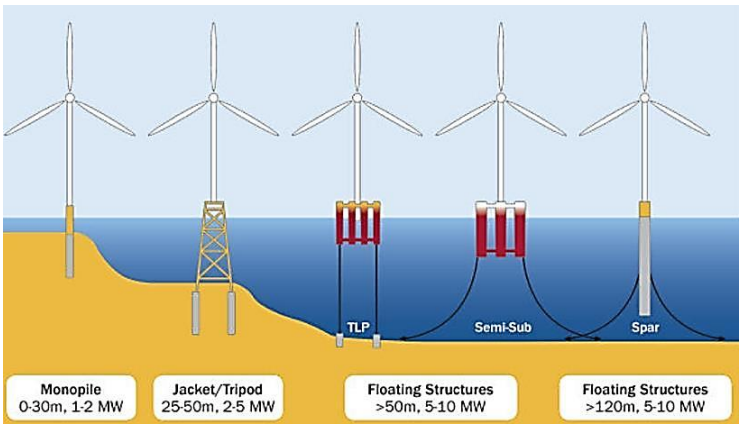

Figure 1. 4：Types of offshore wind turbine foundations[9]

Generally, gravity and monopile offshore wind turbines are used in sea areas with water depth from 0 m to 30 m, which the power is 1MV -2 MV. Considering the economy and ease of installation, the monopile offshore wind turbine is currently the most widely used offshore wind turbine. The tripod/jacket offshore wind turbine is mainly used in sea areas with water depth from 25 m to 50 m, and the power is 2 MW -5 MW. TLP and Semi-sub offshore wind turbine are generally used in sea areas with a water depth greater than 50 meters, power is usually from 5 MW-10 MV. For spar offshore wind turbine which is used in sea areas with water depth greater than 120 m, the power is also from 5 MW – 10 MW.

1.3 Offshore Wind Turbine Installation

Generally speaking, when offshore engineering companies are constructing, they usually choose one foundation of among the gravity, monopile, jacket and tripod foundations for construction[10].

The structure of the monopile is relatively simple, and the subject is a long pipe. In the process of offshore operations, a large hydraulic hammer is generally used to drive the single pile into the seabed for fixing. Generally speaking, this pipe is made of steel and is prepared by welding with can, where the can is rolled into a round shape from steel plates of different sizes and then welded together. The biggest advantage of the monopile is that in the process of offshore operations, the installation work will become relatively simple when the equipment, construction plan, site preparations are fully prepared and the seabed soil data is reliable[10].

In this study, the floating vessel installation of offshore wind turbine blades is the main research focus and difficulty, and the motion of offshore wind turbine is the secondary research objective. Therefore, the object of blade installation of wind turbine is determined as single pile wind turbine in the follow-up research process.

The installation process of single pile offshore wind turbine foundation can be summarized as follows: scour protection installation, foundation installation, transition piece transportation, turbine tower installation, engine room installation and blade installation.

1.3.1 Monopile Offshore Wind Turbine Foundation Installation

The following is the installation process of monopile offshore wind turbine foundation.

1. For the vessel required in the installation process, the preferred installation vessel is a jack-up crane vessel, which can be loaded and installed on the deck of various parts of the offshore wind turbine.

2. The large hydraulic hammer is used for piling when installing a single pile. The hammer is equipped with a power device and a control unit. It can be tested when the single pile is driven to ensure that the installation process is safe and error-free, and the project is safe and error-free.
3. Pile handling tools are mainly used for holding and vertical positioning of single piles before and during pile driving.
4. In order to cast the single pile and transition piece together, grouting equipment is also necessary.
5. In extreme cases, such as the seabed soil is hard or there are rocks, large drilling rigs can be used to drill holes on the seabed to ensure that the single pile can be smoothly driven into the seabed and fixed[10].

For the installation of the nacelle and rotor, they are assembled at the installation site with the crane as shown in figure 1.5

Figure 1. 5： The installation of wind turbines[11]

1.3.2 Installation of Offshore Wind Turbine Blade

In the blade installation technology, single blade installation, bunny ear installation and whole rotor lifting are the most common and effective methods (Uraz,2011). With the continuous exploration and innovation of domestic and foreign experts on the installation process of wind turbine model, the blade installation technology and installation process are constantly making better breakthroughs[9, 12, 13].

The rotor overall lifting is the three blades are first connected to the hub fixed, and then lifted, this method has also become the "rotor installation method."

With the increase of the number of blades, it is difficult to lift the weight of three blades to more than 100 meters by using the existing crane equipment, because it has great requirements for the operation space, so it is difficult to solve this problem.

The "rabbit ear" method solves the problem by lifting the cabin with two blades, just like a rabbit face with two ears. Although the problem can be solved, but in practical of the engineering, this application method is not common.

Figure 1.6 shows the schematic diagram of single blade lifting operation. As shown in the figure, the crane on the vessel is mainly responsible for lifting the blade with steel wire rope. The lifting rope is connected with the lifting head and hook, and the hook is connected with the yoke with sling. The yoke is mainly responsible for fixing the turbine blade and hanging it in the air. The towing cable connecting the boom and yoke is mainly used to reduce the pendulum movement of the blade. The blade system of crane wire rope hook is usually affected by environmental factors such as wind speed, wind direction and so on, in which the average wind load and dynamic wind load will affect the system.

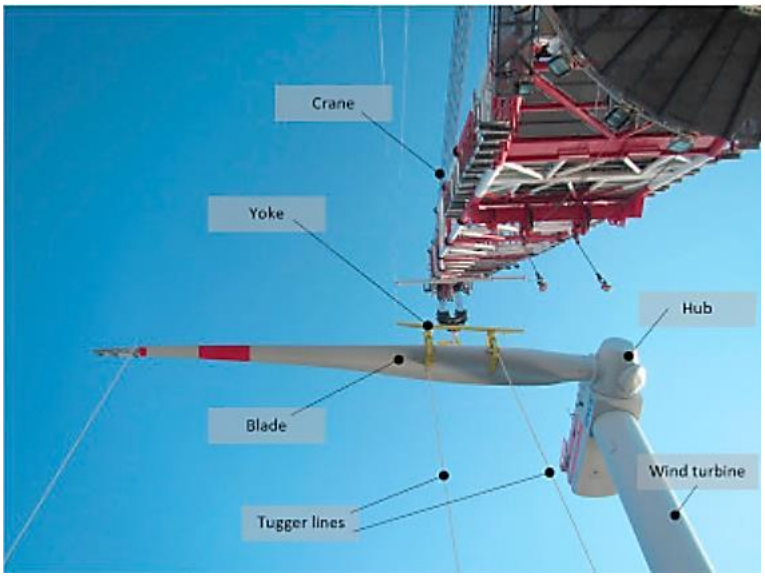

Figure 1. 6：The configuration of a single blade lifting operation[14]

Taking the installation of jack-up vessel as an example, this paper briefly introduces the installation of single blade. Generally, when installing single blade, the jack-up vessel should be installed in the correct position first, and then the single blade should be lifted one by one and connected to the hub. In particular, when rotating the hub, special tools should be used to rotate the turbine hub to the horizontal position. Then fix the blade with yoke and lift it to hub level. It is very important to monitor the movement of blade root during alignment[14]. When the wind speed is too high, resulting in excessive movement, the blade should be suspended near the hub until the weather improves before alignment. If the weather conditions remain bad, it is necessary to lower the yoke system onto the deck with a blade. If the relative movement of the blade meets the requirements, the blade root and hub can be connected accurately by manual operation. In the initial stage of matching, the

guide pin connected to the blade root should be penetrated into the flange hole on the hub. If the guide pin and flange hole can be accurately butted, the blade can be fixed on the hub with bolts, and then the lifting device can be taken out. The above is the installation process of jack-up vessel.

In the above installation process, alignment stage and mating stage are the most important two links, which are also the focus of this study.

It can be seen from figure 1.7 that the blade is lifted on the jack-up vessel by crane. The calibration starts after the blade reaches the hub height. The crane is rotated by selecting the crane and adjusting the lead wire to make the blade root close to the hub. Figure 1.8 shows two possible situations when the blade root and hub are aligned. R_b is the radius of the blade root, R_h is the radius of the hub, and D is the distance between the two centers. The relative movement of the blade root and hub may occur in the process of the calculation, which can be determined by the functional expression of distance and time. If $\mathrm{D} > R_b + R_h$, the offset is too large to be aligned. If $\mathrm{D} < R_b + R_h$, the offset between them is within the controllable range, and the center of blade and hub can be aligned by visual inspection and manual adjustment. According to the above two assumptions, by tracking the relative motion between the two center points on the y and z planes, the radius and the number of moving intersections of R_{sb1} on the circular boundary can be calculated. In a short period of time, if the intersection is small enough, it is possible to realize the alignment between the blade root and hub.

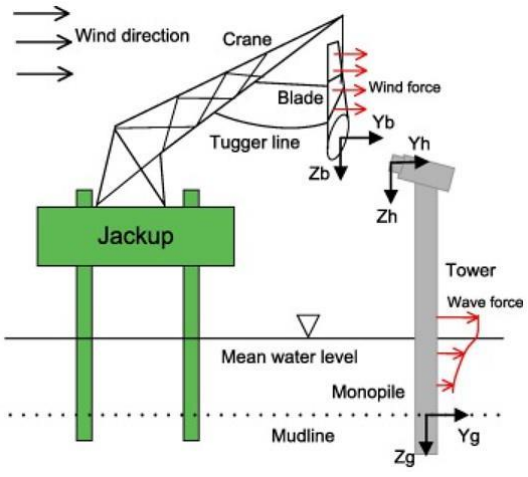

Figure 1. 7：The blade installation [15, 16]

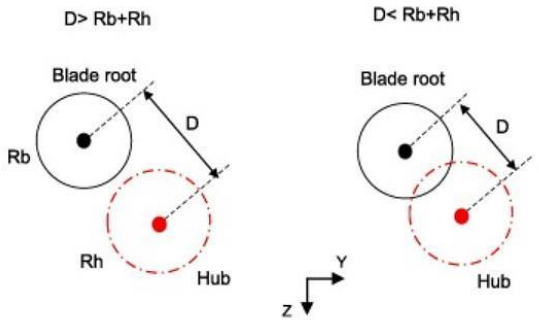

Figure 1. 8：Two possible situations in the alignment process[15, 16]

It can be seen from figure 1.7 that the main components of the blade root and hub. When the work starts in the mating stage, the joint will not be opened until the blade root is aligned with the hub.

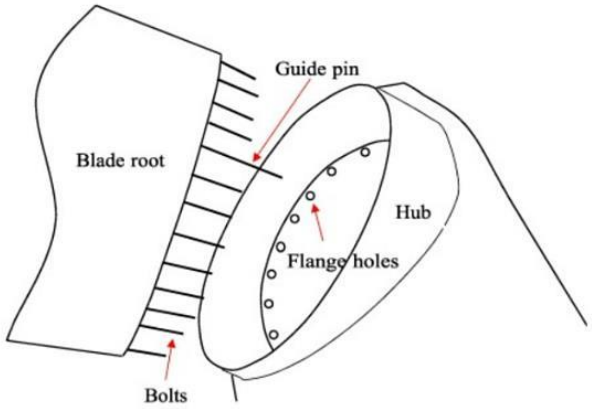

Figure 1. 9：The main components of the blade root and hub[17]

"T-bolt" is usually used for blade root connection, which has low cost and simple connection process. For the guide pin, because the length is longer than the bolt, it can pass through the flange hole first, so that the maintenance bolt can fit with the flange hole smoothly. In order to increase the probability of successful mating, the standard should be more stringent than the calibration stage. Figure 1.10 shows two options for D.

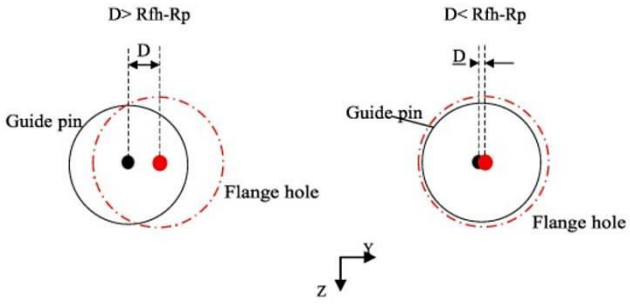

Figure 1. 10：Two options of D [17]

In Figure 1.10, D represents the distance between the two centers, R_{fh} is the moving radius of flange hole, R_p is the moving radius of the guide pin. If $D > R_{fh} - R_p$. It shows that the relative distance is large, and it is impossible for the two to pair. If $D < R_{fh} - R_p$, it means that the relative distance between the two is small, indicating that the two have the possibility of successful pairing. Based on the above assumptions and the evaluation of the success probability, the relative motion between the center of the guide pin and the center of the flange hole in the y and z plane can be tracked, and the radius and R can be calculated_ The number of intersections of the circular boundary motion of SB2. For practical engineering, the low frequency part of the relative motion can be controlled artificially, but the specific control effect mainly depends on the characteristics of the winch towing cable. In the working stage, only when the frequency component is greater than 0.5 Hz, it can be regarded as a parameter related to the coordination stage.

1.3.3 Installation with Floating vessel

Figure 1.11 shows three different kinds of crane vessels used to install offshore wind turbine blades, which are semi-submersible, mono hull and jack-up vessel.

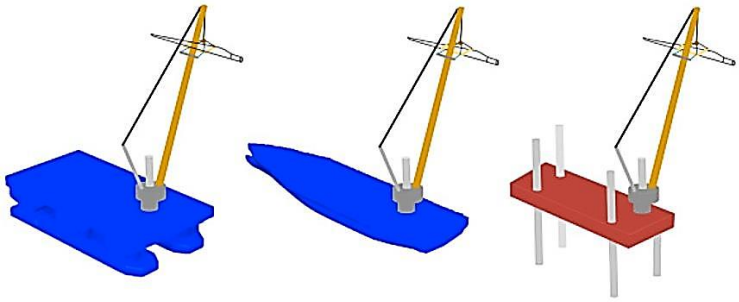

Figure 1. 11：Three different kinds of crane vessels: semi-submersible, mono-hull, jack-up [18]

The research focus of this project is the floating vessel installation of offshore wind turbine blades.

The blade installation system is mainly composed of vessel, crane, blade installation and lifting device.

For floating vessels, semi-submersible vessels have two fully submerged longitudinal pontoons. The pontoon is connected to the main deck by six columns, and the displacement of a single hull is about 40% of that of a semi-submersible[19].

The pedestal crane is mainly composed of crane bracket, suspension steel wire system and lattice arm. The crane is connected to the vessel through the crane bracket as shown in figure 1.12. In the numerical model, the boom is modeled by flexible beam element, and its lower end is hinged on the crane base.

Boom inclination is mainly controlled by boom wire and specifically expressed by rod element.

The deformation effect of crane support (including support, support and rear strut) is ignored in the simulation process[15].

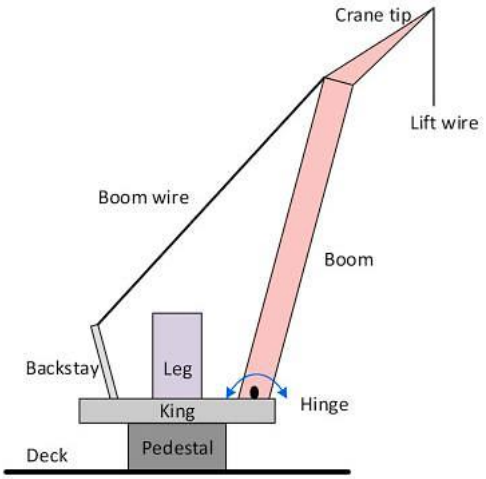

Figure 1. 12：Illustration of a typical offshore pedestal crane[20]

Here are the steps to install offshore wind turbines with floating vessel[21]:

1. Tower ring and lift rigging is attached to the tower on deck
2. Tower is lifted and installed on the transition piece
3. Tower ring remains on the tower but the lift rigging (internal lifting tools) are retrieved
4. Blade is loaded in the blade lift frame
5. The blade lift frame is lifted to installation height
6. Motions are compensated by attaching the blade lift frame to the tower ring in horizontal
   position
7. The blade is upended by lowering the blade lift frame in the hang off points on the tower
   ring
8. The nacelle is turned 90 degrees counter clockwise to align with the blade
9. The blade is inserted using the telescopic beams of the blade lift frame
10. When the blade is attached, the nacelle is turned 90 degrees clockwise to release the blade
11. The blade lift frame is upended and retrieved to deck
12. Step 4 to 11 are repeated for the second blade
13. Vessel is repositioned to retrieve the tower ring

14. Internal lifting tools are inserted into the tower ring
15. Tower ring is opened and retrieved to deck

1.2 The Aim and Scope

As the technology of offshore wind turbines develops better and better, in order to make full use of offshore wind energy, utilization of wind energy in deep water ocean becomes more and more important[22]. The jack-up vessel is limited by its own structure, it is difficult to operate in the ocean environment with a water depth of more than 60 meters. At this time, it is a feasible option to use a floating vessel instead of a jack-up vessel for operation.

This thesis will numerically model and analyze the environment of irregular waves and turbulent winds during the installation of offshore wind turbine blades using a floating vessel.

2 Theory of Blade Installation Using a Floating Vessel

Floating crane vessels are flexible with respect to working water depth and are much faster in relocation. They are thus a promising alternative to install offshore wind turbine components, especially in intermediate and deep water.

In order to determine the blade displacement during the installation of offshore wind turbine blades on the entire floating vessel and to check whether the guide pin can enter the wind turbine, it is necessary to analyze and calculate the load on the vessel and blades during the installation of the wind turbine. Main parts of this research are the load on the floating vessel and offshore wind turbine blade since the main influence in this research are wave and wind. The wave and wind affect the surface part and the underwater part respectively[23].

In the process of the offshore wind turbine blade being lifted and installed, since the offshore wind turbine blade is in the atmosphere, the factor that has the greatest influence on the installation of the offshore wind turbine blade at this stage is the wind speed. The wind load acts on the offshore wind turbine blades, and steel cables are used to connect the wind turbine blades to the crane. Therefore, under the action of the wind load, the blades will shake and cause displacement. The wave acts on the vessel because wave is the main factor causes the hull shaking[24].

Finally, after completing the individual analysis of the above two components, a complete analysis result of the overall structure can be obtained using coupled analysis. By analyzing the motion of the guide needle of the offshore wind turbine blade in the final and complete result, the motion range and change of the guide needle of the offshore wind turbine blade under different sea conditions can be obtained[25]. Comparing this range with the installation standards, it can be determined under what sea conditions this offshore operation is feasible. The installation standards include key parameters such as wave height and period.

2.1 Coupled Simulation Method

It can be seen from figure 2.1 that the coupling simulation method can be obtained by integrating aero code and SIMO By using aerodynamic codes, the aerodynamic force and torque that have been installed on the blade can be obtained. It is mainly composed of dynamic link library (DLL) and SIMO. SIMO is developed by SINTEF

ocean company and has been widely used in offshore wind power, oil and gas industry[26]. It should be pointed out that the offshore wind turbine blade is regarded as a rigid body in SIMO.

Figure 2.1 shows the step-by-step development of the external force model of the blade mounting system in the coupled analysis. The floating vessel is considered in the model[18]. Models of blades and lifting devices (lifting wires, slings and towing ropes) were established in SIMO-Aero[3, 27], and the wave loads on the vessel's hull were also considered.

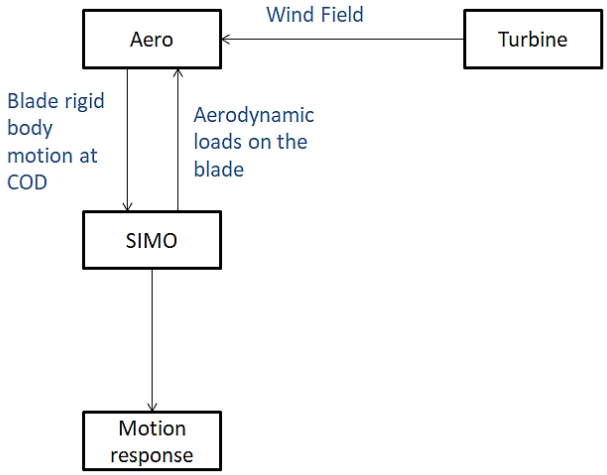

Figure 2. 1： Overview of the coupled simulation method[18]

When the wind speed, effective wave height, and period are obtained, simulation and calculation can be carried out in SIMO based on the above model. The basic formula is as follows:

$$m\ddot{x} + c\dot{x} + kx = f(U) \tag{2.1}$$

The following sections summarize the detailed information of system modeling, including aerodynamic loads, hydrodynamic loads, structural modeling and mechanical coupling. Based on these parts, the calculation and analysis of the entire model can be completed.

2.2 Aerodynamic Loads

The application of SIMO can calculate the contact of the hull, and the calculation of the s aerodynamic load on the blade, also requires an ero code.

Based on the cross flow theory, taking into account the influence of shear wave, turbulent state velocity, Yang and other factors, aeronautical code can be written to obtain the global aerodynamic load on the blade surface.

The aerodynamic load on each blade element needs to be calculated by cross-flow theory. A certain part of the blade element is analyzed as a small unit, which can approximate the actual two-dimensional situation, and can be calculated using the load of the aerodynamic wind turbine blade. When the cross-flow principle is adopted, the inflow velocity perpendicular to the cross section can be ignored, that is, $A_{A,i}$ along yc, the specific process is shown in Figure 2.2.

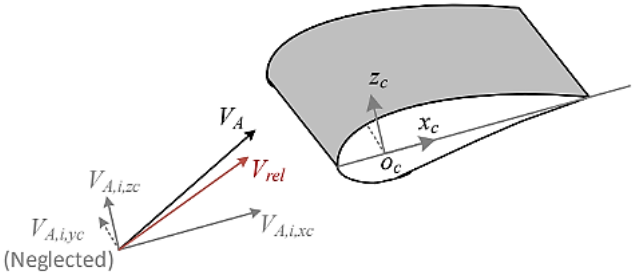

Figure 2. 2：Illustration of cross-flow principle: $\mathbf{A}_{A,i} = [\mathbf{V}_{\mathbf{A,,i,xc}}\ \mathbf{V}_{\mathbf{A,,i,yc}}\ \mathbf{V}_{\mathbf{A,,i,zc}}]^{T}$ **[28]**

When calculating the aerodynamic speed, the relative wind speed V_{rel} used can be carried out by using formula 2.2, which is specifically:

$$A_{A,i} = [V_{A,,i,xc}\ 0\ V_{A,,i,zc}]^{T} \tag{2.2}$$

where $A_{A,i}$ is the relative wind velocity related to element i. $V_{A,,i,xc}$ and $V_{A,,i,zc}$ are respectively its projection on xc and zc. $A_{A,i}$ is obtained by Eqation [14]

$$A_{A,i} = T_{GC,i}(V_{WG,i} - V_i + V_{IG,i}) \tag{2.3}$$

Among them, $V_{WG,i}, -V_i$ *and* $V_{IG,i}$ represents the global wind speed, and i represents the wake induced velocity at unit i. Unlike the motor blades with high rotation speed, the relative movement of the installed blades is relatively small due to the influence of the blade margins during the installation of offshore wind turbine blades. Therefore, the equation can be simplified to the calculation form of 2.4.

$$A_{A,i} = T_{GC,i}(V_{WG,i} - V_i) \tag{2.4}$$

V_{rel} is mainly used to determine the angle of attack α.

After simulating Gupta and Leishman with a helicopter aerodynamic model, Beddoes-Leishman was modified with a dynamic stall model. The improved model can simultaneously simulate offshore wind power and aerodynamic problems. The model mainly includes three parts: unstable adhesion flow, unstable separation flow and dynamic vortex lift. After calculating the above three parts separately, the total load of the airfoil can be obtained by summing them[29].

Then calculate the lift and drag on the blade elements, and finally get the total aerodynamic load on the blade as the sum of all the elements. Figure 2.3 shows the flow chart for calculating the aerodynamic load on the lifting blade.

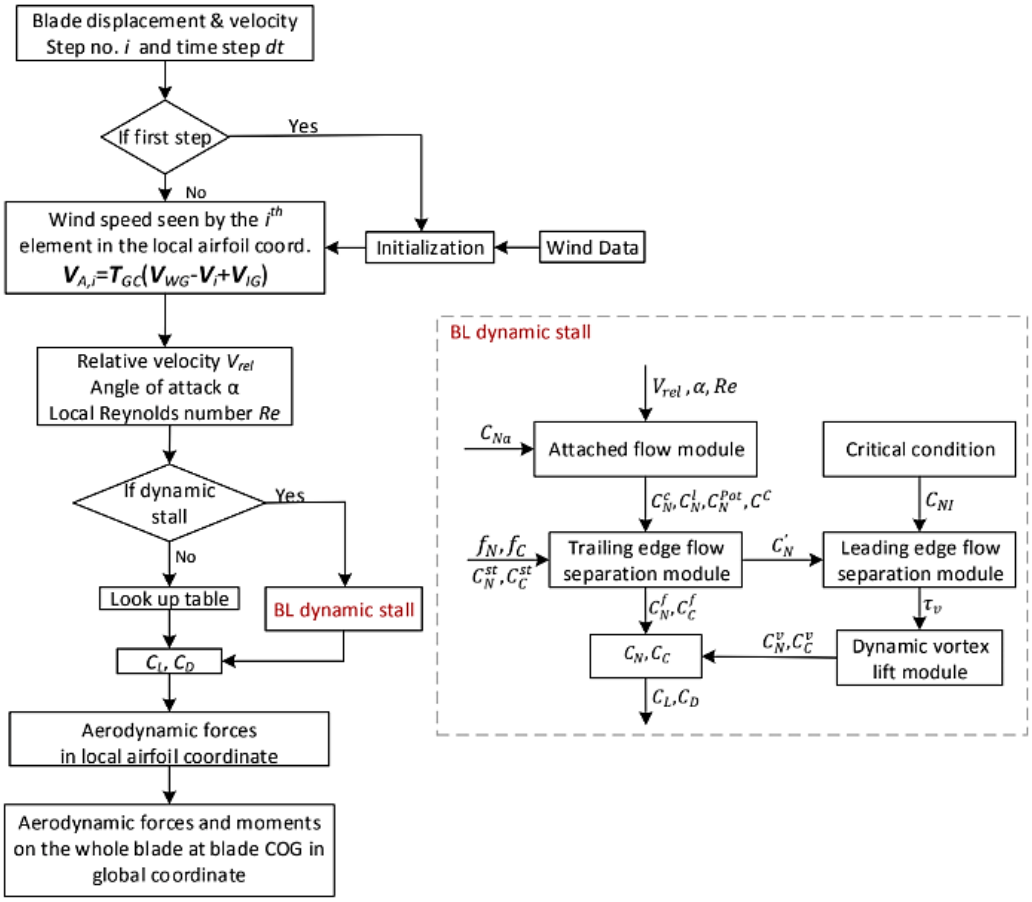

Figure 2. 3：Flow chart for aerodynamic modeling[14, 28]

Figure 2.4 shows the Distribution of lift and drag forces on a blade under rotating condition and lifting condition: blade pitch angle 0° ; rotational speed for the rotating blade 8.029 rpm; constant wind 10m/s, we can see the aerodynamic distribution on the lifting blade It is completely different from the aerodynamic distribution on the rotating blades.

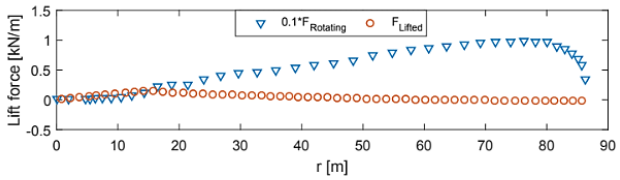

(a) Lift force F_z

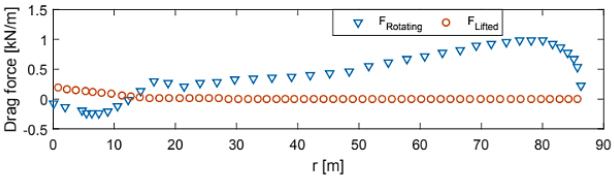

(b) Drag force F_x

Figure 2. 4：Distribution of lift and drag forces on a blade under rotating condition and lifting condition: blade pitch angle 0o; rotational speed for the rotating blade 8.029 rpm; constant wind 10m/s[28]

It can be seen from Figure 2.4 that in offshore wind turbines, the lift and drag of the rotating blades eventually tend to be sharp. According to aerodynamic theory, the center of the rotating blade will remain close to the tip of the blade. This shows that the speed will largely affect the aerodynamic distribution of the rotating blades.

When the blade is lifted, the middle and root of the blade are the main distribution areas of aerodynamic loads. Compared with the inflow wind speed, the wind speed of the blade lift is much smaller than the inflow wind speed, which is basically negligible[30].

When calculating the aerodynamic load, even if the blade speed has a small effect on the aerodynamic load, the influence of the blade speed on it must be taken into account, because the blade speed may play an important role in the damping part of aerodynamics. If the effect of blade speed is not considered in the calculation, the final calculated blade motion may be higher than the actual result.

2.3 Wave Loads on the Floating Vessel

For the floating vessel, the recovery factor of hydrostatic pressure is mainly calculated by the average position of the vessel. The illustration of the semi-submersible, which is used as floating vessel in this thesis is shown in figure 2.5 The floating vessel According to the potential flow theory, the hydrodynamic load can be calculated. The additional mass, potential damping and first-order excitation force can be obtained by using the first-order potential flow model[31, 32]. The additional viscous rolling damping is 3% of the critical rolling damping[33].

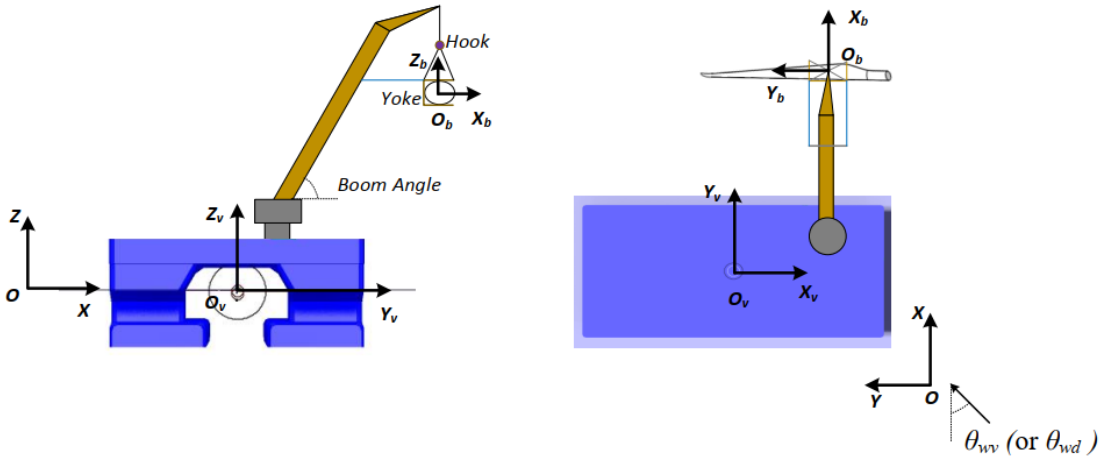

Figure 2. 5：Illustration of semi-submersible vessel

In addition to the first-order hydrodynamic forces described above, the average wave drift load also needs to be considered. The second-order difference frequency wave excitation loads of the monohull vessel in the surge, roll and yaw can be calculated by using the Newman approximation method. For the semi-submersible vessel, the second-order differential frequency wave excitation forces with six degrees of freedom in shallow water should be considered. Therefore, according to the recommendations of DNV-RP-C205 guidelines, the corresponding second-order differential frequency wave loads of the six degrees of freedom of the second-order average wave pressure integral on the wet surface can be used for evaluation[34].

The restoring force of dynamic positioning system can be simplified as equivalent linear stiffness terms of surge, sway and yaw. In addition, the corresponding slow motion can be eliminated or weakened by using large damping, that is, 70% of the critical damping of the vessel's pitch, roll and yaw motion. The above assumption is reasonable because it can be realized by using DP system in practice[31, 35].

2.4 Structural Modeling

Because the flexibility has little effect on the rigid body motion during the blade installation, the blade can be regarded as a rigid body in modeling[36].

In the simulation, the beam element is used to simulate the crane boom. The lower end of the boom is hinged on the crane base. The boom wire controls the boom movement. The boom wire can be represented by the rod element. In this simulation, it is assumed that the deformation of the crane is mainly caused by the flexibility of the boom and the boom wire rope, and the deformation effect of the crane support (including the main support, the base and the rear strut) is ignored.

A 6-DOF rigid body is usually used to model the floating body model. Jack up hull can also be expressed as a rigid body with six degrees of freedom. The flexible jack up leg structure can be considered as beam element. The connection of jack up hull legs is considered as rigid connection.
The Rayleigh damping model is usually used to calculate the structural damping of slender structures such as crane jib and jack-up leg[37]. The damping matrix can be expressed as:

$$\mathrm{c} = \alpha_1 \mathrm{m} + \alpha_2 \mathrm{k} \tag{2.5}$$

where α_1 and α_2 are receptively the mass-proportional and stiffness-proportional damping coefficients. Coefficients of $\alpha_1 = 0$ and $\alpha_1 = 0.005$ were specified for the slender structures.

2.5 Mechanical Couplings

The coupling force modeling of the non-compression traction rope is usually bilinear spring force:

$$\mathrm{T} = \begin{cases} k\Delta L & if \quad \Delta L \geq 0 \\ 0 & therwise \end{cases} \tag{2.6}$$

where T is the tension of steel wire and ΔL is the elongation of steel wire. In addition, k refers to the axial stiffness of the wire. The damping used in the conductor is stiffness proportional damping, usually 1% of the conductor stiffness. Due to the gravity of the blade, the lifting wire and sling are always in tension. In modeling, they are considered as bilinear springs and are represented by rod elements with equivalent stiffness characteristics.

2.6 Blade Motion

For floating crane vessel and jack up cranes, the surge, heave and pitch of blades are mainly caused by the vessel motion caused by waves. There are two main factors that affect the blade motion under other degrees of freedom. When the jack up crane vessel is installed, the aerodynamic load has great influence on the rolling, rolling and rolling motion of the blade. When floating crane vessels are used, the motions caused by aerodynamic loads and waves are more concerned. The vessel motion caused by waves and aerodynamic loads on the blades of the floating body can generate resonance response when the blades roll. In addition, the floating crane vessel can also cause the wave frequency response of blade rolling motion. Compared with the semi-submersible vessel, the wave frequency motion of monohull vessel with blades is more significant, and the double pendulum motion can be excited.

Compared with the semi-submersible vessel and the jack-up vessel, the monohull vessel has larger motion amplitude and is more sensitive to the change of wave direction due to its more obvious wave frequency response. The blade motion of semi-submersible vessel is slightly larger than that of jack-up vessel. However, in general, when the crane vessel is in the top sea state, the installed blade movement is the smallest, and the contribution of the blade motion on the floating vessel to the crane dynamics is relatively small, which is similar to the crane end movement. For the jack-up vessel, the resonance response of crane has more significant influence on blade motion.

By analyzing the eigenvalues, it can be concluded that the blade rigid body has a fixed frequency when the vessel and crane are fixed, based on Eq.(2.5).

$$[-\omega^2 \mathrm{M} + \mathrm{K}] \cdot \mathrm{X} = 0 \tag{2.7}$$

Where M and K represent the mass and recovery matrix of the auxiliary hook respectively. In addition, the recovery matrix K is mainly determined by the gravity of the relevant object, suspension rope, sling and streamer.

2.7 Crane Motion

When the vessel is fixed, the natural period of crane motion can be determined by attenuation test. That is to apply a certain vertical force on the top of the crane and remove it after a period of time. By analyzing the time series of crane end movement, the inherent period of crane is calculated. The deformation of the crane's lower arm is mainly caused by the movement of the crane's lower arm. Compared with the boom itself, the edge deformation of the jib is mainly affected by the natural period of the crane and by the lifting components and lifting devices. The natural cycle of the crane itself is 2.0 s without lifting anything. When considering the installed blades and lifting devices, the natural cycle of the crane is increased to about 2.9 s.

Different from the jack-up crane vessel, the lifting end movement of the crane vessel is mainly caused by the vessel motion caused by the wave, while the flexibility of the lifting machinery has little influence on it, which is much larger than the floating action of the crane on the vessel. In short, the crane top movement of semi-submersible vessel is much smaller than that of the monohull vessel.

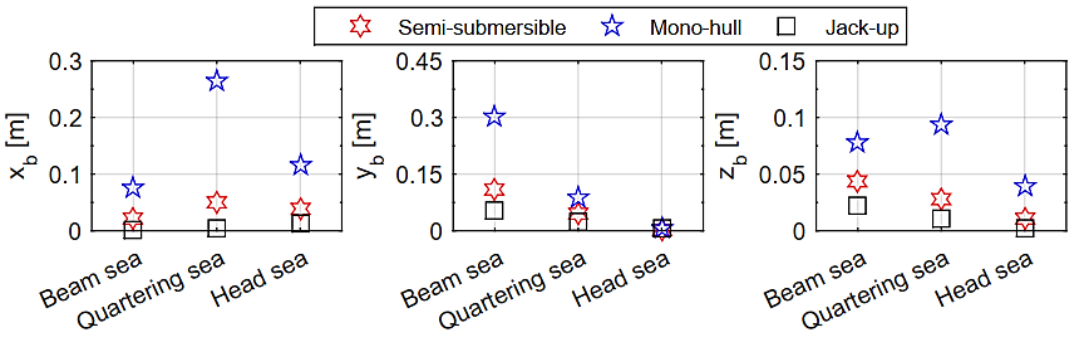

Figure 2. 6 Standard deviations of the crane tip motion with different wave direction: significant wave height is 1 m, period is 7.3s; beam sea θ_{wv} = 0°, quartering sea θ_{wv} = 315° and head sea θ_{wv} = 270°[38]

For the crane operation with large lifting height, the amplitude of crane top motion is usually greater than the translational motion speed of the vessel, because the rotation of the vessel has a greater impact on the top motion of the crane. However, in some cases, the former may be smaller than the latter, because the rolling motion

of the monohull vessel also has a great influence on the former, and when the latter is not synchronized with the latter, the latter cannot be offset.

2.8 Vessel Motions

When considering the motion of the floating vessel, the aerodynamic load on the blades is not taken into consideration, and the hydrodynamic load on the hull caused by waves is mainly considered. Compared with the jacket-up vessel, the motion of the floating vessel is much larger.

When analyzing the motion period of a floating vessel, it is necessary to use eigenvalues for analysis. It should be noted that the crane on the floating vessel and the blades connected by the crane using the sling are not considered in this part.

For the floating vessels, the natural frequencies are obtained by Eq. 2.8.

$$[-\omega^2(\mathrm{M} + A_\infty) + \mathrm{K}] \cdot \mathrm{x} = 0 \tag{2.8}$$

where M is the vessel mass matrix, A_∞ is the added mass matrix at infinite frequency, K is the restoring matrix. The restoring matrix is obtained by the hydrostatic restoring and the equivalent restoring from the DP system.

2.9 Time Domain Simulations

In time domain analysis, turbosim can be used to simulate three-dimensional turbulent wind field[39], which is mainly based on IEC Kaimal model defined in IEC 61400, which is based on the IEC Kaimal Model defined in IEC 61400[40, 41].

When calculating the wind speed above Z m above the sea surface, the calculation formula of wind speed U_Z is usually calculated by 2.9.

$$\mathrm{U}(\mathrm{z}) = U_{ref}(\frac{z}{z_{ref}})^{\alpha} \tag{2.9}$$

Where, UreF represents the reference average wind speed at the reference height zref. According to Yuna Zhao's research report, when the height of zref is 119 m, it can be used as the design hub height of DTU 10 MW wind turbine. According to IEC 61400-3. Since the selected sea area is the North Sea, according to JONSWAP spectrum, the waves here can be simulated as long peak irregular waves:

$$\mathrm{S}(\omega) = \frac{\alpha g^2}{\omega^5} exp[-\beta(\frac{\omega_p}{\omega})^4]\gamma^{\exp[\frac{(\frac{\omega}{\omega_p}-1)^2}{2\sigma^2}]} \tag{2.10}$$

where α is the spectral parameter, β is the form parameter, ω_p is the wave peak frequency and γ is the peakedness parameters[34].

In the steady-state simulation, it is usually necessary to simulate 30-42 samples, and the simulation time is about 20 minutes. In order to improve the accuracy of the

final analysis, the simulation results of the first 10 minutes need to be deleted and not included in the valid data. By analyzing the results in time domain, the motion response eigenvalues of the blade in the meshing stage can be obtained[42].

2.10 Blade Root Motion

During the installation of a single hull vessel, the motion of the blade root is highly dependent on the wave conditions. Among them, the blade root motion of single hull vessel is the largest, followed by semi-submersible vessel, and finally jack-up vessel. Under the top sea condition, the value of blade root motion can reach the minimum value.

The motion caused by jack-up crane vessel is the smallest, followed by semi-submersible vessel and single hull vessel. On the jack-up platform, the motion of blade root decreases with the increase of TP, because the wave excitation of jack-up vessel is smaller and smaller. On the contrary, the blade root movement of floating crane vessel increased significantly. The increase range of semi-submersible vessel is much smaller than that of monohull vessel, because the wave frequency response of the semi-submersible vessel in blade root motion is relatively small.

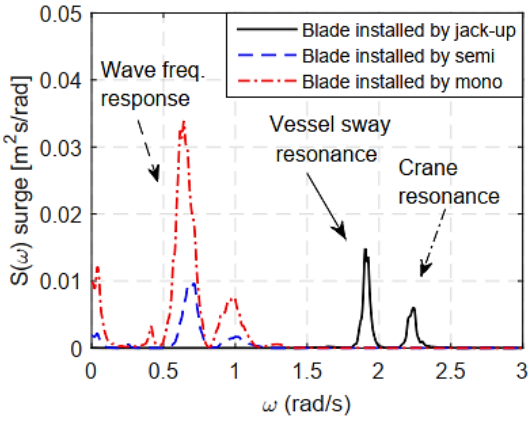

Figure 2. 7：Power spectra of blade surge motion: U_w = 7m/s, θ_{wd} = 0°, significant wave height is 1 m, period is 7.3s, quartering sea θ_{wv} = 315°[38]

2.11 Gumbel Distribution

Gumbel distribution can model and analyze the maximum or minimum distribution. For standard Gumbel distribution, the cumulative distribution function and the probability density function is shown as below.

$$F(x) = e^{-e^{(-x)}} \tag{2.11}$$

$$f(x) = e^{-(x+e^{-x})} \tag{2.12}$$

3 Numerical Model

SIMA software can provide a complete solution for the simulation and analysis of offshore operations and floating systems. The software can convert high-level concepts in engineering and theory into low-level definitions that are convenient for calculation and analysis. At the same time, the software can easily visualize a large amount of data, and the result display is more intuitive, which is extremely important for analysis and interpretation in engineering applications [43].

With the maturity of the SIMA software, its application range has become wider and wider. Offshore lifting operations, lifting of roofs and modules, installation of offshore equipment, installation of underwater equipment, offshore towing operations, the floating vessel and the jack-up vessel can all be completed by SIMA software. The use of SIMA software is extremely common in the marine industry, and its functions can better meet the requirements of this project. Therefore, in the research process of this project, SIMA was also selected for analysis, calculation and research[43].

3.1 Floating Vessel Model

The floating vessel model in the ocean in SIMA is shown as below in figure 3.1:

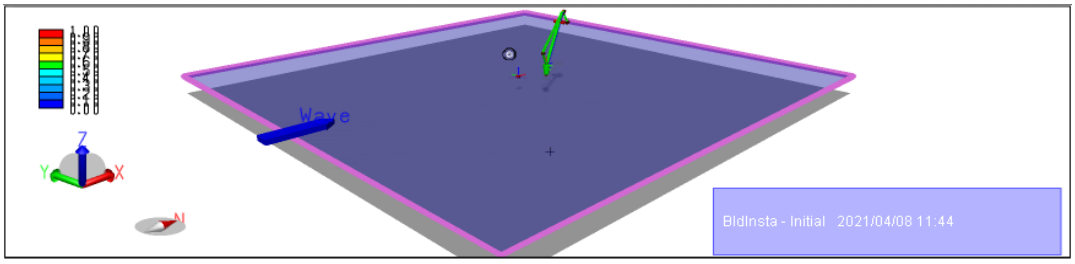

Figure 3. 1: Floating vessel model in the ocean in SIMA

In this model, there are two main parts, which are floating vessel and the crane with blade lifted on it with lift wire which is shown in figure 3.2.

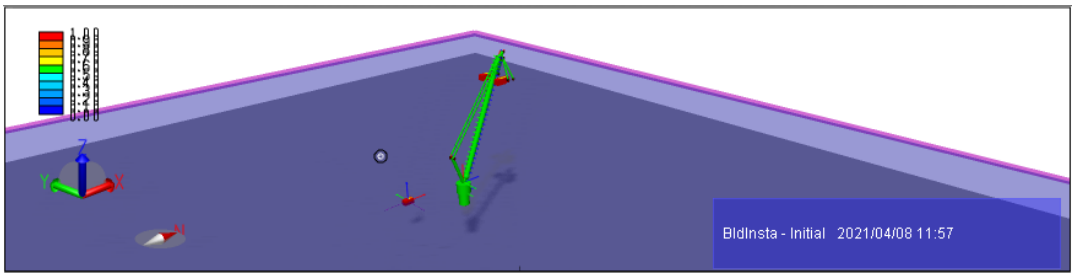

Figure 3. 2: Floating vessel and crane with blade model

Due to the characteristics of the SIMA software, the floating vessel model equipped with the crane used to lift the blades of the offshore wind turbine can be displayed in two parts. Among them, the specific example of floating vessel in this study is semi-submersible vessel, and the crane used to lift the blades of offshore wind turbines is established in the consent model. In this model, the semi-submersible model is established as shown in figure 3.3:

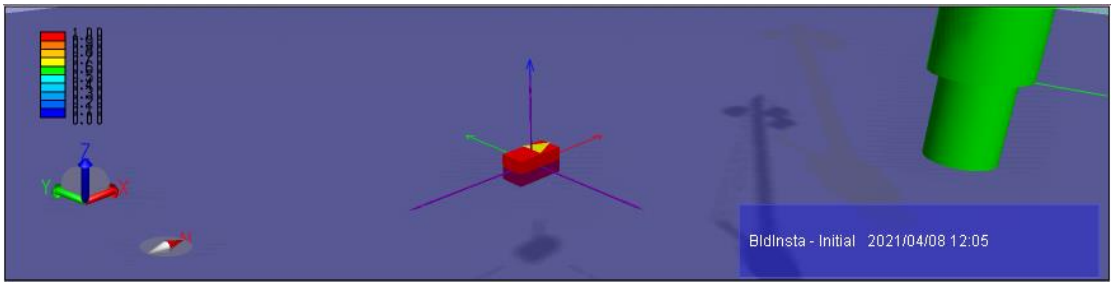

Figure 3. 3：Semi-submersible model in SIMA

The semi-submersible model is set as six degrees of freedom, total motion is simulated in time domain and no estimation of low frequency motion. The parameter of the floating vessel is shown as below:

Table 3. 1: Main parameters of the floating vessels

parameters	Semi-submersible	Mono-hull
Length [m]	175	183
Breadth [m]	87	47
Operational draught [m]	26.1	12
Displacement [m]	1.638*105	6.190*104

And the crane model is shown as figure 3.4:

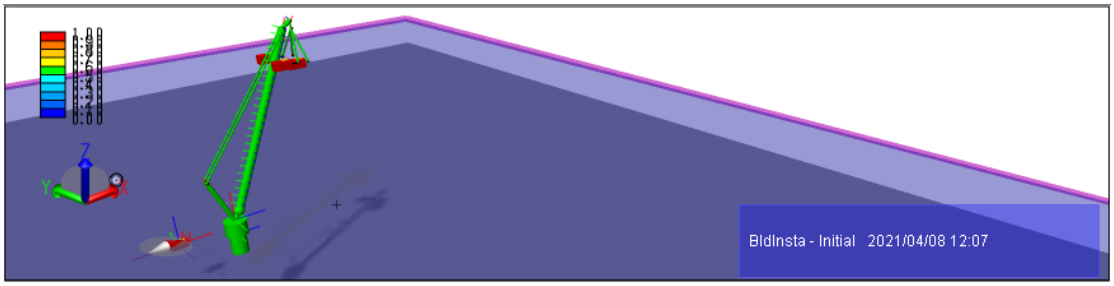

Figure 3. 4：The crane model

In the model figure, the green part is used to simulate the crane. It combines different lines together to establish the crane model. It is worth noting that the offshore wind turbine blade is connected to the crane by lift wire for lifting procedure. The main parameters of the crane is shown as below:

Table 3. 2：The main parameters of the crane

Crane Properties	
Boom length [m]	107.6
Crane boom angle [deg]	67.6
No. Of equipment boom wires [-]	2
Equivalent boom wire stiffness [KN/m]	9048
Equivalent boom wire damping [KNs/m]	90.5
Crane tip position on the vessels	
Semi-submersible vessel	(66m,65.3m,144.9m)
Mono-hull vessel	(74.2m,65.6m,144.9m)
Jack-up vessel	(34.2m,49.3m,133.2m)

- It is given in the vessle-related coordinate system. The height of crane tip on all three vessel are the same in the global coordinate system,i.e.,144.9m above the mean sea surface.

The blade model is the highlight cube as shown in figure 3.5.

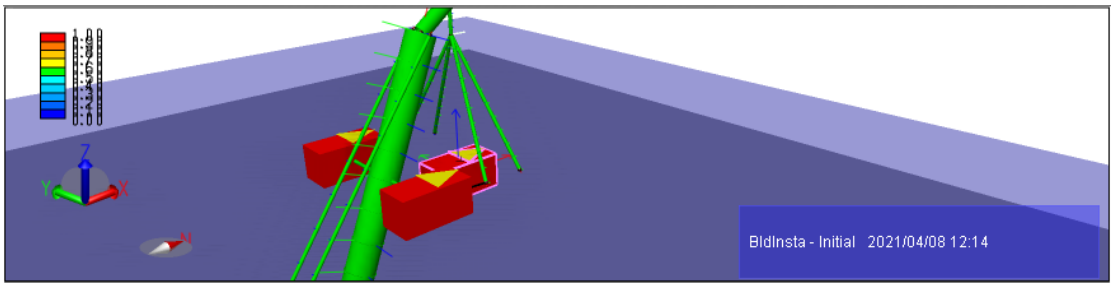

Figure 3. 5：The blade model

And the parameter of blade is shown as below:

Table 3. 3: Main properties of the blade lifting system

Parameter	Value	Unit
Hook mass	10	tons
Yoke mass	47	tons
Blade mass	41.67	tons
Blade length	86.37	m
Blade COG*	26.2	m
Installation height	119	m
Tugger line arm length	10	m

3.2 Loads on the Model

In this article, as it's mentioned before, there are two main loads on the model, which are wind and wave. The wind mainly acts on the blade and the wave mainly acts on the semi-submersible vessel.

3.2.1 Wave Spectrum

The JONSWAP spectrum model with different significant wave height and wave peak period for irregular wave is used to simulate the wave environment. The JONSWAP spectrum is a modification of Pierson-Moskowitz spectrum, which is suitable for the evolving ocean state under limited access conditions. The JONSWAP spectrum is obtained by equation 3.1 as shown below:

$$S_{JONSWAP}(\omega) = A_\gamma \frac{5}{16} H_s^2 \omega_p^4 \omega^{-5} \exp(-\frac{5}{4}(\frac{\omega}{\omega_p})^{-4}) \gamma^{\exp(-0.5(\frac{\omega-\omega_p}{\sigma\omega_p})^2)} \quad (3.1)$$

For parameters A_γ, ω_p and σ, expessions are shown as equation 3.2, 3.3 and 3.4:

$$A_\gamma = 1 - 0.287\ln(\gamma) \quad (3.2)$$

$$\omega_p = \frac{2\pi}{T_p} \quad (3.3)$$

$$\sigma = \begin{cases} 0.07 & when\ \omega < \omega_p \\ 0.09 & when\ \omega \geq \omega_p \end{cases} \quad (3.4)$$

The parameter γ is expressed as equation 3.5.

$$\gamma = \begin{cases} 5 & when\ \ \frac{T_p}{\sqrt{H_s}} \leq 3.6 \\ \exp\left(5.75 - 1.15\frac{T_p}{\sqrt{H_s}}\right) & when\ 3.6 < \frac{T_p}{\sqrt{H_s}} < 5 \\ 1 & when\ \ 5 \leq \frac{T_p}{\sqrt{H_s}} \end{cases} \quad (3.5)$$

3.2.2 Spectral Density

For the wave spectrum, the spectral density is a very important function. The expression is shown as below:

$$S_{xy}(\omega) = \frac{1}{2\pi}\int_{-\infty}^{\infty} R_{xy}\tau e^{-i\omega\tau} d\tau \quad (3.6)$$

$$R_{xy}(\omega) = \int_{-\infty}^{\infty} S_{xy}\omega e^{-i\omega\tau} d\omega \quad (3.7)$$

$$S_{yx}(\omega) = \frac{1}{2\pi}\int_{-\infty}^{\infty} R_{yx}\tau e^{-i\omega\tau} d\tau \quad (3.8)$$

$$R_{yx}(\omega) = \int_{-\infty}^{\infty} S_{yx}\omega e^{-i\omega\tau} d\omega \quad (3.9)$$

When there is a certain frequency, the wave elevation can be expressed as equation 3.11.

$$\zeta_a(\omega_n) = \sqrt{2S_\zeta(\omega_n)\Delta\omega} \quad (3.10)$$

$$\zeta(\omega_n, \mathrm{t}) = \zeta_a sin(\omega_n t + \phi) \quad (3.11)$$

3.2.3 Wind Load

TurbSim is used to create the wind field generation. It is a stochastic, full-field turbulent wind simulator. It uses statistical models (as opposed to physics-based models) to numerically simulate the time series of three-component wind speed

vectors at points in a fixed two-dimensional vertical rectangular grid in space. TurbSim output can be used as input for AeroDyn-based [1] codes (such as FAST [2], YawDyn [3] or MSC.ADAMS®[4]). AeroDyn uses Taylor's frozen turbulence hypothesis to obtain local wind speeds and interpolates the fields generated by TurbSim in time and space. The frequency spectrum and spatial coherence of the velocity components are defined in the frequency domain, and then the time series are generated through the inverse Fourier transform. The theoretical assumption behind this method of simulating time series is a smooth process. In order to simulate non-stationary components, TurbSim (used with AeroDyn) can superimpose coherent turbulence structures on the time series it generates. The basic simulation method is summarized in Figure 3.6.

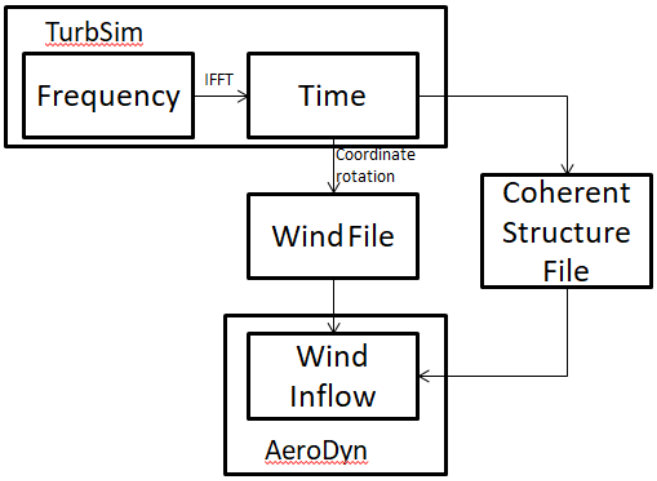

Figure 3. 6：Simulation method

The basic idea of TurbSim simulation method is the conversion from frequency domain to time domain. Calculate through model data and required wind field parameter input files and generate AeroDyn-compatible wind output; optional coherent structures are written in a separate file and superimposed in AeroDyn (they require a full-field background wind file)

To creat the turbulent wind in this thesis work, the Kaimal turbulence model is used. The Kaimal spectrual model with exponential coherence is shown as below:

$$\frac{fS_k(f)}{\sigma_k^2} = \frac{4f^{L_k}/_{V_{hub}}}{(1+6f^{L_k}/_{V_{hub}})^{5}/_{3}} \tag{3.12}$$

$$\mathrm{Coh(r,f)} = \exp[-12((f * {}^{r}/_{V_{hub}})^{2} + (0.12 * {}^{r}/_{L_c})^{2})^{0.5}] \tag{3.13}$$

The coefficients vary for different components(u,v,w). Different coefficients may be used based on measurements, but IEC standard suggests no correlation in v,w.

The wind field input setting is shown as below:

Table 3. 4：Wind field input setting

Vertical grid-point matrix dimension	32
Horizontal grid-point matrix dimension	50
Hub height [m]	119
Grid height [m]	190
Grid width [m]	300
Turbulence model	IECKAI (for turbulent wind cases) and NONE (for constant wind cases)
Power law exponent	0.14 (for turbulent wind cases) and 0 (for constant wind cases)
Surface roughness lenght [m]	0.0003

3.2.4 Hydrodynamic Loads

Hydrodynamic loads mainly work on the floating vessel, which uses semi-submersible model to simulate. Incient wave causes hydrodnamic loads according to Jonswap spectrum and the wave period varies from 2s to 15s. In this thesis topic, the simulation doesn't involve swell and current since the motion caused by current and swell can be neglected compared with the motion caused by wave and wind. The wave height is 1 m in regular wave cases. For the irregular wave cases, the wave height varies from 0.5 m to 2 m.

During the installation procedure, the environment includes the irregular wave and turbulent wind. For the irregular wave, there are first order wave force and seconed order wave force. According to the linear potential flow theory, the first order wave force can be expressed using transfer function and wave elevaton. The final equation can be expressed as below:

$$S_{F^1}(\omega) = H^{(1)}(\omega_n)H^{(1)} * (\omega_n)S_\eta(\omega) \tag{3.14}$$

The wave elevation is shown as equation 3.15 and 3.16.

$$F^1(x,y,t) = R\{\sum_{n=1}^{N}\sum_{m=1}^{M}|H(\omega_n,\theta_m)|\sqrt{2S_\eta(\omega_n)D(\theta_m)\Delta\omega\Delta\theta}\exp(i(\omega_n t - k_n x cos(\theta_m) - k_n y sin(\theta_m) + \epsilon_{nm} + \phi_{H^1_{nm}})) \tag{3.15}$$

The second order wave force is shown as equation 3.5.

$$F^2(x,y,t) = R\{\sum_{n=1}^{N}\sum_{m=1}^{M}|H(\omega_n,\theta_m)|\sqrt{2S_\eta(\omega_n)D(\theta_m)\Delta\omega\Delta\theta}\exp(i(\omega_n t - k_n x cos(\theta_m) - k_n y sin(\theta_m) + \epsilon_{nm} + \phi_{H^1_{nm}})) \tag{3.16}$$

The calculation for the first order wave force and second order wave force will be done by SIMA based on the equation mentioned above.

4 Results

4.1 Installation Model System Characteristics

To understand the installation model system characteristics, the constant wind and regular wave are considered with applying external loads to examine the response of the system.

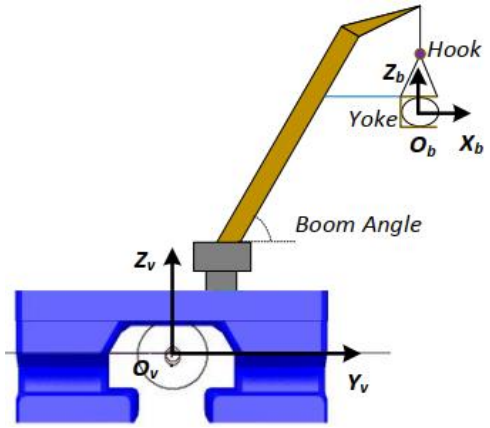

Figure 4. 1: Installation Model

4.1.1 Initial Condition

To check the initial condition, there is no external load applied. The blade position results of the six degrees of freedom of x, y, z, rx, ry, rz are shown in the following table respectively.

Table 4. 1：Blade position without wind and wave condition

	x[m]	y[m]	z[m]	rx [deg]	ry [deg]	rz [deg]
Blade Position	62.064	-66.000	119.35	-4.5200e-07	9.0125	-6.5519e-08

The x, y and z are global position. The rotational angles for x, y, z are represented as rx, ry and rz.

4.1.2 Installation System Behavior in Constant Wind

The constant wind cases require no wave, the wind speeds are 2 m, 5 m and 10 m respectively. Since the blades of the wind turbine are lifted horizontally during the installation of the offshore wind turbine, the wind can blow from any direction at this time. It is necessary to consider different directions of the incoming wind. And the incoming wind speed directions are 0° , 90° , 180° and 270° respectively. The blade position for different constant wind speed cases are shown as below:

Table 4. 2：Blade position for constant wind

Wind speed (m/s)	Wind direction (deg)	x (m)	y(m)	z(m)	rx (deg)	ry (deg)	rz (deg)
2	0	62.07	-66	119.4	-0.002274	9.013	3.71E-04
2	90	62.07	-66	119.4	-0.001711	9.013	2.33E-04
2	180	62.07	-66	119.4	-7.09E-05	9.013	3.11E-04
2	270	62.07	-66	119.4	-0.001711	9.013	2.33E-04
5	0	62.07	-66	119.4	-0.01187	9.011	0.002666
5	90	62.07	-66	119.4	-0.008352	9.011	0.0018
5	180	62.07	-66	119.4	0.001893	9.013	0.002287
5	270	62.07	-66	119.4	-0.008352	9.011	0.0018
10	0	62.07	-66.01	119.4	-0.04616	9.005	0.01086
10	90	62.07	-66.01	119.4	-0.03209	9.007	0.007395
10	180	62.07	-65.99	119.4	0.00877	9.012	0.009324
10	270	62.07	-66.01	119.4	-0.03209	9.007	0.007395

It can be seen from Table 4.2 that even when the wind speed reaches 10m/s, the motion of the blades is extremely small and almost negligible. The blade movement is not significant under different wind speeds and different incoming wind directions.

The floating vessel position for different constant wind speed cases are shown in table 4.3.

Table 4. 3：Floating vessel position for constant wind

Wind speed (m/s)	Wind direction (deg)	x (m)	y(m)	z(m)	rx (deg)	ry (deg)	rz (deg)
2	0	4.71E-05	-9.64E-07	-0.003143	-0.0009042	9.35E-05	9.70E-05
2	90	3.21E-05	-1.21E-06	-0.003144	-0.0009026	9.35E-05	6.61E-05
2	180	1.52E-05	-2.01E-06	-0.003143	-0.0009029	8.40E-05	3.15E-05
2	270	3.21E-05	-1.21E-06	-0.003144	-0.0009026	9.35E-05	2.33E-04
5	0	0.0002959	5.26E-07	-0.003131	-0.0009313	9.42E-05	6.61E-05
5	90	0.0002025	-1.08E-06	-0.003135	-0.0009211	9.40E-05	0.0006062
5	180	9.65E-05	-6.12E-06	-0.003133	-0.0009234	3.44E-05	0.0004133
5	270	0.0002025	-1.08E-06	-0.003135	-0.0009211	9.40E-05	0.0001967
10	0	0.001184	8.04E-06	-0.003088	-0.001028	9.69E-05	0.0004133
10	90	0.0008108	9.01E-07	-0.003106	-0.0009874	9.62E-05	0.001655
10	180	0.0003868	-1.99E-05	-0.003095	-0.0009965	-0.0001414	0.0007878
10	270	0.0008108	9.01E-07	-0.003106	-0.0009874	9.62E-05	0.001655

As shown in Table 4.3, the motion of the floating vessel is extremely small. This is mainly due to the fact that the wave conditions need to be set for the calculation to be normal when the sima is performing the simulation calculation. Here, a wave small enough to be ignored is used for simulation.

4.1.3 Installation System Behavior in Regular Wave

In order to understand the basic influence of waves on the installed system, it is necessary to perform the simulation in the case of regular wave.

The environmental setting for regular wave involves amplitude and period. The period varies from 2 s to 15 s and amplitude is setted as 1 m, the wave elevation result is shown as below:

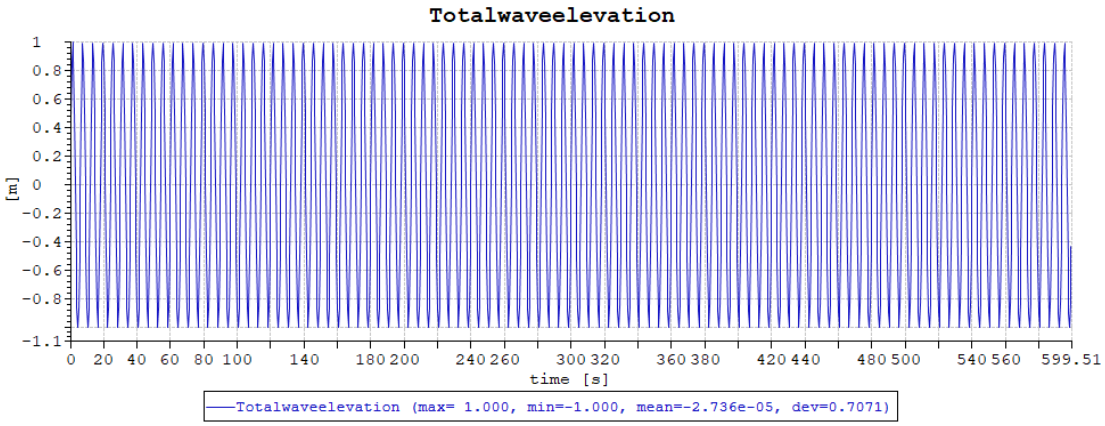

Figure 4. 2：Wave elevation in regular wave

Taking the amplitude of 1 meter and the wave period of 4 seconds as an example, the simulation calculation results of two incident waves in different directions are shown in figure 4.3 and 4.4.

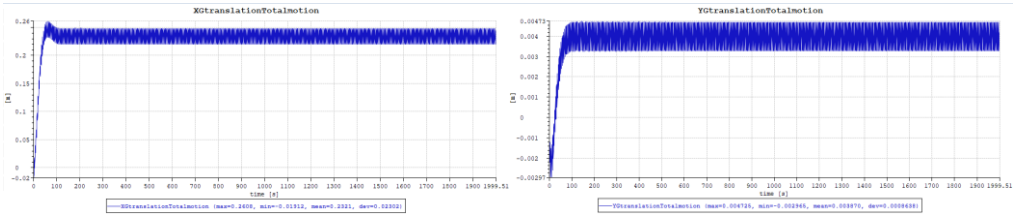

(a)X translation floating vessel motion (b)Y translation floating vessel motion

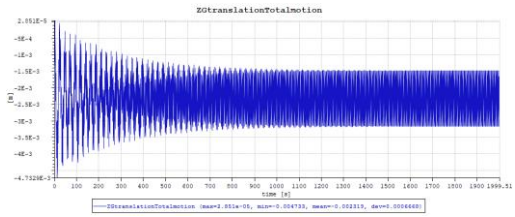

(c)Z translation floating vessel motion

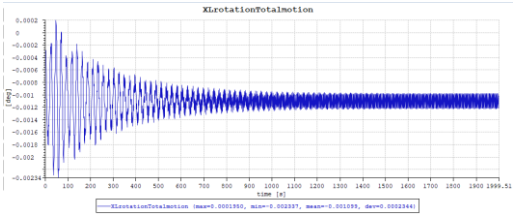

(d)X rotation floating vessel motion

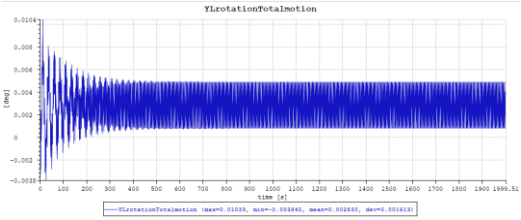

(e)Y rotation floating vessel motion

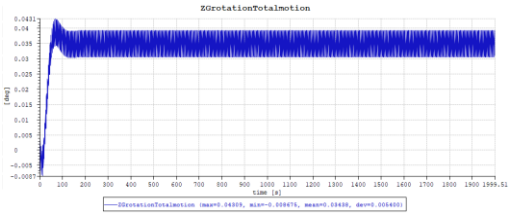

(f)Z rotation floating vessel motion

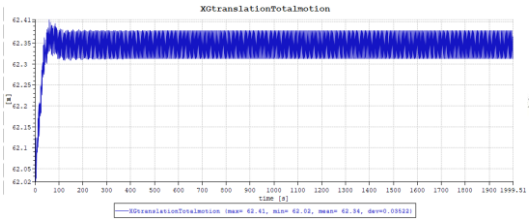

(g) X translation blade motion

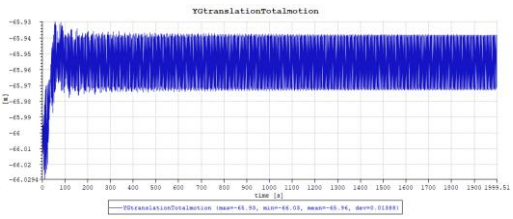

(h) Y translation blade motion

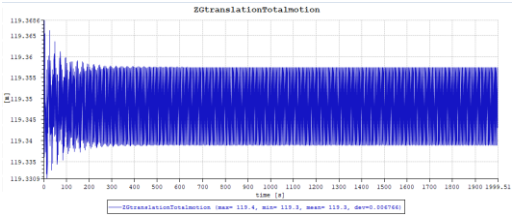

(i) Z translation blade motion

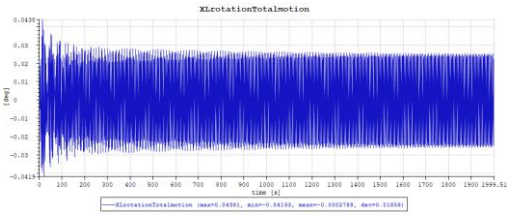

(j) X rotation blade motion

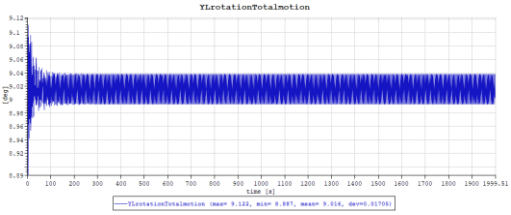

(k) Y rotation blade motion

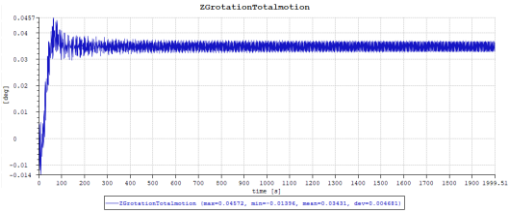

(l) Z rotation blade motion

Figure 4. 3：Installation system motion for incoming wave direction 0°

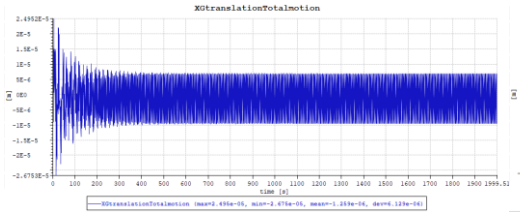

(a)X translation floating vessel motion

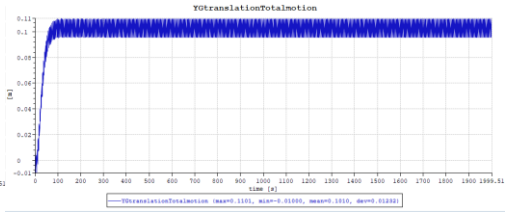

(b)Y translation floating vessel motion

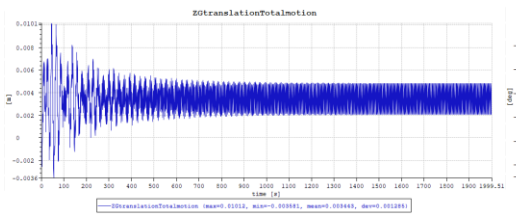

(c)Z translation floating vessel motion

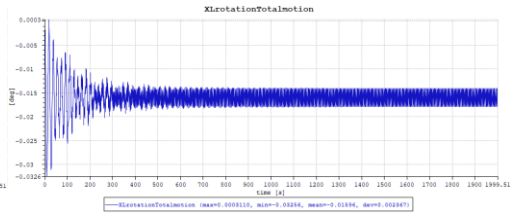

(d)X rotation floating vessel motion

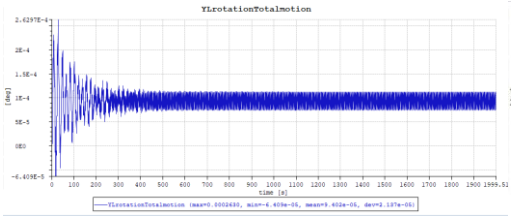

(e)Y rotation floating vessel motion

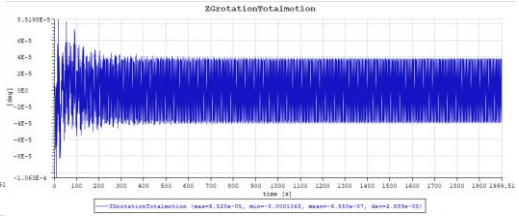

(f)Z rotation floating vessel motion

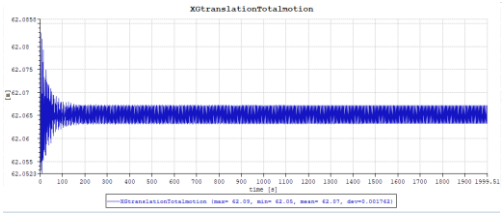

(g) X translation blade motion

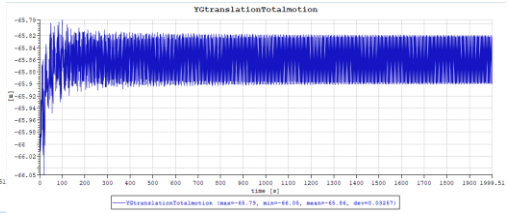

(h) Y translation blade motion

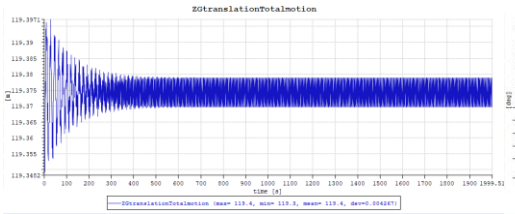

(i) Z translation blade motion

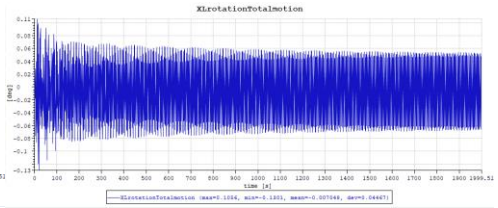

(j) X rotation blade motion

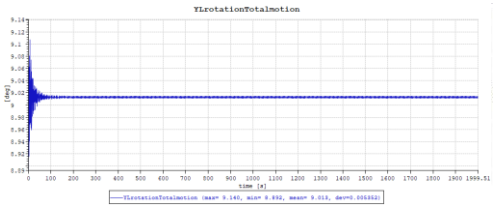

(k) Y rotation blade motion

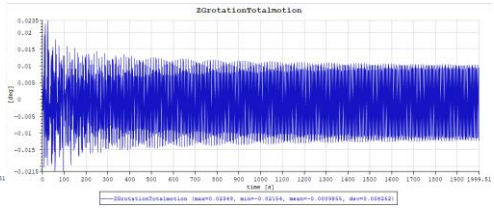

(l) Z rotation blade motion

Figure 4. 4：Installation system motion for incoming wave direction 90°

By comparing Figure 4.3 and Figure 4.4, it can be found that for the simulation of regular waves in different incident directions, the translation results of the floating vessel in the x-axis direction and the y-axis direction are slightly different. Due to the special structure of the floating vessel, when the incident wave enters from the direction along the x-axis, the translational motion in the x-axis direction is much greater than the result when the incident wave enters along the y-axis, but the translational motion in the y-axis direction is larger.

In the case of different incident wave directions, the motion of offshore wind turbine blades does not change much.

The motion of floating vessel for regular wave analysis result is shown as below:

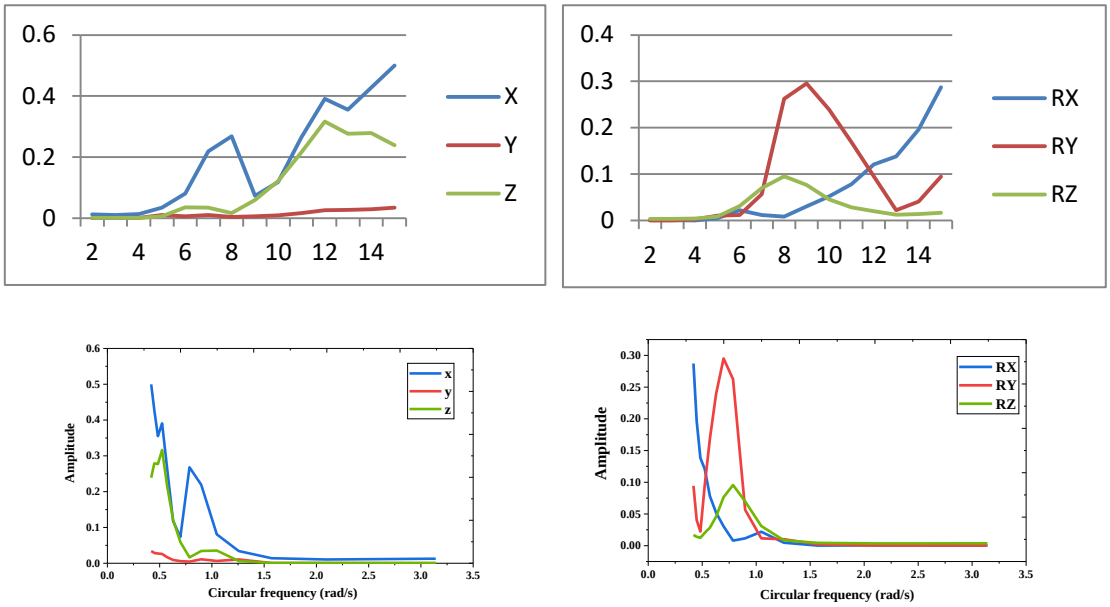

(a) Incident wave amplitude 1m, wave direction 0°

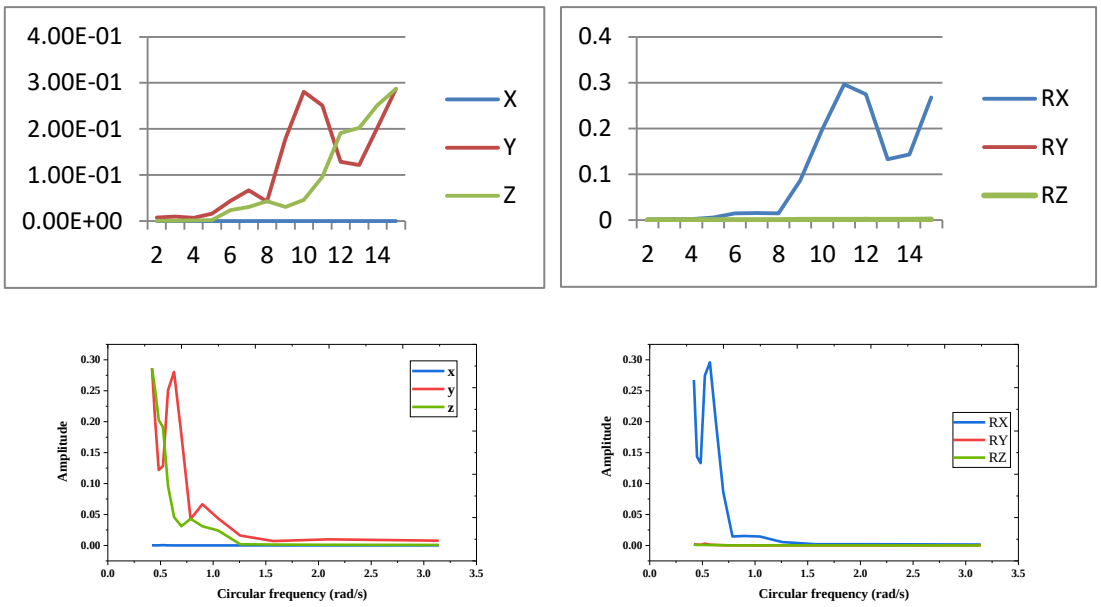

(b) Incident wave amplitude 1m, wave direction 90°

Figure 4. 5：The RAOs of the floating vessel motions for incident wave with amplitude 1 m

According to the figure 4.5, when the incident wave comes from 0 degree, which is x-axial, the dominant motion of the floating vessel is surge, heave, roll and pitch but the motion is very small since the existence of the mooring system in floating vessel. Translations of total motion in x, y and z axis are all smaller than 1 m while the wave amplitude is 1 m, so translation motions are acceptable. The rotation motion is even

smaller than 1 degree so it is acceptable as well. The semi-submersible is used as floating vessel. There is force in positive x-direction on the column which incident wave meets first and there is also reverse force in the negative x-direction on column which the incident wave meets second. These two forces which happen all the time work together to make the semi-submersible has motion. When the wave period is twice than the distance between the two columns in semi-submersible, there will be a minimum force in semi-submersible so that the translation motion will be also small compared with the neighbor wave period. The mooring system can provide damping effect and inertia effect for floating vessels to slow down the movement of the floating structure in the ocean and stabilize the floating structure. When the wave period is 20 s, compared with the wave length, semi-submersible is small so that the x-direction translation motion will be around 1 m as shown in figure 4.6.

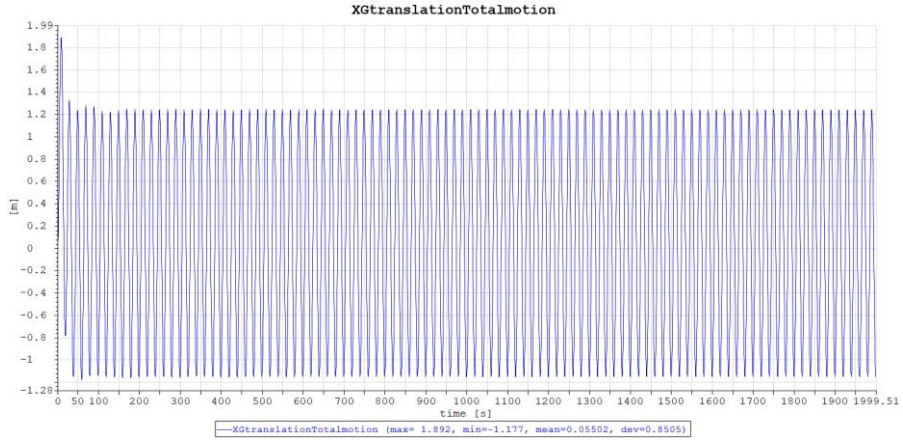

Figure 4. 6：Translation motion in x-direction for wave period 20 s and wave amplitude 1 m

The response of the blade for incident wave with amplitude 1 m is shown in figure 4.7.

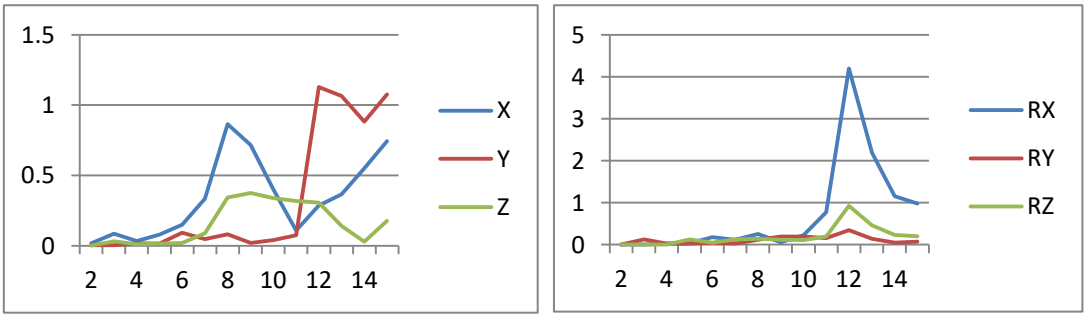

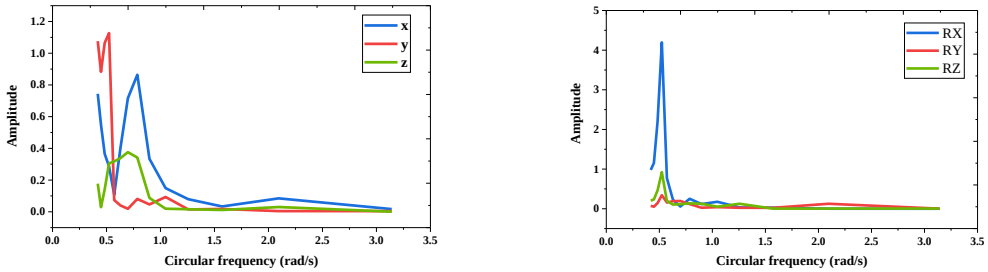

(a) Incident wave amplitude 1m, wave direction 0°

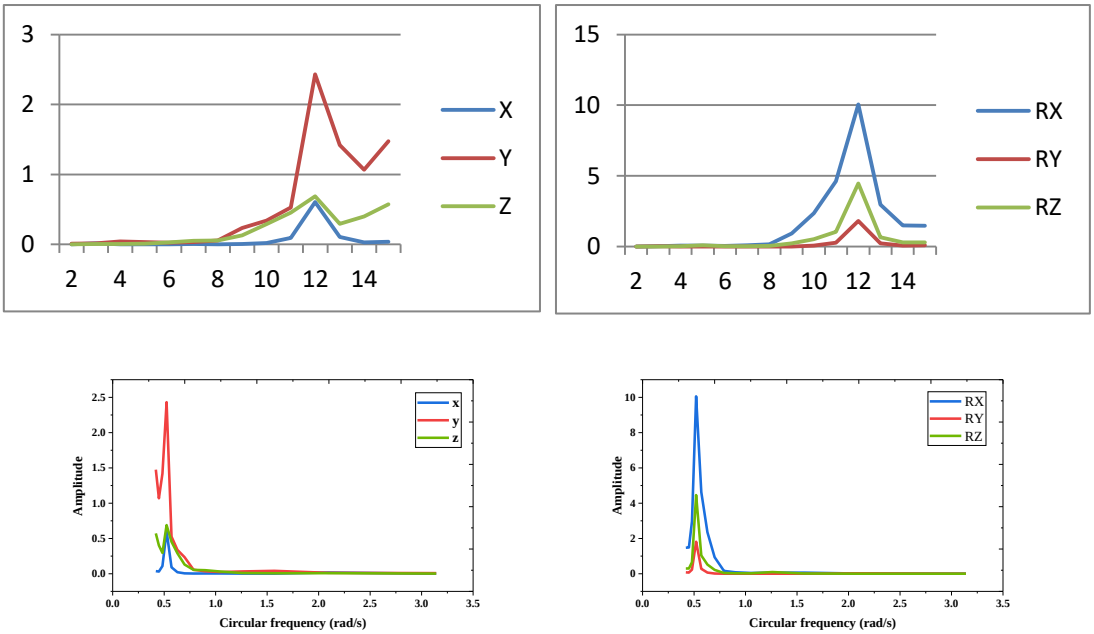

(a) Incident wave amplitude 1m, wave direction 90°

Figure 4. 7：The response of the blade for incident wave with amplitude 1 m

According to the response of the blade for incident wave with amplitude 1 m from figure 4.7, it can be seen that when the incident wave direction is 90 degrees, the natural period is around 12 sec so that the natural frequency is around 0.52 rad/s. While when the incident wave comes from 0 degree, the incident wave is affected by the structure of the floating vessel. Since the semi-submersible vessel uses two pontoons with several columns to provide buoyancy, the direction of the incident wave has a great influence on the movement of the vessel. When the direction of the incoming wave is perpendicular to the placement direction of the pontoon, the incoming wave will affect the force acting on the second pontoon because of the existence of the first pontoon.

The blade motion is larger compared with semi-submersible vessel motion. The load of semi-submersible vessel will be transfer to the blade due to the blade is lifted up by the crane attached on the floating vessel which is semi-submersible vessel.

4.1.4 The Blade Pitch Angle Result

To understand the blade pitch angle, the forces and moments on the blade is shown as below in table 4.4.

Table 4. 4：The force and moments on the blade with different blade pitch angle

Blade pitch angle [deg]	x-direction force [kN]	y-direction force [kN]	z-direction force [kN]	Moment about x-axis [kN -m]	Moment about y-axis [kN -m]	Moment about z-axis [kN -m]
0	1.7	0.0	10.4	62.05	0.0	37.31
30	12.1	0.0	23.3	291.0	0.0	-76.1
45	19.7	0.0	21.9	211.1	0.0	-195.3
60	26.3	0.0	15.4	256.5	0.0	-291.0
9	3.6	0.0	16.0	147.8	0.0	24.5
-9.01	1.3	0.0	4.0	-27.11	0.0	29.1

The translation and rotation motion of the blade is shown in table 4.5.

Table 4. 5：The translation and rotation moment of the blade

Blade pitch angle [deg]	Displacement in x-direction [m]	Displacement in y-direction [m]	Displacement in z-direction [m]	Rotational angle about x-axis [deg]	Rotational angle about y-axis [deg]	Rotational angle about z-axis [deg]
0	62.07	-65.95	119.4	0.1501	9.001	0.04877
30	62.11	-65.8	119.3	0.5781	8.943	0.06539
45	62.06	-65.8	119.3	0.5652	8.899	0.008841
60	62.17	-65.84	119.3	0.3997	8.86	-0.00734
9	62.07	-66.01	119.4	-0.04616	9.005	0.01086
-9.01	62.08	-65.89	119.4	0.3283	8.99	0.07309

According to the table 4.5, all translation motion for different axises are smaller than 1 m and all rotation motion for different axises are smaller than 1 degree. From the table 4.4, it can be seen that the force in the y axis is always 0 N regardless of the blade pitch angle. The displacement of the blade in y axis is small but compared with the displacement in other axis, it is large due to the blade is not limited in the y axis.

There are lift force which is caused by the lift wire connected to the crane and the drag force caused by the incoming wind on the blade as well during the installation process according to the results as shown in table 4.4.

The dynamic calculation is relative to the static calculation, the original position of the dynamic calculation based on the static calculation result. The static calculation result for the translation and rotation position is shown in table 4.6.

Table 4. 6：The translation and rotation position for the static calculation

Blade pitch angle [deg]	Displacement in x-direction [m]	Displacement in y-direction [m]	Displacement in z-direction [m]	Rotational angle about x-axis [deg]	Rotational angle about y-axis [deg]	Rotational angle about z-axis [deg]
All angles	62.064	-66.000	119.35	-4.5200e-07	9.0125	-6.5519e-08

It can be seen from the table 4.6 that the blade rotational angle about y axis is always around 9 degrees no matter how much the blade pitch angle is. Since the initial pitch angle of the blade is determined by the DLL input file, the initial pitch angle can be set directly in the DLL input file, and the angle is not directly transferred to SIMA. SIMA just combines dynamic calculation results to static calculation results. The actual angle of the blade is the sum of the initial blade angle input by the DLL file and the angle change of the dynamic results.

As results showed according to the table 4.4 and 4.5, it is suggested to set the blade pitch angle as around -9 degrees since with small displacement for all cases, forces and moments of the blade with -9 degrees original blade pitch angle is smallest.

4.1.5 The Turbulent Wind and Irregular Wave Result

During the real installation process, the environment includes the turbulent wind and irregular wave. The turbulent wind causes aerodynamic loads on the blade and the effect on the floating vessel is very small. The irregular wave mainly works on the semi-submersible vessel to cause hydrodynamic loads, the crane on the floating vessel will transfer the motion to the blade as well.

Here the individual case for the turbulent wind on the installation model and the individual case for the irregular wave on the installation model are considered.

When there is only turbulent wind without wave, the incoming wind angle for these cases are 0 degree. The blade position result is shown in table 4.7.

Table 4. 7：The blade motions under different turbulent wind cases

(a) Average positions of the blade						
Wind speed [m/s]	Displacement in x-direction [m]	Displacement in y-direction [m]	Displacement in z-direction [m]	Rotational angle about x-axis [deg]	Rotational angle about y-axis [deg]	Rotational angle about z-axis [deg]
5	62.07	-66.00	119.40	-0.0004	9.013	-0.0001
10	62.07	-66.01	119.40	-0.0321	9.002	0.0149

(b) Standard deviation of the position of the blade						
Wind speed [m/s]	Displacement in x-direction [m]	Displacement in y-direction [m]	Displacement in z-direction [m]	Rotational angle about x-axis [deg]	Rotational angle about y-axis [deg]	Rotational angle about z-axis [deg]
5	0.0003	0.0014	0.0003	0.0007	0.0014	0.0001
10	0.0015	0.0248	0.0004	0.0723	0.0031	0.0165

According to the table 4.7, mean positions of the blade in six digree of freedom don't change for different wind speed while the standard deviation of the blade positions is slightly affected by the wind speed.

When there is only irregular wave with wave period 9 s without wind. The blade postion result is shown in table 4.8

Table 4. 8：The blade motion under irregular wave cases with different significant wave height

(a) Mean positions of the blade						
Significant wave height [m]	Displacement in x-direction [m]	Displacement in y-direction [m]	Displacement in z-direction [m]	Rotational angle about x-axis [deg]	Rotational angle about y-axis [deg]	Rotational angle about z-axis [deg]
1	62.11	-65.99	119.30	0.00	9.017	0.00
2	62.24	-65.97	119.30	0.00	9.032	0.03
4	62.73	-65.88	119.30	0.00	9.110	0.12

(b) Standard deviation of the position of the blade						
Significant wave height [m]	Displacement in x-direction [m]	Displacement in y-direction [m]	Displacement in z-direction [m]	Rotational angle about x-axis [deg]	Rotational angle about y-axis [deg]	Rotational angle about z-axis [deg]
1	0.17	0.10	0.08	0.27	0.04	0.06
2	0.35	0.21	0.16	0.58	0.09	0.13
4	0.79	0.58	0.34	1.46	0.21	0.33

Table 4. 9：The floating vessel motion under irregular wave cases with different significant wave height

(a) Mean positions of the floating vessel						
Significant wave height [m]	Displacement in x-direction [m]	Displacement in y-direction [m]	Displacement in z-direction [m]	Rotational angle about x-axis [deg]	Rotational angle about y-axis [deg]	Rotational angle about z-axis [deg]
1	0.03	0.0	0.0	0.0	0.0	0.01
2	0.11	0.0	0.01	0.0	0.01	0.03
4	0.44	0.0	0.05	0.01	0.05	0.13

(b) Standard deviation of the position of the floating vessel						
Significant wave height [m]	Displacement in x-direction [m]	Displacement in y-direction [m]	Displacement in z-direction [m]	Rotational angle about x-axis [deg]	Rotational angle about y-axis [deg]	Rotational angle about z-axis [deg]
1	0.05	0.0	0.02	0.01	0.06	0.02
2	0.11	0.01	0.05	0.03	0.12	0.05
4	0.32	0.01	0.16	0.10	0.28	0.11

The result in table 4.9 shows that the displacement in the floating vessel is very small, it can be neglected compared with the structure scale. According to the table 4.8, the blade motion will vary with the changing of the irregular wave. With the significant wave height increasing, the mean blade position increases, the deviation fo the blade position increases as well. The main reason for this phenomenon is the use of floating vessel during the installation process. In the process of offshore operations, in order to ensure that the position of the vessel does not move, and to avoid large deviations due to the displacement of the vessel during installation, a mooring system is used. Compared with jack-up vessel, the mooring system can only provide a certain amount of damping to reduce the displacement when the movement is small, so as to reduce the influence of the wave to a certain extent, but it cannot completely avoid the influence of the wave. The legs of a jack-up vessel can sit directly on the seabed and lift the jack-up vessel away from the sea surface, thereby avoiding the influence of waves.

Under the irregular wave cases with different wave peak periods and same significant wave height as 1 m and there is no wind. The result is shown in table 4.10.

Table 4. 10：The blade motion under irregular wave cases with different wave peak period

(a) Mean positions of the blade						
Wave peak periods [sec]	Displacement in x-direction [m]	Displacement in y-direction [m]	Displacement in z-direction [m]	Rotational angle about x-axis [deg]	Rotational angle about y-axis [deg]	Rotational angle about z-axis [deg]
4	62.09	-65.99	119.30	0.00	9.01	0.00
5	62.10	-66.00	119.30	0.00	9.01	0.00
6	62.10	-65.99	119.30	0.00	9.01	0.00
7	62.10	-65.99	119.30	0.00	9.02	0.01
8	62.10	-65.99	119.30	0.00	9.02	0.01
9	62.11	-65.99	119.30	0.00	9.02	0.01
10	62.11	-65.99	119.40	0.00	9.03	0.01
11	62.11	-65.99	119.40	0.00	9.03	0.01
12	62.09	-65.99	119.40	0.00	9.06	0.01

(b) Deviation of the position of the blade						
Wave peak periods [sec]	Displacement in x-direction [m]	Displacement in y-direction [m]	Displacement in z-direction [m]	Rotational angle about x-axis [deg]	Rotational angle about y-axis [deg]	Rotational angle about z-axis [deg]
4	0.02	0.00	0.00	0.01	0.02	0.01
5	0.03	0.01	0.00	0.01	0.03	0.01
6	0.06	0.02	0.02	0.03	0.01	0.03
7	0.10	0.02	0.04	0.03	0.02	0.03
8	0.15	0.06	0.06	0.18	0.03	0.05
9	0.16	0.09	0.08	0.26	0.04	0.06
10	0.14	0.24	0.08	0.68	0.04	0.14
11	0.13	0.29	0.08	0.79	0.04	0.16
12	0.14	0.52	0.09	1.42	0.07	0.29

Table 4. 11：The floating vessel motion under irregular wave cases with different wave peak period

(a) Mean positions of the floating vessel						
Wave peak periods [sec]	Displacement in x-direction [m]	Displacement in y-direction [m]	Displacement in z-direction [m]	Rotational angle about x-axis [deg]	Rotational angle about y-axis [deg]	Rotational angle about z-axis [deg]
4	0.02	0.00	0.00	0.00	0.00	0.00
5	0.03	0.00	0.00	0.00	0.00	0.00
6	0.03	0.00	0.00	0.00	0.00	0.00
7	0.03	0.00	0.00	0.00	0.00	0.01
8	0.02	0.00	0.00	0.00	0.00	0.01

9	0.03	0.00	0.00	0.00	0.00	0.01
10	0.04	0.00	0.00	0.00	0.00	0.01
11	0.04	0.00	0.00	0.00	0.00	0.01
12	0.04	0.00	0.00	0.00	0.00	0.01

(b) Standard deviation of the position of the floating vessel						
Wave peak periods [sec]	Displacement in x-direction [m]	Displacement in y-direction [m]	Displacement in z-direction [m]	Rotational angle about x-axis [deg]	Rotational angle about y-axis [deg]	Rotational angle about z-axis [deg]
4	0.01	0.00	0.00	0.00	0.00	0.00
5	0.02	0.00	0.00	0.00	0.00	0.00
6	0.04	0.00	0.01	0.00	0.01	0.01
7	0.05	0.00	0.01	0.01	0.03	0.02
8	0.06	0.00	0.01	0.01	0.05	0.02
9	0.05	0.00	0.02	0.01	0.06	0.02
10	0.05	0.00	0.03	0.02	0.06	0.02
11	0.07	0.00	0.05	0.03	0.05	0.01
12	0.09	0.00	0.06	0.06	0.04	0.01

According to the table 4.10 and table 4.11, the floating vessel motion and blade motion are very small, which are not affected by the different wave peak period significantly. The deviation of the balde and the floating vessel motion is also small.

Based on the results of separate analysis for turbulent wind and irregular wave, the turbulent wind and irregular wave are combined for a comprehensive analysis to obtain more realistic calculation results about model for offshore wind turbine blade installation.

The setting about the environmental condition parameters for the turbulent wind and irregular wave is listed in the table 4.12.

Table 4. 12：The environmental parameter setting

Wave height (m)	Wave period (s)	Wind speed (m/s)
0.5	5, 7, 9, 11	5
1.0	5, 7, 9, 11	5, 10
2.0	5, 7, 9, 11	10

For the conbination of the turbulent wind and irregular wave, the incident wave direction is 0 degree, which is along x axis. The wave spectrum used for these cases is JONSWAP. The turbulence model is KAIMAL and the trbulent intensity is 15% with power law exponent as 0.14.

The blade motion result of the combination cases for turbulent wind and irregular wave is shown in table 4.13

Table 4. 13：The blade motion caused by the combination of turbulent wind and irregular wave

Environment setting	Mean displacement in x axis (m)	Mean displacement in y axis (m)	Mean displacement in z axis (m)	Mean rotation angle in x axis (deg)	Mean rotation angle in y axis (deg)	Mean rotation angle in z axis (deg)
Hs 0.5 m Tp 5 s Uw 5 m/s	62.07	-65.82	119.4	0.58	9.016	0.08
Hs 0.5 m Tp 7 s Uw 5 m/s	62.07	-65.82	119.4	0.58	9.016	0.08
Hs 0.5 m Tp 9 s Uw 5 m/s	62.07	-65.81	119.4	0.58	9.017	0.08
Hs 0.5 m Tp 11 s Uw 5 m/s	62.08	-65.82	119.4	0.58	9.017	0.08
Hs 1 m Tp 5 s Uw 5 m/s	62.09	-65.82	119.4	0.58	9.017	0.08
Hs 1 m Tp 7 s Uw 5 m/s	62.10	-65.81	119.4	0.58	9.018	0.08
Hs 1 m Tp 9 s Uw 5 m/s	62.11	-65.81	119.4	0.58	9.019	0.09
Hs 1 m Tp 11 s Uw 5 m/s	62.12	-65.81	119.4	0.58	9.019	0.08
Hs 1 m Tp 5 s Uw 10 m/s	62.05	-65.33	119.4	2.16	9.090	0.29
Hs 1 m Tp 7 s Uw 10 m/s	62.06	-65.32	119.4	2.17	9.091	0.30
Hs 1 m Tp 9 s Uw 10 m/s	62.07	-65.32	119.4	2.16	9.093	0.30
Hs 1 m	62.08	-65.32	119.4	2.164	9.092	0.30

Tp 11 s Uw 10 m/s						
Hs 2 m Tp 5 s Uw 10 m/s	62.14	-65.32	119.4	2.165	9.093	0.30
Hs 2 m Tp 7 s Uw 10 m/s	62.16	-65.30	119.4	2.167	9.097	0.32
Hs 2 m Tp 9 s Uw 10 m/s	62.20	-65.30	119.4	2.166	9.105	0.33
Hs 2 m Tp 11 s Uw 10 m/s	62.23	-65.30	119.4	2.165	9.103	0.32

(a) The mean displacement and rotation angle for combination cases

Environment setting	Deviation of displacement in x axis (m)	Deviation of displacement in y axis (m)	Deviation of displacement in z axis (m)	Deviation of rotation angle in x axis (deg)	Deviation of rotation angle in y axis (deg)	Deviation of rotation angle in z axis (deg)
Hs 0.5 m Tp 5 s Uw 5 m/s	0.01	0.04	0.00	0.12	0.01	0.02
Hs 0.5 m Tp 7 s Uw 5 m/s	0.05	0.04	0.02	0.13	0.03	0.02
Hs 0.5 m Tp 9 s Uw 5 m/s	0.08	0.04	0.04	0.13	0.05	0.2
Hs 0.5 m Tp 11 s Uw 5 m/s	0.06	0.06	0.04	0.14	0.05	0.02
Hs 1 m Tp 5 s Uw 5 m/s	0.03	0.04	0.01	0.12	0.02	0.03
Hs 1 m Tp 7 s Uw 5 m/s	0.10	0.04	0.04	0.13	0.06	0.03
Hs 1 m Tp 9 s Uw 5 m/s	0.16	0.05	0.08	0.14	0.11	0.03
Hs 1 m Tp 11 s Uw 5 m/s	0.12	0.10	0.07	0.17	0.09	0.03

Hs 1 m Tp 5 s Uw 10 m/s	0.03	0.15	0.01	0.46	0.04	0.08
Hs 1 m Tp 7 s Uw 10 m/s	0.10	0.15	0.04	0.47	0.07	0.08
Hs 1 m Tp 9 s Uw 10 m/s	0.16	0.15	0.08	0.47	0.11	0.08
Hs 1 m Tp 11 s Uw 10 m/s	0.12	0.17	0.07	0.47	0.10	0.08
Hs 2 m Tp 5 s Uw 10 m/s	0.08	0.15	0.02	0.46	0.05	0.08
Hs 2 m Tp 7 s Uw 10 m/s	0.23	0.16	0.08	0.47	0.14	0.10
Hs 2 m Tp 9 s Uw 10 m/s	0.33	0.17	0.15	0.49	0.22	0.09
Hs 2 m Tp 11 s Uw 10 m/s	0.26	0.24	0.15	0.50	0.19	0.09

(b) The standard deviation of displacement and rotation angle for combination cases

According to the table 4.13 (a) and (b), it can be seen that the blade mean position is affected by the wind and wave at the same time. Though wind speed becomes larger, the motion of displacement in x become smaller, while the mean position of y is larger, the rotation of the blade of x, y and z become larger as well. The variation of x axis displacement is slightly affected by the wave with different peak period and significant wave height. The wave with different significant wave height and peak period also affects the y rotation of the blade. The displacement in z axis of the blade is not affected by neither wind speed nor wave. The deviation of displacement in y axis and deviation of rotation in x axis are affected by wind speed. When the peak period of wave changes, the deviation of x axis changes, especially when the peak period reaches at 9 s, the deviation has highest value. The other deviation of motions for six degree of freedom are slightly affected by the wave as well. On consider the x displacement is not changed with different wind speed, when the wind speed increases, the change in the position of the blades becomes slightly smaller, which may be affected by the change in the position of the floating vessel.

The motion of the floating vessel is shown in table 4.14 which is shown as below:

Table 4. 14: The floating vessel motion caused by the combination of turbulent wind and irregular wave

Environment setting	Mean displacement in x axis (m)	Mean displacement in y axis (m)	Mean displacement in z axis (m)	Mean rotation angle in x axis (deg)	Mean rotation angle in y axis (deg)	Mean rotation angle in z axis (deg)
Hs 0.5 m Tp 5 s Uw 5 m/s	0.01	0.00	0.00	0.00	0.00	0.00
Hs 0.5 m Tp 7 s Uw 5 m/s	0.00	0.00	0.00	0.00	0.00	0.00
Hs 0.5 m Tp 9 s Uw 5 m/s	0.01	0.00	0.00	0.00	0.00	0.00
Hs 0.5 m Tp 11 s Uw 5 m/s	0.01	0.00	0.00	0.00	0.00	0.00
Hs 1 m Tp 5 s Uw 5 m/s	0.03	0.00	0.00	0.00	0.00	0.00
Hs 1 m Tp 7 s Uw 5 m/s	0.02	0.00	0.00	0.00	0.00	0.01
Hs 1 m Tp 9 s Uw 5 m/s	0.03	0.00	0.00	0.00	0.00	0.01
Hs 1 m Tp 11 s Uw 5 m/s	0.04	0.00	0.00	0.00	0.00	0.01
Hs 1 m Tp 5 s Uw 10 m/s	0.03	0.00	0.00	0.00	0.00	0.00
Hs 1 m Tp 7 s Uw 10 m/s	0.02	0.00	0.00	0.00	0.00	0.01
Hs 1 m Tp 9 s Uw 10 m/s	0.03	0.00	0.00	0.00	0.00	0.01
Hs 1 m Tp 11 s Uw 10 m/s	0.04	0.00	0.00	0.00	0.00	0.01

Hs 2 m Tp 5 s Uw 10 m/s	0.11	0.00	0.00	0.00	0.00	0.00
Hs 2 m Tp 7 s Uw 10 m/s	0.10	0.00	0.01	0.00	0.01	0.02
Hs 2 m Tp 9 s Uw 10 m/s	0.11	0.00	0.01	0.00	0.01	0.03
Hs 2 m Tp 11 s Uw 10 m/s	0.15	0.00	0.01	0.00	0.01	0.03

(a) The mean displacement and rotation angle for combination cases

Environment setting	Deviation of displacement in x axis (m)	Deviation of displacement in y axis (m)	Deviation of displacement in z axis (m)	Deviation of rotation angle in x axis (deg)	Deviation of rotation angle in y axis (deg)	Deviation of rotation angle in z axis (deg)
Hs 0.5 m Tp 5 s Uw 5 m/s	0.01	0.00	0.00	0.00	0.00	0.00
Hs 0.5 m Tp 7 s Uw 5 m/s	0.03	0.00	0.00	0.00	0.01	0.01
Hs 0.5 m Tp 9 s Uw 5 m/s	0.02	0.00	0.01	0.00	0.03	0.01
Hs 0.5 m Tp 11 s Uw 5 m/s	0.03	0.00	0.02	0.01	0.02	0.01
Hs 1 m Tp 5 s Uw 5 m/s	0.02	0.00	0.00	0.00	0.00	0.00
Hs 1 m Tp 7 s Uw 5 m/s	0.06	0.00	0.01	0.01	0.03	0.02
Hs 1 m Tp 9 s Uw 5 m/s	0.05	0.00	0.02	0.01	0.06	0.02
Hs 1 m Tp 11 s Uw 5 m/s	0.07	0.00	0.05	0.03	0.05	0.01
Hs 1 m Tp 5 s Uw 10 m/s	0.02	0.00	0.00	0.00	0.00	0.00

Hs 1 m Tp 7 s Uw 10 m/s	0.06	0.00	0.01	0.01	0.03	0.02
Hs 1 m Tp 9 s Uw 10 m/s	0.05	0.00	0.02	0.01	0.06	0.02
Hs 1 m Tp 11 s Uw 10 m/s	0.07	0.01	0.05	0.03	0.05	0.01
Hs 2 m Tp 5 s Uw 10 m/s	0.06	0.01	0.01	001	0.01	0.01
Hs 2 m Tp 7 s Uw 10 m/s	0.13	0.01	0.03	0.02	0.06	0.04
Hs 2 m Tp 9 s Uw 10 m/s	0.11	0.01	0.05	0.03	0.12	0.05
Hs 2 m Tp 11 s Uw 10 m/s	0.15	0.01	0.10	0.07	0.10	0.03

(b) The standard deviation of displacement and rotation angle for combination cases

It can be seen there is almost no motion and deviation in other degrees of freedom for the floating vessel except in x axis. For the motion in a axis, it is dominated by different waves with significant wave height and wave peak period.

The wave force mainly acts on the floating vessel, which will cause displacement movement in x, y and z aixs. Due to the presence of the crane which is regarded as a rigid bod on floating vessel, part of the wave force given to the floating vessel by the incident wave is transmitted to the blade through the crane on the deck and the lift wire connected to the blade on the crane, causing the blade has motion as well. In a turbulent wind field, the blade is subjected to a certain wave force at the same time as the aerodynamic force given by the wind, which mainly causes the blade to rotate and insignificant translation motion. The lift wire and tugger line used to connect the crane and the blade and lift the blade can limit the displacement of the blade in the x-direction and z-direction to a certain extent.

Taking into account the above-mentioned influencing factors, during the installation of the offshore wind turbine blades, due to the extremely small displacement of the floating vessel used, the influence of wave forces and wind forces need to be considered carefully.

4.2 Spectral Density

Under the irregular wave with significant wave height is 2 m, wave peak period is 9 s and 10 m/s turbulent wind, the motion result for combination cases with different wave seed and wind seed is shown in table 4.15.

Table 4. 15：The blade motion for different wave and wind seeds cases

Wave seed and wind seed	Mean displacement in x axis (m)	Mean displacement in y axis (m)	Mean displacement in z axis (m)	Mean rotation angle in x axis (deg)	Mean rotation angle in y axis (deg)	Mean rotation angle in z axis (deg)
Wind seed:1380469326 Wave seed:100	62.34	-65.26	119.36	2.21	9.12	0.35
Wind seed:744903028 Wave seed:101	62.11	-65.01	119.4	3.13	9.18	0.46
Wind seed:-1931013759 Wave seed:102	62.31	-65.35	119.36	1.99	9.09	0.31
Wind seed:-1801367361 Wave seed:103	62.15	-65.00	119.39	3.17	9.20	0.47
Wind seed:1711922163 Wave seed:104	62.30	-65.25	119.37	2.33	9.12	0.37
Wind seed:-1659124769 Wave seed:200	62.20	-65.12	119.38	2.71	9.14	0.41
Wind seed:-1261119636 Wave seed:201	62.17	-65.29	119.37	2.20	9.10	0.33
Wind seed:1899248659 Wave seed:202	62.24	-65.32	119.37	2.38	9.12	0.37
Wind seed:1899248659 Wave seed:203	62.24	-65.41	119.37	2.12	9.10	0.32
Wind seed:1089447476	62.19	-65.26	119.36	1.81	9.07	0.27

Wave seed:204						
Wind seed:-139118402 Wave seed:300	62.24	-65.39	119.37	1.84	9.08	0.28
Wind seed:-77431392 Wave seed:301	62.15	-65.18	119.37	2.56	9.13	0.38
Wind seed:-1035971066 Wave seed:302	62.11	-65.30	119.38	2.20	9.10	0.31
Wind seed:590771239 Wave seed:303	62.28	-65.19	119.37	2.49	9.13	0.38
Wind seed:132450265 Wave seed:304	62.24	-65.34	119.37	2.04	9.10	0.31
Wind seed:-1220293325 Wave seed:400	62.23	-65.22	119.37	2.43	9.12	0.36
Wind seed:-132430614 Wave seed:401	62.22	-65.28	119.37	2.22	9.11	0.33
Wind seed:-963395014 Wave seed:402	62.21	-65.32	119.36	2.08	9.10	0.31
Wind seed:-104419964 Wave seed:403	62.20	-65.38	119.37	1.93	9.08	0.30
Wind seed:2088778182 Wave seed:404	62.13	-65.23	119.38	2.36	9.11	0.35

(a) The mean displacement and rotation angle for different wave and wind seeds cases

Wave seed and wind seed	Mean displacement in x axis (m)	Mean displacement in y axis (m)	Mean displacement in z axis (m)	Mean rotation angle in x axis (deg)	Mean rotation angle in y axis (deg)	Mean rotation angle in z axis (deg)
Wind seed:1380469326 Wave seed:100	0.39	0.19	0.19	0.48	0.11	0.11
Wind seed:744903028 Wave seed:101	0.18	0.19	0.09	0.59	0.08	0.10

Wind seed:-1931013759 Wave seed:102	0.27	0.13	0.13	0.27	0.08	0.08
Wind seed:-1801367361 Wave seed:103	0.40	0.15	0.18	0.45	0.11	0.10
Wind seed:1711922163 Wave seed:104	0.27	0.26	0.14	0.40	0.09	0.09
Wind seed:-1659124769 Wave seed:200	0.22	0.16	0.11	0.50	0.08	0.08
Wind seed:-1261119636 Wave seed:201	0.27	0.15	0.12	0.43	0.07	0.09
Wind seed:1899248659 Wave seed:202	0.39	0.18	0.18	0.49	0.11	0.11
Wind seed:1899248659 Wave seed:203	0.25	0.22	0.13	0.60	0.08	0.11
Wind seed:1089447476 Wave seed:204	0.21	0.15	0.11	0.40	0.06	0.08
Wind seed:-139118402 Wave seed:300	0.33	0.15	0.15	0.33	0.08	0.09
Wind seed:-77431392 Wave seed:301	0.27	0.12	0.12	0.36	0.08	0.08
Wind seed:-1035971066 Wave seed:302	0.16	0.23	0.08	0.67	0.07	0.12
Wind seed:590771239 Wave seed:303	0.32	0.15	0.18	0.43	0.11	0.09
Wind seed:132450265 Wave seed:304	0.24	0.20	0.13	0.48	0.08	0.10
Wind seed:-1220293325 Wave seed:400	0.24	0.13	0.13	0.33	0.09	0.08
Wind seed:-132430614	0.34	0.16	0.16	0..48	0.09	0.11

Wave seed:401						
Wind seed:-963395014 Wave seed:402	0.33	0.14	0.16	0.33	0.08	0.08
Wind seed:-104419964 Wave seed:403	0.23	0.15	0.13	0.33	0.08	0.07
Wind seed:2088778182 Wave seed:404	0.19	0.22	0.09	0.57	0.06	0.09

(b) The standard deviation of displacement and rotation angle for different wave and wind seeds cases

The floating vessel motion result for combination cases is shown in table 4.16.

Table 4. 16：The floating vessel motion for different wave and wind seeds cases

Wave seed and wind seed	Mean displacement in x axis (m)	Mean displacement in y axis (m)	Mean displacement in z axis (m)	Mean rotation angle in x axis (deg)	Mean rotation angle in y axis (deg)	Mean rotation angle in z axis (deg)
Wind seed:1380469326 Wave seed:100	0.13	0.00	0.01	0.00	0.01	0.03
Wind seed:744903028 Wave seed:101	0.11	0.00	0.01	0.00	0.01	0.03
Wind seed:-1931013759 Wave seed:102	0.12	0.00	0.01	0.00	0.01	0.04
Wind seed:-1801367361 Wave seed:103	0.15	0.00	0.01	0.00	0.02	0.03
Wind seed:1711922163 Wave seed:104	0.13	0.00	0.01	0.00	0.01	0.03
Wind seed:-1659124769 Wave seed:200	0.15	0.00	0.01	0.00	0.01	0.04
Wind seed:-1261119636 Wave seed:201	0.11	0.00	0.01	0.00	0.01	0.02
Wind	0.11	0.00	0.01	0.00	0.01	0.03

seed:1899248659 Wave seed:202						
Wind seed:1899248659 Wave seed:203	0.15	0.00	0.01	0.00	0.01	0.03
Wind seed:1089447476 Wave seed:204	0.09	0..00	0.01	0.00	0.01	0.02
Wind seed:-139118402 Wave seed:300	0.15	0.00	0.01	0.00	0.02	0.03
Wind seed:-77431392 Wave seed:301	0.14	0.00	0.01	0.00	0.01	0.02
Wind seed:-1035971066 Wave seed:302	0.11	0.00	0.01	0.00	0.01	0.03
Wind seed:590771239 Wave seed:303	0.11	0.00	0.01	0.00	0.01	0.02
Wind seed:132450265 Wave seed:304	0.15	0.00	0.01	0.00	0.01	0.02
Wind seed:-1220293325 Wave seed:400	0.17	0.00	0.01	0.00	0.02	0.03
Wind seed:-132430614 Wave seed:401	0.13	0.00	0.01	0.00	0.01	0.03
Wind seed:-963395014 Wave seed:402	0.11	0.00	0.01	0.00	0.01	0.02
Wind seed:-104419964 Wave seed:403	0.14	0.00	0.01	0.00	0.02	0.04
Wind seed:2088778182 Wave seed:404	0.10	0.00	0.01	0.00	0.01	0.04

(a) The mean displacement and rotation angle for different wave and wind seeds cases

Wave seed and wind seed	Mean displacement in x axis (m)	Mean displacement in y axis (m)	Mean displacement in z axis (m)	Mean rotation angle in x axis (deg)	Mean rotation angle in y axis (deg)	Mean rotation angle in z axis (deg)

Wind seed:1380469326 Wave seed:100	0.10	0.01	0.05	0.03	0.12	0.05
Wind seed:744903028 Wave seed:101	0.11	0.01	0.05	0.03	0.11	0.05
Wind seed:-1931013759 Wave seed:102	0.10	0.00	0.06	0.04	0.11	0.05
Wind seed:-1801367361 Wave seed:103	0.11	0.01	0.05	0.03	0.13	0.04
Wind seed:1711922163 Wave seed:104	0.13	0.01	0.07	0.05	0.11	0.04
Wind seed:-1659124769 Wave seed:200	0.11	0.01	0.06	0.04	0.11	0.04
Wind seed:-1261119636 Wave seed:201	0.10	0.01	0.05	0.03	0.11	0.04
Wind seed:1899248659 Wave seed:202	0.10	0.01	0.05	0.03	0.10	0.03
Wind seed:1899248659 Wave seed:203	0.15	0.01	0.05	0.03	0.11	0.04
Wind seed:1089447476 Wave seed:204	0.11	0.01	0.05	0.03	0.10	0.03
Wind seed:-139118402 Wave seed:300	0.12	0.01	0.06	0.04	0.13	0.04
Wind seed:-77431392 Wave seed:301	0.11	0.01	0.06	0.03	0.11	0.04
Wind seed:-1035971066 Wave seed:302	0.11	0.01	0.05	0.03	0.10	0.03
Wind seed:590771239 Wave seed:303	0.09	0.00	0.05	0.03	0.10	0.03
Wind seed:132450265	0.13	0.01	0.07	0.04	0.12	0.06

Wave seed:304						
Wind seed:-1220293325 Wave seed:400	0.14	0.01	0.06	0.04	0.14	0.06
Wind seed:-132430614 Wave seed:401	0.11	0.01	0.05	0.03	0.11	0.04
Wind seed:-963395014 Wave seed:402	0.11	0.01	0.07	0.04	0.10	0.03
Wind seed:-104419964 Wave seed:403	0.12	0.01	0.06	0.04	0.12	0.04
Wind seed:2088778182 Wave seed:404	0.18	0.01	0.07	0.04	0.15	0.07

(b) The standard deviation of displacement and rotation angle for different wave and wind seeds cases

Based on the result of combination cases, the spectral density analysis is done and the peak value is shown in table 4.17.

Table 4. 17：The spectral density analysis results of different wind seeds and wave seeds when installing offshore wind turbine blades with floating vessel

Wave seed and wind seed	X translation	Y translation	Z translation	X rotation	Y rotation	Z rotation	Wave elevation	Lift wire
Wind seed:1380469326 Wave seed:100	0.71	0	0.69	0	0.69	0.74	0.69	0
Wind seed:744903028 Wave seed:101	0.71	0	0.69	0	0.66	0	0.69	0
Wind seed:-1931013759 Wave seed:102	0.74	0.18, 0.27	0.71	0	0.69	0.74, 1.2	0.74	0
Wind seed:-1801367361 Wave seed:103	0.74	0	0.71	0	0.25, 0.69	0.76	0.74	0
Wind seed:1711922163 Wave seed:104	0.74	0.27	0.69	0	0.66	0	0.79	0
Wind seed:-1659124769 Wave seed:200	0.031, 0.25, 0.76	0	0.25, 0.64, 0.75	0	0.25, 0.64, 0.75	0.79	0.64, 0.75, 0.88, 1	0

Wind seed:-1261119636 Wave seed:201	0.76	0	0.74	0	0.26, 0.69	0.79	0.69, 0.78, 0.98	0
Wind seed:1899248659 Wave seed:202	0.74	0.28	0.71	0	0.69	0.79	0.74	0
Wind seed:1899248659 Wave seed:203	0.74	0	0.69	0	0.69	0.83	0.79	0
Wind seed:1089447476 Wave seed:204	0.26, 0.77	0	0.27, 0.72	0	0.25, 0.71	0.79	0.79, 0.97	0
Wind seed:-139118402 Wave seed:300	0.71	0	0.69	0	0.69	0.76	0.69	0
Wind seed:-77431392 Wave seed:301	0.74	0	0.69	0	0.25, 0.69	0.79	0.74	0
Wind seed:-1035971066 Wave seed:302	0.7	0	0.68, 0.79	0	0.66	0.81	0.68, 0.81, 1	0
Wind seed:590771239 Wave seed:303	0.74	0	0.71	0	0.69	0.76	0.74	0
Wind seed:132450265 Wave seed:304	0.71	0.26	0.27, 0.69	0	0.031, 0.68, 0.25	0.79	0.69	0
Wind seed:-1220293325 Wave seed:400	0.71	0	0.71	0	0.69	0.71	0.69	0
Wind seed:-132430614 Wave seed:401	0.76	0.049, 0.26, 0.55	0.25, 0.74	0	0.25, 0.71	0.79	0.74	0
Wind seed:-963395014 Wave seed:402	0.74	0.27, 0.47, 0.64	0.69	0	0.65	0.79	0.65	0
Wind seed:-104419964 Wave seed:403	0.74	0	0.69	0	0.69	0.74	0.69	0
Wind seed:2088778182 Wave seed:404	0.76	0	0.74	0	0.69	0.79	0.74	0

According to the table 4.17 about the spectral density analysis result, most motions are dominated by the wave. Surge, heave, pitch, and yaw motions show very close peak frequency with the wave peak frequency. The blade motion is dominated by the wind at the same time. The effects of irregular waves and turbulent wind are similar to a considerable extent.

4.3 Gumbel Distribution

In the setting of environmental conditions, for the same turbulent wind speed, significant wave height and wave peak period, different wave seeds and wind seeds are used to change the wind and wave conditions. The Gumbel distribution is usually suitable for the maximum value, so here the Gumbel distribution is used to analyze the results of different wind seeds and wave seeds cases.

The Gumbel distribution results of 20 different wave seeds and wind seeds are shown in Figure 4.8.

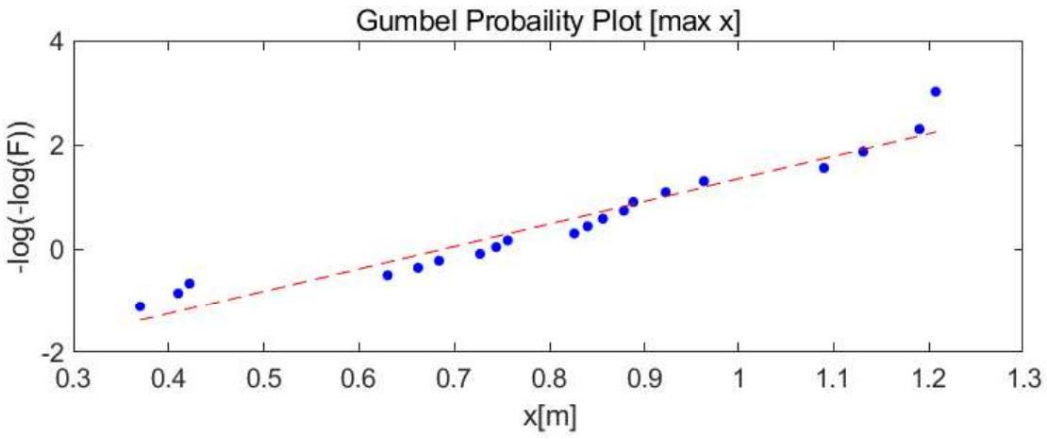

(a) The Gumbel distribution for surge

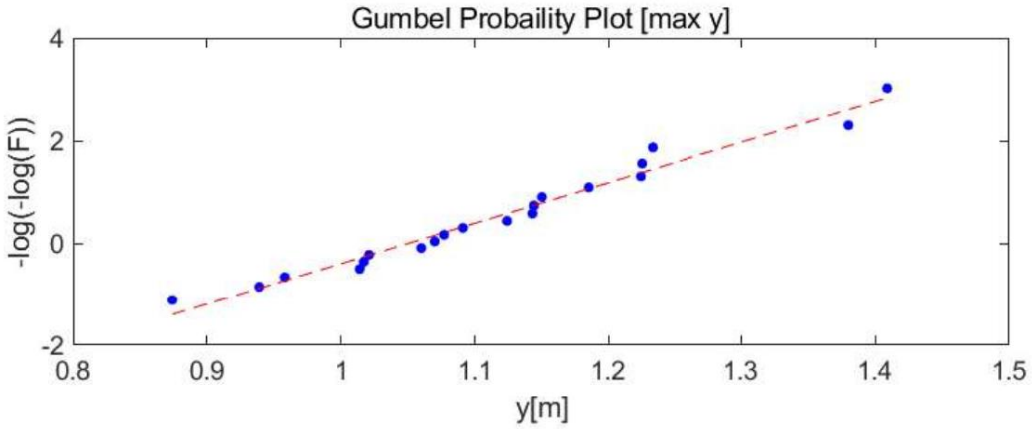

(b) The Gumbel distribution for sway

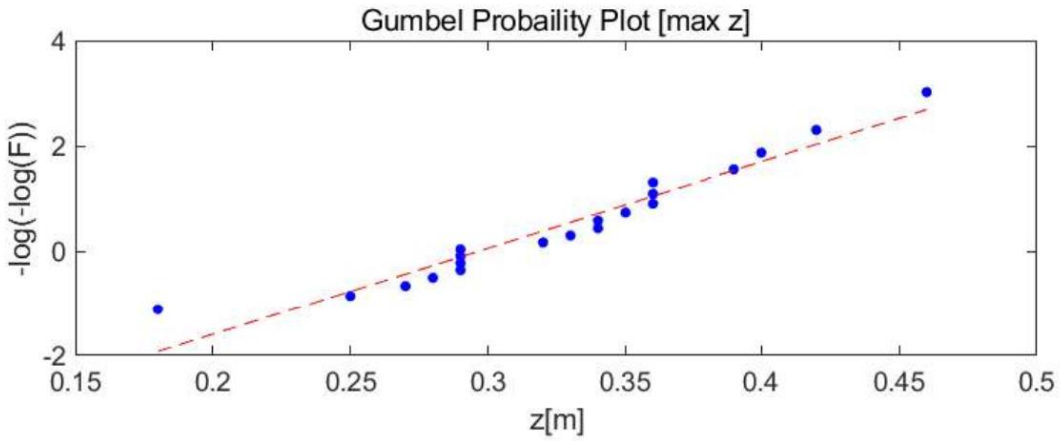

(c) The Gumbel distribution for heave

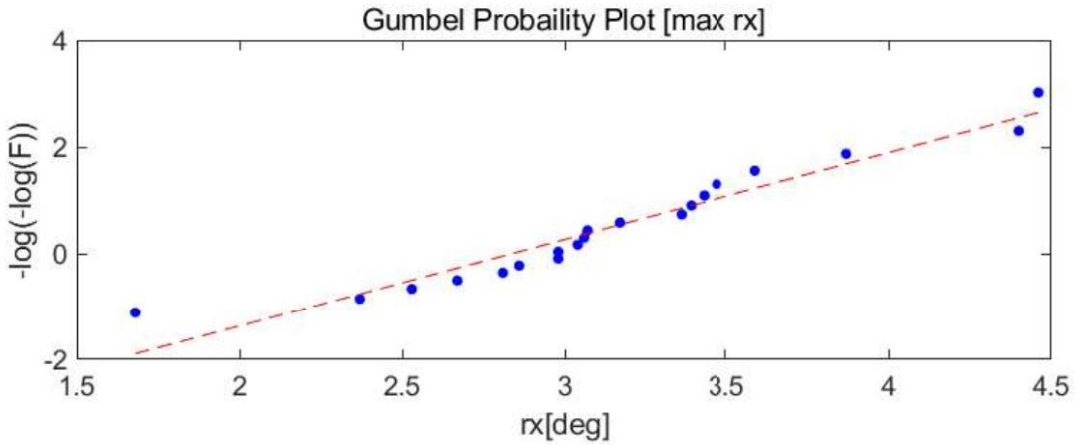

(d) The Gumbel distribution for roll

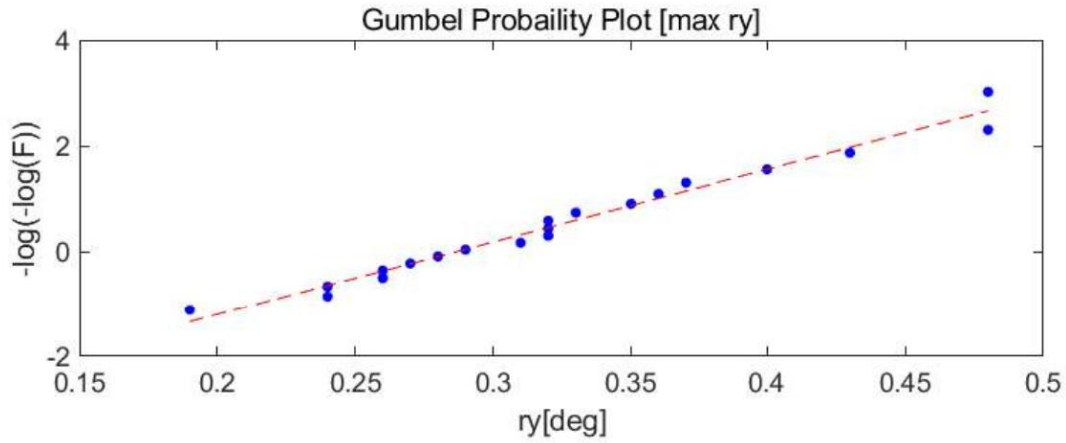

(e) The Gumbel distribution for pitch

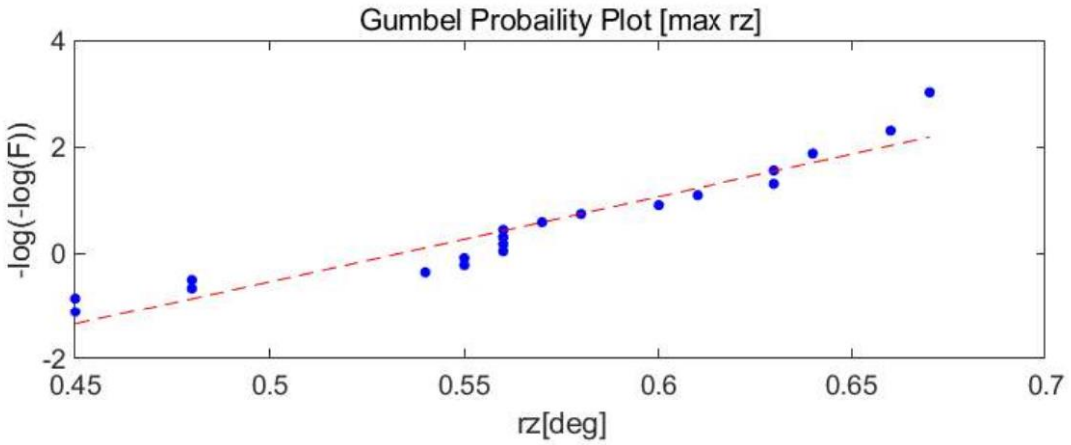

(f) The Gumbel distribution for yaw

Figure 4. 8：The Gumbel distribution results of 20 different wave seeds and wind seeds

It can be seen that Gumbel distribution fits very well, represented by the linear curve on the Gumbel probability paper. The most probable value from the Gumbel distribution is shown in the table 4.18 as below, parameter b is the most probable value. For the blade motion in surge, the most probable value is 0.6889, the most probable value range for sway motion of the blade is 1.0507, for the heave motion is 0.2967. For the rotation motion of the blade, in the x-axis, the most probable value is 2.8384, in the y-axis is 0.2870 and the most probable value for the rotation in z-axis is 0.5338. The datas comes from Gumbel distribution can be used for design check.

Table 4. 18: Gumbel distribution coefficients of 6 degrees of freedom motion

	a	b
Surge	0.2310	0.6889
Sway	0.1264	1.0507
Heave	0.0608	0.2967
Roll	0.6133	2.8384
Pitch	0.0726	0.2870
Yaw	0.0624	0.5338

5 Discussion

5.1 Simulation Results with the Scheme of Installing Offshore Wind Turbine Blades on Jack-up Vessel

For the installation of offshore wind turbine blades, this paper uses a floating vessel to lift and install the blades. Another option is to use a jack-up vessel for installation. This chapter compares and discusses the simulation results of two offshore wind turbine blade installation methods. The research on the use of jack-up vessels for offshore wind turbine blade installation was completed by Taewoo Kim.

5.1.1 Simulation of Spectral Density Analysis Using the Scheme of installing Offshore Wind Turbine Blades Using Jack-up vessels

Under the same ocean environmental conditions, the jack-up vessel is simulated exactly the same. The turbulent wind speed is 10 m/s and the wind direction is 0 degrees. The significant wave height is 2.0 m/s. The peak period of this wave is 9 seconds. The wave direction is 0 degree. Wave particles and wind particles are the same as those of jack-up containers, as shown in Table 5.1.

Table 5. 1：The blade motion due to the turbulent winds and irregular wave combinations for jack-up vessel

(a) Displacement in x-direction

Average						Standard deviation					
		Tp [sec.]						Tp [sec.]			
Hs [m]	Uw [m/s]	5	7	9	11	Hs [m]	Uw [m/s]	5	7	9	11
0.5	5.0	61.39	61.39	61.39	61.39	0.5	5.0	0.06	0.04	0.02	0.02
1.0	5.0	61.39	61.39	61.39	61.39	1.0	5.0	0.12	0.07	0.04	0.03
1.0	10.0	61.37	61.37	61.37	61.37	1.0	10.0	0.12	0.07	0.04	0.03
2.0	10.0	61.37	61.37	61.37	61.37	2.0	10.0	0.24	0.14	0.09	0.07

(b) Displacement in y-direction

Average						Standard deviation					
		Tp [sec.]						Tp [sec.]			
Hs [m]	Uw [m/s]	5	7	9	11	Hs [m]	Uw [m/s]	5	7	9	11
0.5	5.0	-34.03	-34.0	-34.03	-34.03	0.5	5.0	0.04	0.04	0.04	0.04

			3		
1.0	5.0	-34.03	-34.03	-34.03	-34.03
1.0	10.0	-33.74	-33.74	-33.74	-33.74
2.0	10.0	-33.74	-33.74	-33.74	-33.74

1.0	5.0	0.04	0.04	0.04	0.04
1.0	10.0	0.11	0.11	0.11	0.11
2.0	10.0	0.11	0.11	0.11	0.11

(c) Displacement in z-direction

Average					
		Tp [sec.]			
Hs [m]	Uw [m/s]	5	7	9	11
0.5	5.0	119.29	119.29	119.29	119.29
1.0	5.0	119.29	119.29	119.29	119.29
1.0	10.0	119.30	119.30	119.30	119.30
2.0	10.0	119.30	119.30	119.30	119.30

Standard deviation					
		Tp [sec.]			
Hs [m]	Uw [m/s]	5	7	9	11
0.5	5.0	0.02	0.01	0.01	0.01
1.0	5.0	0.04	0.03	0.02	0.01
1.0	10.0	0.04	0.03	0.02	0.01
2.0	10.0	0.08	0.05	0.03	0.02

(d) Rotational angle about the x-axis

Average					
		Tp [sec.]			
Hs [m]	Uw [m/s]	5	7	9	11
0.5	5.0	0.38	0.38	0.38	0.38
1.0	5.0	0.38	0.38	0.38	0.38
1.0	10.0	1.32	1.32	1.32	1.32
2.0	10.0	1.32	1.32	1.32	1.32

Standard deviation					
		Tp [sec.]			
Hs [m]	Uw [m/s]	5	7	9	11
0.5	5.0	0.12	0.12	0.12	0.12
1.0	5.0	0.12	0.12	0.12	0.12
1.0	10.0	0.35	0.35	0.35	0.35
2.0	10.0	0.35	0.36	0.35	0.35

(e) Rotational angle about the y-axis

Average					
		Tp [sec.]			
Hs [m]	Uw [m/s]	5	7	9	11
0.5	5.0	9.02	9.02	9.02	9.02
1.0	5.0	9.02	9.02	9.02	9.02
1.0	10.0	9.05	9.05	9.05	9.05
2.0	10.0	9.06	9.05	9.05	9.05

Standard deviation					
		Tp [sec.]			
Hs [m]	Uw [m/s]	5	7	9	11
0.5	5.0	0.08	0.04	0.03	0.02
1.0	5.0	0.16	0.09	0.05	0.04
1.0	10.0	0.16	0.09	0.06	0.04
2.0	10.0	0.34	0.18	0.11	0.08

(f) Rotational angle about the z-axis

Average					
		Tp [sec.]			
Hs [m]	Uw [m/s]	5	7	9	11

Standard deviation					
		Tp [sec.]			
Hs [m]	Uw [m/s]	5	7	9	11

0.5	5.0	0.05	0.05	0.05	0.05	0.5	5.0	0.02	0.02	0.02	0.02
1.0	5.0	0.05	0.05	0.05	0.05	1.0	5.0	0.02	0.02	0.02	0.02
1.0	10.0	0.19	0.19	0.19	0.19	1.0	10.0	0.06	0.06	0.06	0.06
2.0	10.0	0.19	0.19	0.19	0.19	2.0	10.0	0.07	0.06	0.06	0.06

According to the table 5.1, the mean position variation of x axis is affected by the wind speed, the motion on y axis is dominated by the wind speed as well. The motion for z axis is not affected significantly by the wave or wind, but the standard deviation will become larger with wave peak period becoming smaller and significant wave height becoming larger. Compared with the result of offshore wind turbine blade motion during installation procedure with jack-up vessel, the standard deviations of the six degrees of freedom motions of the blade installed by the floating vessel are larger than the motion of the jack-up vessel due to the exist of the legs in jack-up vessel. Normally, The jack-up vessel will lower its legs and put it on the bottom of the sea, and then use the same mechanical movement to lift the jack-up vessel away from the ocean surface while the legs are sitting on the bottom of the sea without moving. This feature of the jack-up vessel ensures that its hull is hardly affected by the waves, which is the biggest difference between a jack-up vessel and a floating vessel.

Table 5. 2：The spectral density analysis results of different wind seeds and wave seeds when installing offshore wind turbine blades with jack-up vessel

Wave seed and wind seed	X translation	Y translation	Z translation	X rotation	Y rotation	Z rotation	Wave elevation	Lift wire
Wind seed:1380469326 Wave seed:100	1.9	0	1.9	0	1.9	1.2	0.69	1.8
Wind seed:744903028 Wave seed:101	1.9	0	1.9	0	1.9	0	0.69	1.8
Wind seed:-1931013759 Wave seed:102	1.9	0	1.9	0	1.9	0	0.74	1.8
Wind seed:-1801367361 Wave seed:103	1.9	0	1.9	0	1.9	0	0.74	1.8
Wind seed:1711922163 Wave seed:104	1.9	0	1.9	0	1.9	0	0.79	1.8
Wind	1.9	0	1.9	0	1.9	0	0.64,	1.8

seed:-1659124769 Wave seed:200							0.75, 0.88, 1	
Wind seed:-1261119636 Wave seed:201	1.9	0	1.9	0	1.9, 2.1	1.2	0.69, 0.78, 0.98	2.1
Wind seed:1899248659 Wave seed:202	1.9	0	1.9	0	1.9	0	0.74	1.8
Wind seed:1899248659 Wave seed:203	1.9	0	1.9	0	1.9	0.47, 1.2	0.79	1.8
Wind seed:1089447476 Wave seed:204	1.9	0	1.9	0	1.9	0	0.79, 0.97	1.8
Wind seed:-139118402 Wave seed:300	1.9	0	1.9	0	1.9	1.2	0.69	1.8
Wind seed:-77431392 Wave seed:301	1.9	0	1.9	0	1.9, 2.1	1.2	0.74	2.1
Wind seed:-1035971066 Wave seed:302	1.9	0	1.9	0	1.9	0	0.68, 0.81, 1	1.8
Wind seed:590771239 Wave seed:303	1.9	0	1.9	0	1.9, 2.1	0	0.74	1.8
Wind seed:132450265 Wave seed:304	1.9	0	1.9	0	1.9	0	0.69	1.8
Wind seed:-1220293325 Wave seed:400	1.9	0	1.9	0	1.9	0	0.69	1.8
Wind seed:-132430614 Wave seed:401	1.9	0	1.9	0	2	0	0.74	1.8
Wind seed:-963395014 Wave seed:402	1.9	0	1.9	0	1.9	0	0.65	1.8
Wind seed:-104419964 Wave seed:403	1.9	0	1.9	0	1.9, 2.1	1.2	0.69	1.8

Wind seed:2088778182 Wave seed:404	1.9	0	1.9	0	1.9	0	0.74	1.8

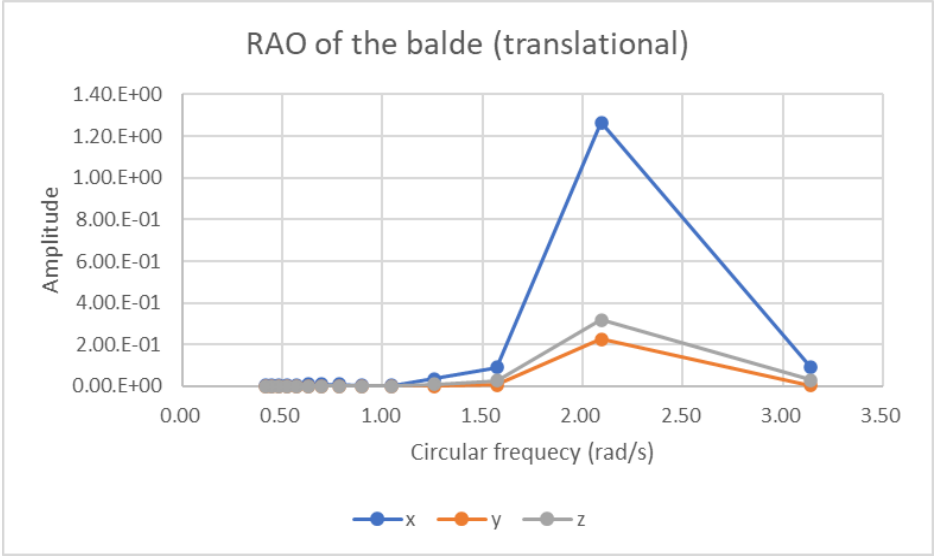

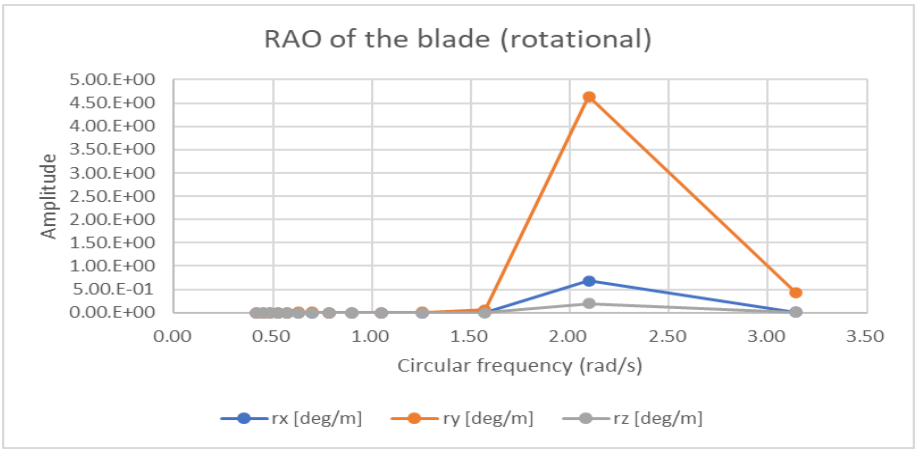

Figure 5. 1: The responses of the blade for incident wave with 1m amplitude when wave direction is 0 degree.

The figure 5.1 shows that the natural frequency when the offshore wind turbine blade is installed by the jack-up vessel is 2.09 rad/s. According to the spectral density analysis result from table 5.2, the blade motion has relation to the surge, heave and pitch peak frequency, the wave elevation has relation to the blade motion as well but smaller than the peak frequency of parameters mentioned before. This result is different with the spectral density analysis results of different wind seeds and wave seed when installing offshore wind turbine blade with floating vessel. For the motion of the blade installed by the floating vessel, most motions are dominated by the wave. Surge, heave, pitch, and yaw motions show very close peak frequency with the wave peak frequency. The blade motion is dominated by the wind at the

same time. For the peak frequency of the sway and roll motion is 0 rad/s, this result is same as the floating vessel. This difference needs to be noted during the installation of offshore wind turbine blades, especially in the installation process using floating vessels, because floating vessels are usually used in the construction of offshore wind turbine blades in the deep sea.

5.1.2 Gumbel Distribution of the Simulation Results of the Installation of Offshore Wind Turbine Blades Using Jack-up Vessels

When the offshore wind blade is installed by the jack-up vessel, the Gumbel distribution coefficient is shown as below.

Table 5. 3: Gumbel distribution coefficients of 6 degrees of freedom motion

	a	b
(a) Displacement in x-direction (surge)	0.0322	0.1977
(b) Displacement in y-direction (sway)	0.0962	0.7936
(c) Displacement in y-direction (heave)	0.0111	0.0907
(d) Rotational angle about x-axis (roll)	0.2919	2.4907
(e) Rotational angle about the y-axis (pitch)	0.0344	0.3020
(f) Rotational angle about the z-axis (yaw)	0.0448	0.3985

The most probable value from the Gumbel distribution is shown in the table 5.3 as below, parameter b is the most probable value. For the blade motion in surge, the most probable value is 0.1977, the most probable value range for sway motion of the blade is 0.7936, for the heave motion is 0.0907. For the rotation motion of the blade, in the x-axis, the most probable value is 2.4907, in the y-axis is 0.3020 and the most probable value for the rotation in z-axis is 0.3985.

5.2 Discussion Based on the Results of Using the Floating Vessel for Offshore Wind Turbine Blade Installation

When a floating vessel is used for installation of offshore wind turbine blades, due to the special structure of the floating vessel, the movement is more complicated than that of a jack-up vessel for installation of offshore wind turbine blades.

The wind mainly acts on the blades of offshore wind turbines. During the hoisting process of offshore wind turbine blades, the blades are raised horizontally by the crane. When the incoming wind encounters the blades, aerodynamic force is generated. For constant winds with different speeds and angles of incidence, the

position of the blades is almost unchanged and relatively constant. Since the wind field has minimal impact on floating vessels, floating vessels will not be affected in this case either.

On the basis of the influence of wind on blade movement, waves also have a greater influence on the installation of offshore wind turbine blades. Although the floating vessel uses anchor chains for mooring and positioning, compared with the jack-up vessel, floating vessels still has not left the sea. In the case of regular waves, different incident wave directions cause the vessel to have different motions, mainly in the x-axis direction and the y-axis direction. Due to the use of the semi-submersible vessel as a floating vessel for simulation, the part of semi-submersible vessel on the sea surface includes pontoons and the columns structure above pontoons, so the direction of the incident wave will affect the motion of the floating vessel. When the incident wave hits a floating vessel, the special sea surface structure of the floating vessel will cause the cancellation phenomenon. When the wavelength of the incident wave reaches twice the distance between the two columns, the cancellation phenomenon is most obvious. Affected by the wave force on the floating vessel, the crane used to lift the offshore wind turbine blade on the floating vessel is regarded as a rigid body. The wave force will be transmitted to the blade along with the connection structure between the floating vessel and the offshore wind turbine blade resulting in the blade small motion. By analyzing the motion of the offshore wind turbine blade with different incident wave directions, it can be found that when the incident wave is 90 degrees, the natural frequency is about 0.52 rad/s.

In TurbSIm, the initial pitch angle of offshore wind turbine blades is set to different values, and the wind force DLL file calculated by TurbSim is imported into SIMA for calculation. By comparing the aerodynamic forces received by offshore wind turbine blades, it is found that the initial When the pitch angle is about -9 degrees, the wind load on the blades is the smallest. Therefore, it is recommended to set the blade pitch angle to -9 degrees during the installation of offshore wind turbine blades to avoid the aerodynamic force brought by the wind. In this case, it can also ensure that the motion of offshore wind turbine blades is small.

In the comprehensive simulation of irregular wave and turbulent wind, with the increase of significant wave height, wave peak period and wind speed, the motion of offshore wind turbine blades also gradually increases, especially the translation motion in the x-axis and y-axis directions and the rotational motion of the x-axis, y-axis and z-axis. However, it should be noted that when only considering the difference of turbulent wind speed or only considering the waves of different

significant wave height and wave peak period, the difference in the results of the motion of the offshore wind turbine blades is not large.

This is because in this study, the floating vessel, the crane on the floating vessel and lifted offshore wind turbine blades are regarded as rigid bodies, and the lift wires used to lift the blade can move freely. In a complex simulation situation that includes the irregular wave and the turbulent wind, considering the coupling effect of the three structures, the wave force received by the floating vessel has a certain effect on the blades at the same time. The turbulent wind mainly acts on the blades, but the phenomenon is not obvious when it acts alone. Based on the analysis of coupling theory, the effect of turbulent wind speed is more obvious when the significant wave height and wave peak period of the wave are taken into account, which leads to larger motion of the offshore wind turbine blade during the installation process.

Analyze 16 different significant wave height, wave peak period and turbulent wind speed. The environmental conditions when the significant wave height is 2m, the wave peak period is 9s, and the turbulent wind speed is 10m/s are used as specific conditions for further study.

When the turbulent wind speed and wave conditions are the same, the simulation and spectrum analysis based on the simulation results of different wind seeds and wave seeds can show that the effects of wind and waves on the blade motion are similar in the case of coupling.

In the research of Gumbel distribution, it is found that in the motion of six degrees of freedom, the most probable values of the motion of each degree of freedom are respectively 0.6889 for surge, 1.0507 for sway, 0.2967 for heave, 2.8384 for roll, 0.2870 for pitch and 0.5338 for yaw. In the installation process of offshore wind turbine blades, attention should be paid to the most likely installation situation to determine whether it is suitable for installation operations, avoid exceeding the acceptable operating range of motion and avoid accidents.

6 Conclusion

This thesis is related to the installation of offshore wind turbine blades, and does the research about the motion of the blades during the installation of offshore wind turbine blades using floating vessels. Based on the coupling method developed by Dr. Yuna Zhao, dynamic analysis of the response of the installation system under different environmental conditions is carried out. This chapter introduces the main conclusions and suggestions for future work.

6.1 Conclusions

The installation process of the offshore wind turbine blade using the floating vessel is simulated under various environmental conditions.

For constant winds with different speeds and incident angles, the position of the blade is relatively stable without significant changes, and the standard deviation of the blade slightly increases as the wind speed increases. Wind has no effect on the movement of floating vessels.

When only regular wave is considered, different incident wave directions lead to different motions of the floating vessel, mainly in the x-axis direction and the y-axis direction. The lifted blade has tiny motion as well.

After calculating different initial blade pitch angles, it is found that when the initial blade pitch angle is about -9 degrees, the blade receives the least force and the motion of the blade is relatively small. During the installation process, it is recommended to set the initial angle to -9 degrees to minimize the motion of the blade.

Generally, in the installation process of offshore wind turbine blades, the environment faced is the coexistence of irregular waves and turbulent wind. With the increase of significant wave height, wave peak period and wind speed, the motion of the blade will increase significantly. According to the simulation of the environment with different wind seeds and wave seeds, the spectral density analysis is adopted to analyze the result. It is found that the effects of irregular waves and turbulent wind speed on the blade motion are similar. During the installation of offshore wind turbine blades, large waves and high wind speeds should be avoided as much as possible.

If the significant wave height is 2 m, the wave peak period is 9 s, and the turbulent wind speed is 10 m/s, the Gumbel distribution analysis shows that the most probable values of the six degrees of freedom are 0.6889 for surge, 1.0507 for sway, 0.2967 for heave, 2.8384 for roll, 0.2870 for pitch and 0.5338 for yaw. It is recommended that the most probable value of each degree of freedom should be paid attention to before the installation of offshore wind turbine blades to ensure that the installation can be carried out in most cases of this sea state to avoid accidents.

6.2 Future Work

Based on the phenomena and laws that have been discovered, it is meaningful to further analyze the specific wave forces and wind forces experienced by the lifted offshore wind turbine blades on the basis of still using the coupling method of Dr. Yuna Zhao.

Based on the coupling method, further analyze the blade movement in extreme cases.

Further study the distribution of exceeding the installation standards under extreme conditions.

Explore the motion of the root of the blade in the mating phase, and find the sea conditions that allow the blade to be installed according to the blade installation standards.

References

[1] WIKIPEDIA. Offshore wind power [M].

https://en.m.wikipedia.org/wiki/Offshore_wind_power.

[2] COUNCIL. G W E. Global offshore wind report 2020. [M]. https://gwec.net/global-offshore-wind-report-2020/. 2020.

[3] YUNNA ZHAO Z C, PETER CHRISTIAN SANDVIK. An Integrated Dynamic Analysis Method for Simulating Installation of a Single Blade for Wind Turbines[J]. Ocean Engineering, 2018, 152.

[4] WWW.HXNY.COM. The first demonstration project of offshore wind power and marine ranching will be built in Shandong Province [M]. (http://www.hxny.com/nd-42171-0-17.html. 2019.

[5] HAO ZHANG F L, HAIBING CHEN. Seismic response of offshore composite caisson-piles foundation with different pile configurations and soil conditions in centrifuge tests[J]. Ocean Engineering, 2021, 221: 108561.

[6] O. MAURICIO HERNANDEZ C M S, MOJTABA MAALI AMIRI, CORBINIANO SILVA, SEGEN F. ESTEFEN, EMILIO LA ROVERE. Environmental impacts of offshore wind installation, operation and maintenance, and decommissioning activities: A case study of Brazil[J]. Renewable and Sustainable Energy Reviews, 2021, 144: 110994.

[7] CHEN J H Z. Experimental investigation of aerodynamic effect–induced dynamic characteristics of an OC4 semi-submersible floating wind turbine.[J]. Proceedings of the Institution of Mechanical Engineers，Journal of Engineering for the Maritime Environment, 2018, 232: 19-36.

[8] ADARAMOLA M E. Wind Resources and Future Energy Security: Environmental Social, and Economic Issues[J]. Apple Academic Press, 2015.

[9] BAILEY H, BROOKES K, THOMPSON P. Assessing Environmental Impacts of Offshore Wind Farms: Lessons Learned and Recommendations for the Future[J]. Aquatic biosystems, 2014, 10: 8.

[10] THOMSEN K E. Offshore Wind - A comprehensive Guide to Successful Offshore Wind Farm Installation[M]. City, 2014

[11] EUROPE W. Offshore wind in Europe- Key trends and statistics 2017[R]. City, 2018.

[12] AL. L L E. Joint distribution of environmental condition at five european offshore sites for design of combined wind and wave energy devices[J]. Journal of Offshore Mechanics and Arctic Engineering, 2015, 137:031901.

[13] WANG W, BAI, Y.. J. Investigation on installation of offshore wind turbines[J]. Marine Sci Appl, 2010, 9: 175–180.

[14] ZHAO. Y. Numerical Modeling and Dynamic Analysis of Offshore Wind Turbine Blade Installation.[D]. City: NTNU, 2019.

[15] JIANG Z G Z, REN Z, LI Y, DUAN L. . A parametric study on the final blade installation process for monopile wind turbines under rough environmental conditions.[J]. Engineer Structure, 2018, 172: 1042–1056.

[16] CHANNEL. G W. How to build an offshore wind farm. [M]. https://www.youtube.com/watch?v=kg-bJB-stQs&list=PLUCbklMxQPodNX9r50inaiTdYSe2HziTU. 2017.

[17] AL Z J E. A parametric study on the final blade installation process for monopile wind turbines under rough environmental conditions[J]. Engineering Structures, 2018, (172): 1042–1056.

[18] YUNA ZHAOA Z C, ZHEN GAO, PETER CHRISTIAN SANDVIKD. Numerical study on the feasibility of offshore single blade installation by floating crane vessels[J]. Marine Structures, 2019, 64: 442-462.

[19] SHI W, PARK, H.-C., CHUNG, C.-W., KIM, Y.-C., ET AL. Comparison of dynamic response of monopile, tripod and jacket foundation system for a 5-mw wind turbine [M]. The Twenty-first International Offshore and Polar 20 Engineering Conference. Hawaii, USA. 2011: 19-24.

[20] YUNA ZHAO Z C, PETER CHRISTIAN SANDVIK, ZHEN GAO. Numerical modeling and analysis of the dynamic motion response of an offshore wind turbine blade during installation by a jack-up crane vessel[J]. Ocean Engineering, 2018, 165: 353–364.

[21] CORBETTA G A P, I. AND WILKES, J. Wind in power - 2014 European statistics [J]. The European Wind Energy Association, 2014.

[22] WU YX L H, CHI HM, LIU LY, CAI AM, NING HC. . The Marine Environment Impacts on the Supporting Structure of the Offshore Wind Turbines and Discussions on the Protective Measures[J]. AMR, 2014: 1065–1069:1381–1069.

[23] DAYUN W O. Single pile foundation transportation of offshore wind power abroad [M]. http://www.sgcio.com/eduinfo/eduzx/2018/0508/71386.html. 2018.

[24] SARKAR A, GUDMESTAD, O. T., 2013. . 33, 160–187. Study on a new method for installing a monopile and a fully integrated offshore wind turbine structure[J]. Marine Structures, 2013, 33: 160-187.

[25] WU Y X, ET AL. The Marine Environment Impacts on the Supporting Structure of the Offshore Wind Turbines and Discussions on the Protective Measures[J]. Advanced Materials Research, 2014, 1065–1069: 1381–1389.

[26] ZHENGSHUN CHENG T R W, MUK CHEN ONG, KAI WANG. Power performance and dynamic responses of a combined floating vertical axis wind turbine and wave energy converter concept[J]. Energy, 2019, 171: 190-204.

[27] A. S. VERMA Y Z, Z. GAO, AND N. P. VEDVIK. . Explicit structural response-based methodology for assessment of operational limits for single blade installation for offshore wind turbines. I [M]. Proceedings of the 4th International Conference in Ocean Engineering. Chennai, India. 2018: 18-21.

[28] ZHAO Y, CHENG Z, SANDVIK P C, et al. An integrated dynamic analysis method for simulating installation of single blades for wind turbines[J]. Ocean Engineering, 2018, 152: 72-88.

[29] CHENG Z, MADSEN, H. A., GAO, Z., MOAN, T. A fully coupled method for numerical modeling and dynamic analysis of floating vertical axis wind turbines[J]. Renewable Energy 2017: 604–619.

[30] VERITAS D N. Modelling and analysis of marine operations[J]. standard DNV-RP-H103, 2011.

[31] OCEAN S. SIMO-theory manual version 4.10[M]. City, 2017.

[32] OCEAN S. RIFLEX- Theory Manual 4.10.1[M]. City, 2017.

[33] PEDERSEN. E A. Motion analysis of semi-submersible[D]. City: Norwegian University of Science and Technology Department of Marine Technology, 2012.

[34] DNV-RP-C205 D. Environmental conditions and environmental loads [M]. DET NORSKE VERITAS. Olso, Norway. 2007.

[35] OCEAN. S. SIMO-User Manual Version 4.10.[M]. City: SINTEF Ocean, 2017.

[36] M. GAUNAA L B, S. GUNTUR, F. ZAHLE. . First-order aerodynamic and aeroelastic behavior of a single-blade installation setup [M]. Journal of Physics: Conference Series. 2014.

[37] RAYLEIGH L. Theory of Sound (two volumes)[M]. City: Dover Publications,, 1877.

[38] PATERSON J, DAMICO, F., THIES, P., KURT, E., HARRISON, G. Offshore wind installation vessels–a comparative assessment for uk offshore rounds 1 and 2[J]. Ocean Engineering, 2017.

[39] JONKMAN B J. Turbsim user's guide: Version 1.50[M]. City, 2009.

[40] IEC. International standard 61400-1, [M]. wind turbines, part 1: Design requirements. 2005.

[41] IEC I-. wind turbines, part 3: Design requirements for offshore wind turbines[J]. 2009.

[42] MOAN. A N A T. Stochastic dynamics of marine structures[D]. City: Cambridge University Press, UK, 2013.

[43] SINTEF.COM. Sima [M]. https://www.sintef.no/en/software/sima/. 2013.

Appendices

Appendix 1: The time series plots and the spectral density plots of the 20 simulations of the blade motion

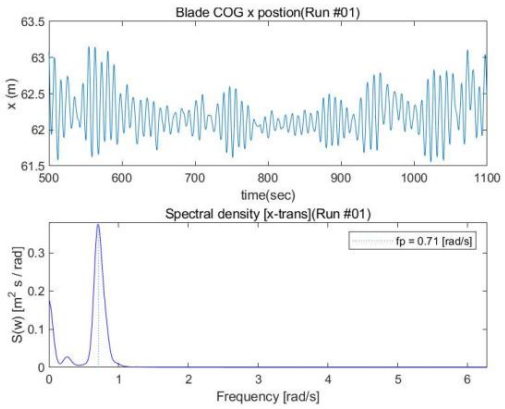

(a) Displacement in the x-direction

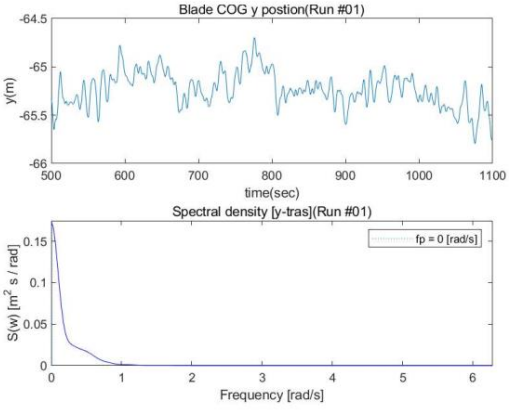

(b) Displacement in the y-direction

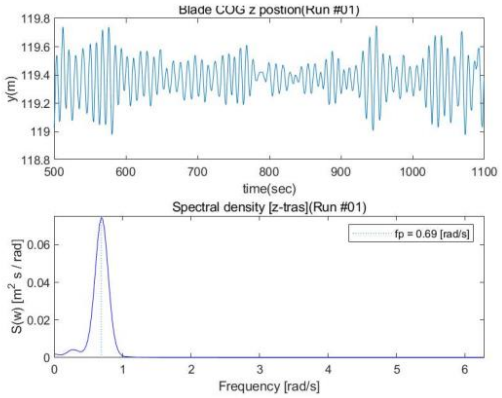

(c) Displacement in the z-direction

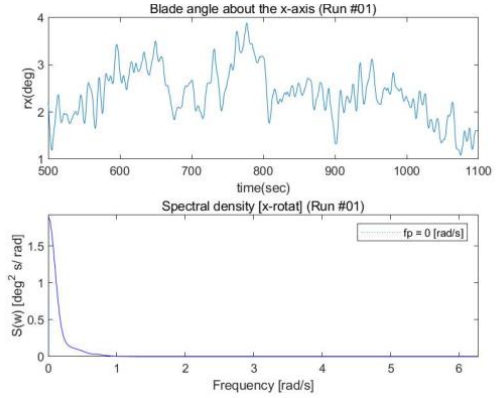

(d) Rotational angle about the x-axis

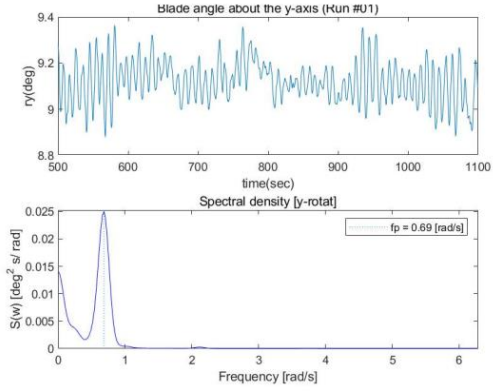

(e) Rotational angle about the y-axis

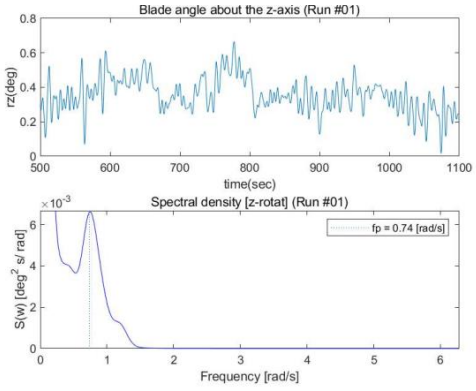

(f) Rotational angle about the z-axis

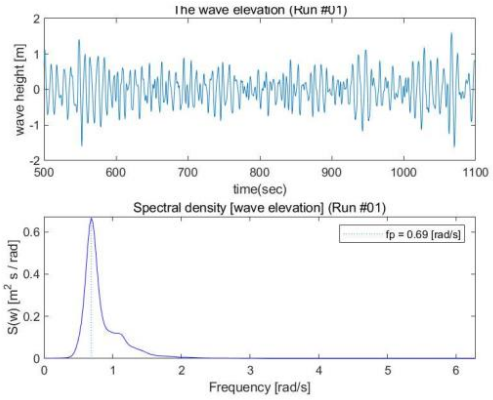

(g) Wave elevation

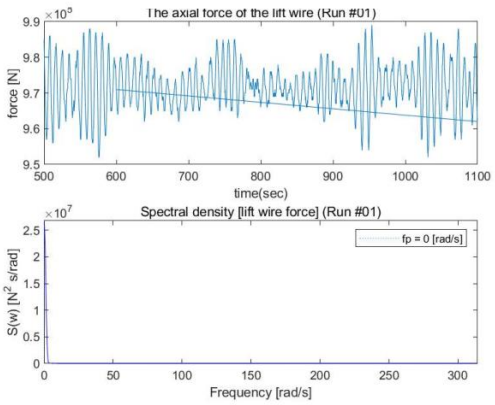

(h) Lift wire axial force

Figure 7. 1: Time series and spectral density plots of wind seed 1380469326, wave seed 100

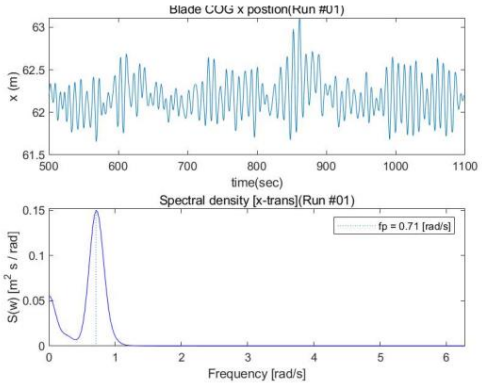

(a) Displacement in the x-direction

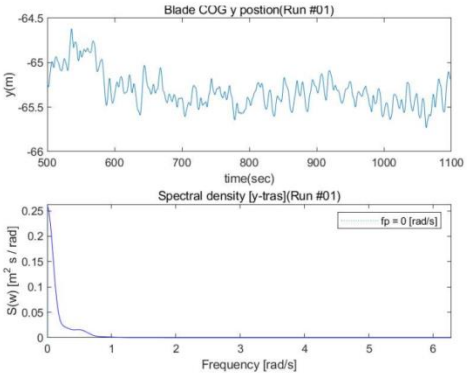

(b) Displacement in the y-direction

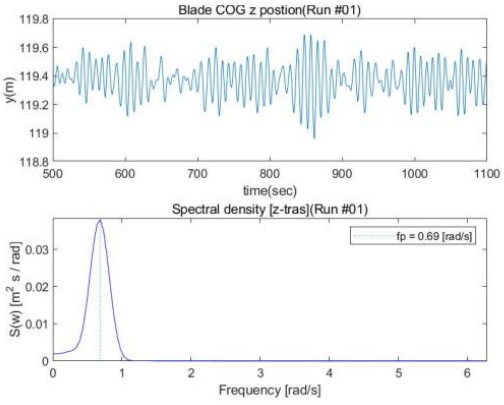

(c) Displacement in the z-direction

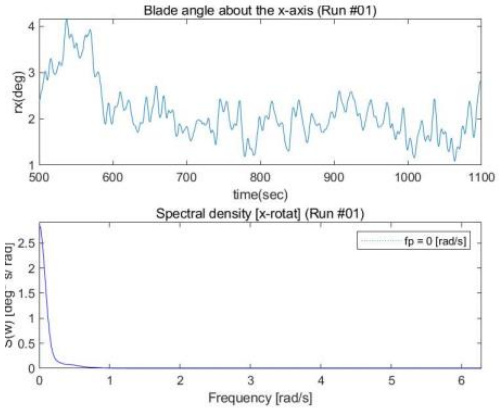

(d) Rotational angle about the x-axis

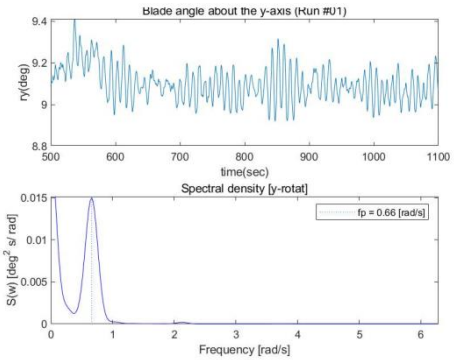

(e) Rotational angle about the y-axis

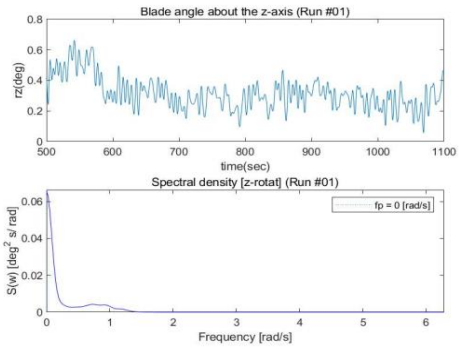

(f) Rotational angle about the z-axis

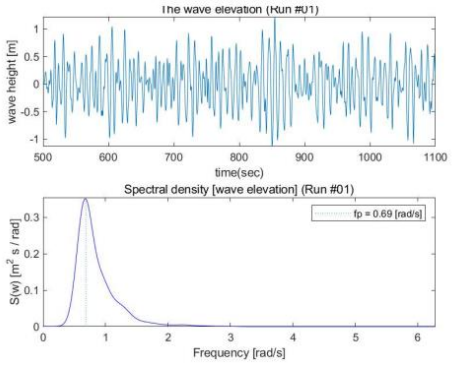

(g) Wave elevation

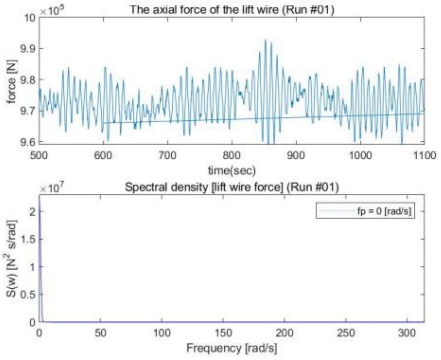

(h) Lift wire axial force

Figure 7. 2: Time series and spectral density plots of wind seed 744903028, wave seed:101

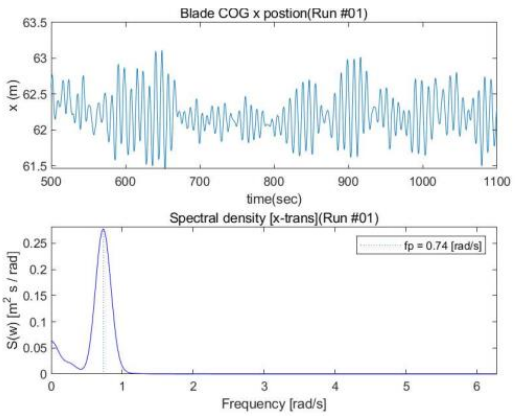

(a) Displacement in the x-direction

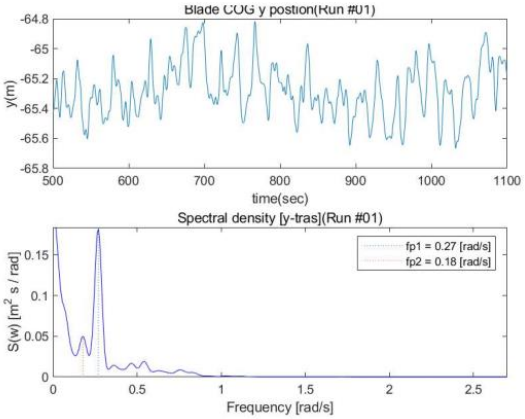

(b) Displacement in the y-direction

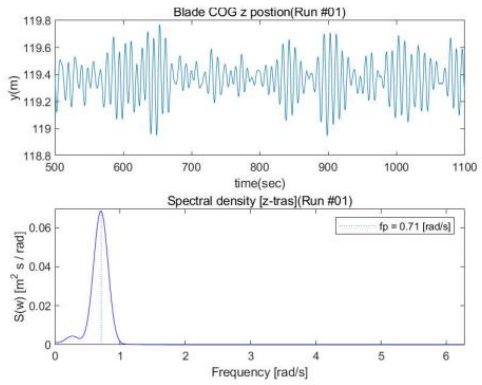

(c) Displacement in the z-direction

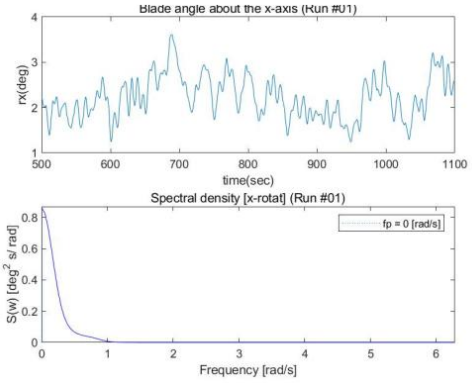

(d) Rotational angle about the x-axis

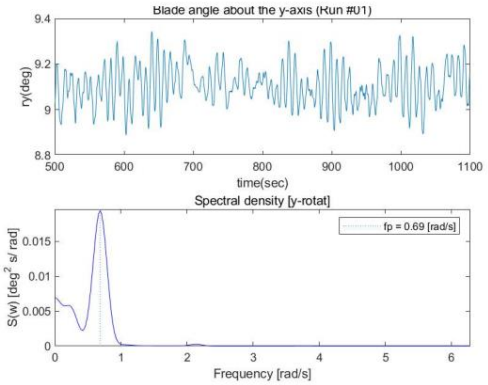

(e) Rotational angle about the y-axis

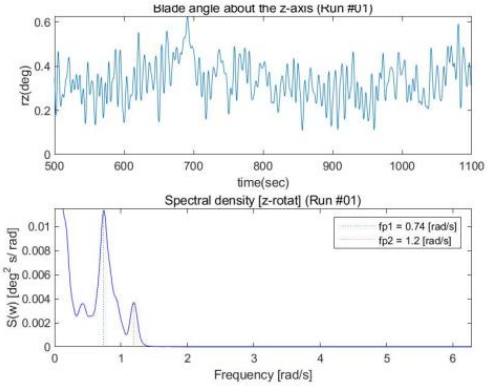

(f) Rotational angle about the z-axis

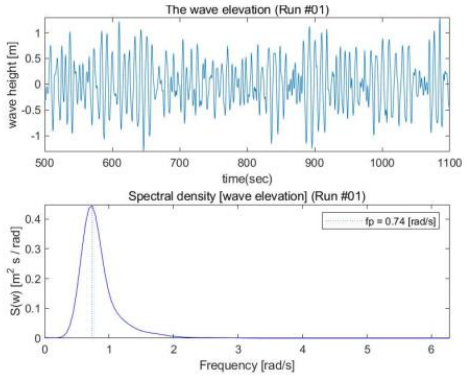

(g) Wave elevation

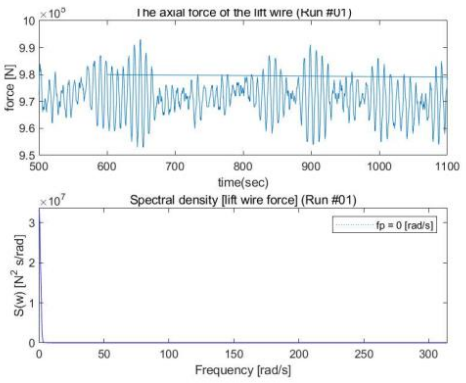

(h) Lift wire axial force

Figure 7. 3: Time series and spectral density plots of Wind seed -1931013759, wave seed 102

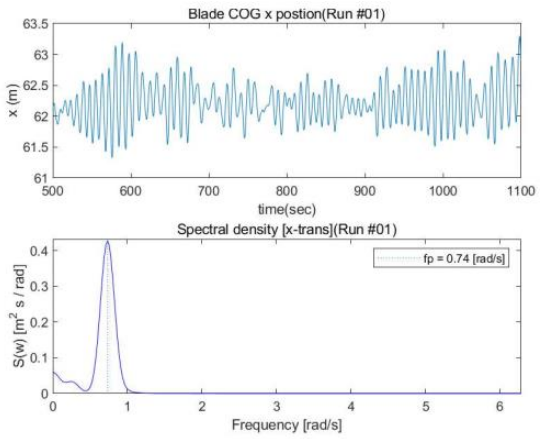

(a) Displacement in the x-direction

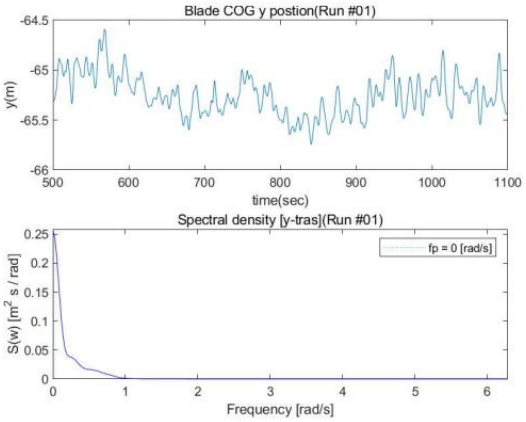

(b) Displacement in the y-direction

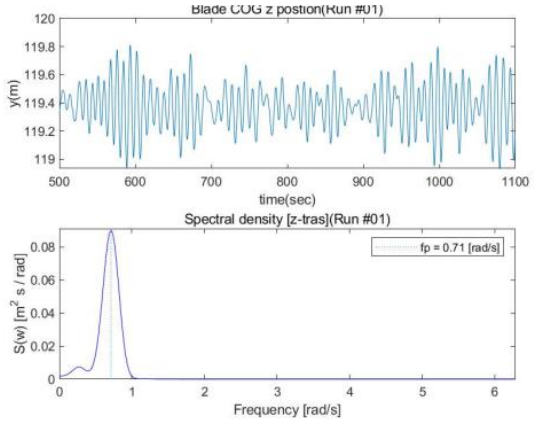

(c) Displacement in the z-direction

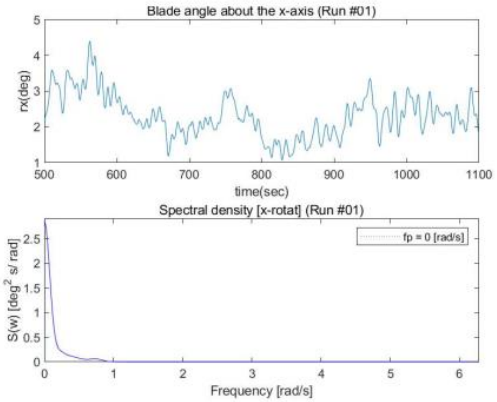

(d) Rotational angle about the x-axis

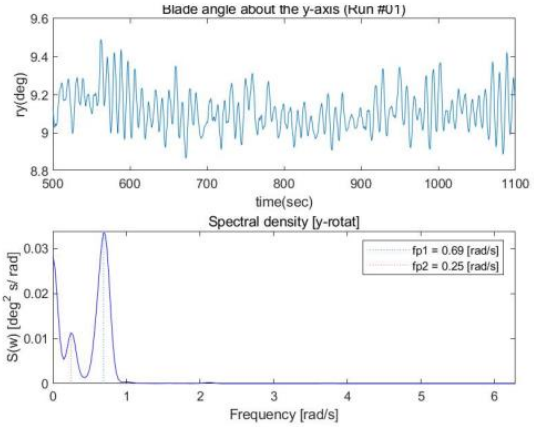

(e) Rotational angle about the y-axis

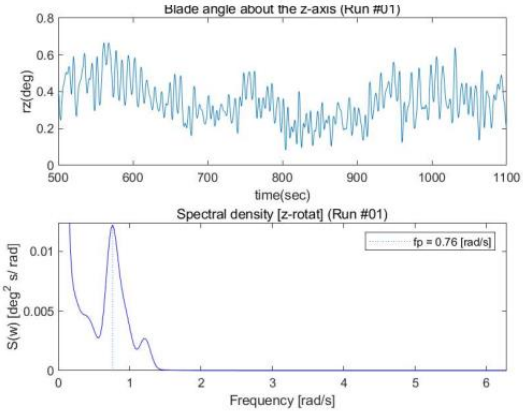

(f) Rotational angle about the z-axis

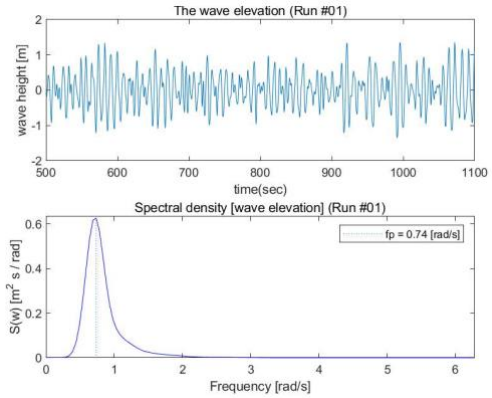

(g) Wave elevation

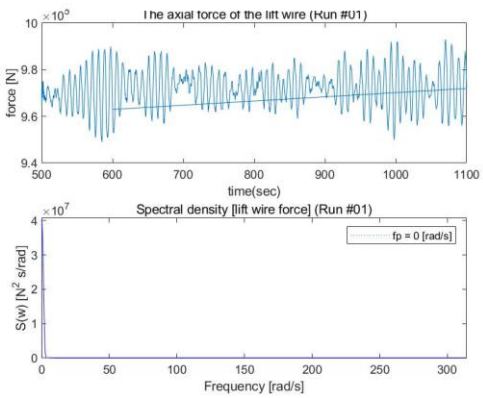

(h) Lift wire axial force

Figure 7. 4: Time series and spectral density plots of wind seed -1801367361, wave seed 103

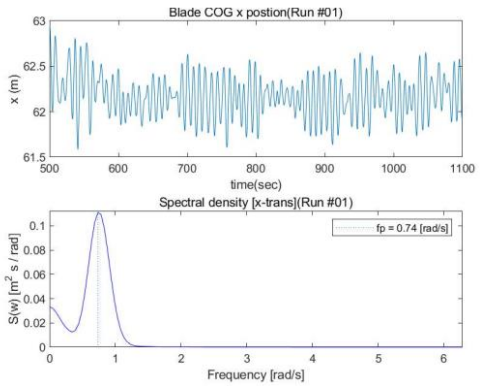

(a) Displacement in the x-direction

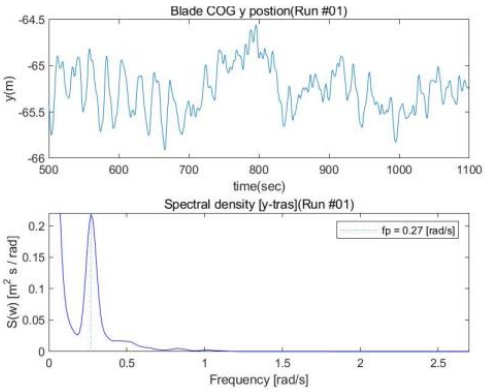

(b) Displacement in the y-direction

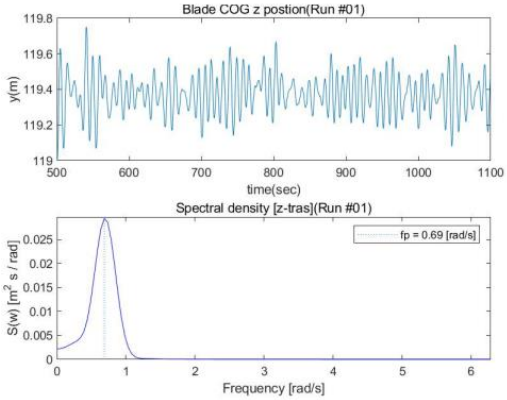

(c) Displacement in the z-direction

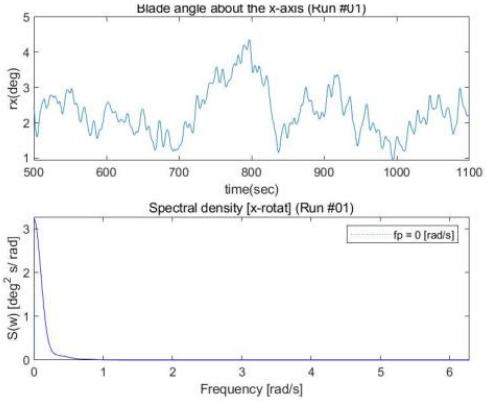

(d) Rotational angle about the x-axis

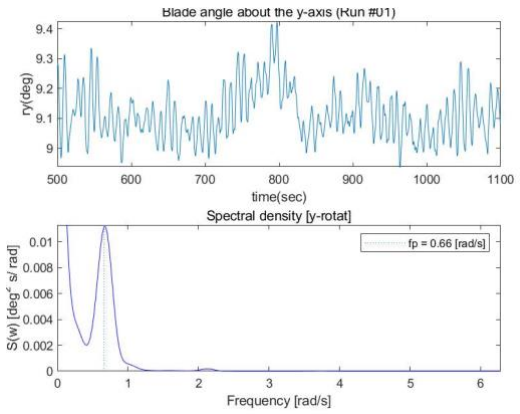

(e) Rotational angle about the y-axis

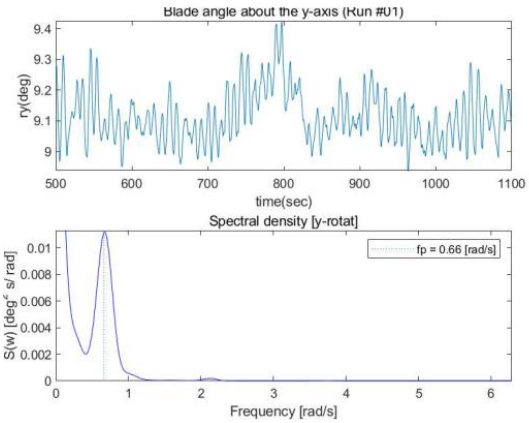

(f) Rotational angle about the z-axis

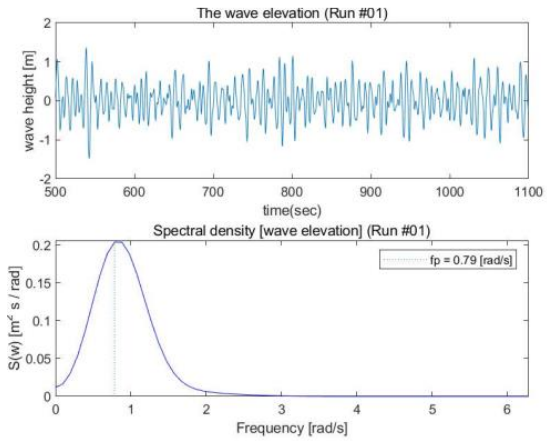

(g) Wave elevation

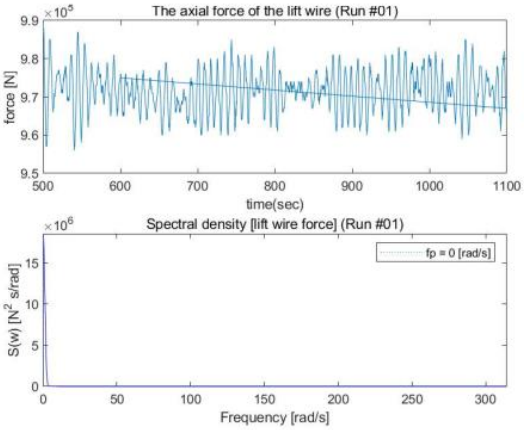

(h) Lift wire axial force

Figure 7. 5: Time series and spectral density plots of wind seed 1711922163, wave seed 104

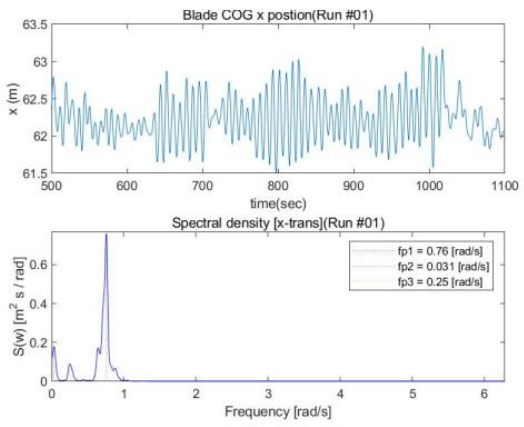

(a) Displacement in the x-direction

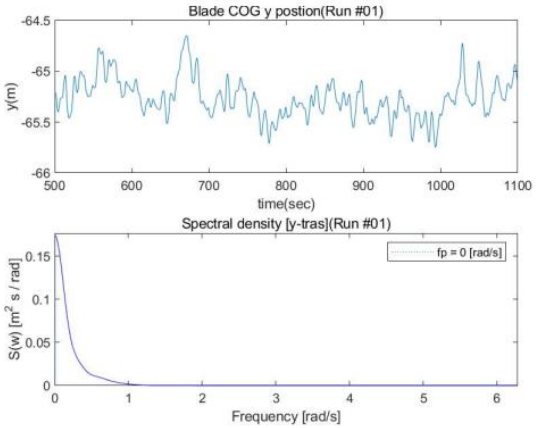

(b) Displacement in the y-direction

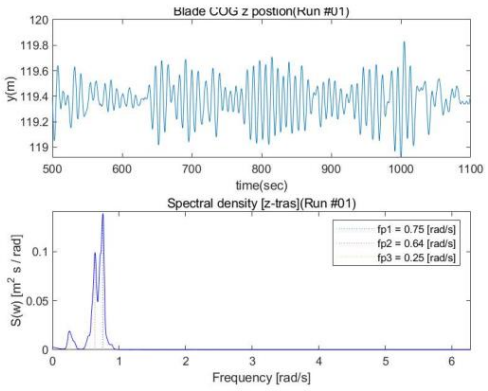

(c) Displacement in the z-direction

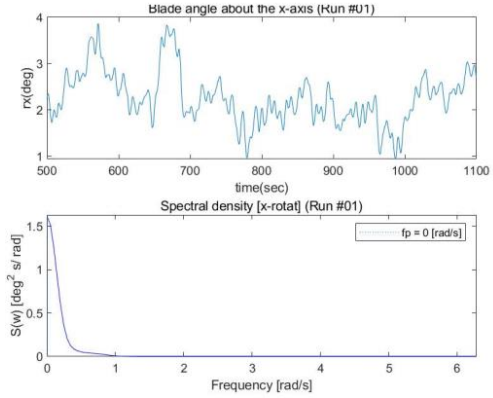

(d) Rotational angle about the x-axis

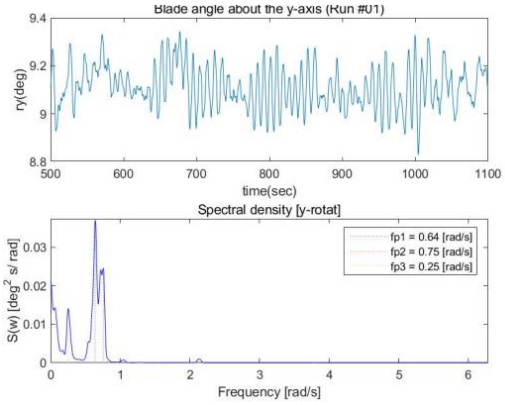

(e) Rotational angle about the y-axis

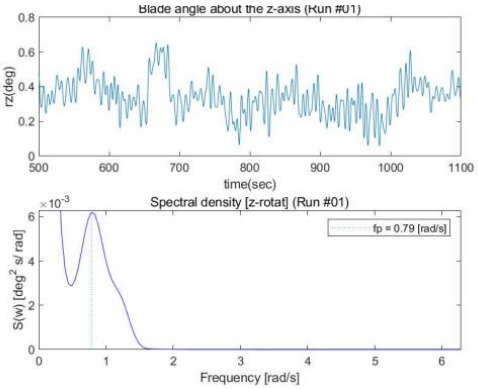

(f) Rotational angle about the z-axis

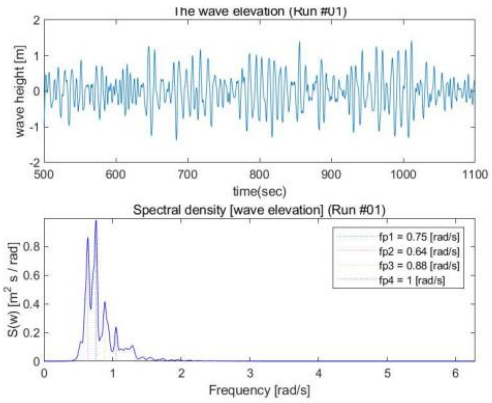

(g) Wave elevation

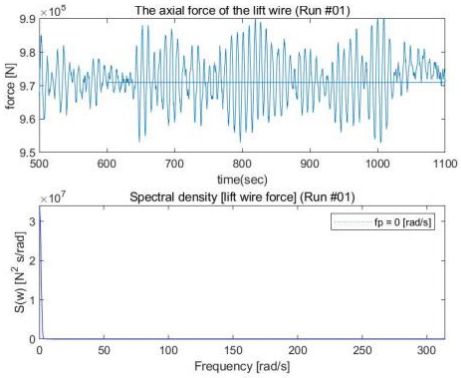

(h) Lift wire axial force

Figure 7. 6: Time series and spectral density plots of wind seed -1659124769, wave seed 200

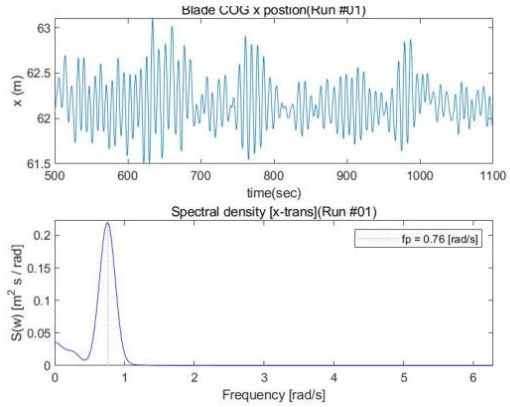

(a) Displacement in the x-direction

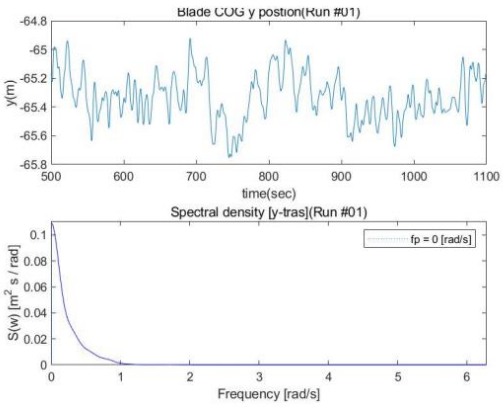

(b) Displacement in the y-direction

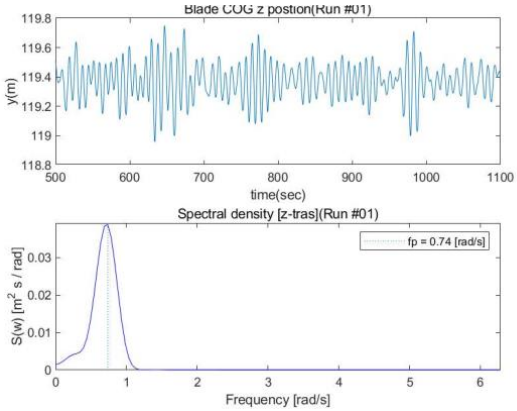

(c) Displacement in the z-direction

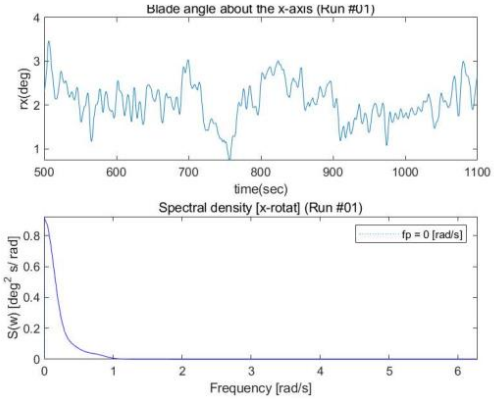

(d) Rotational angle about the x-axis

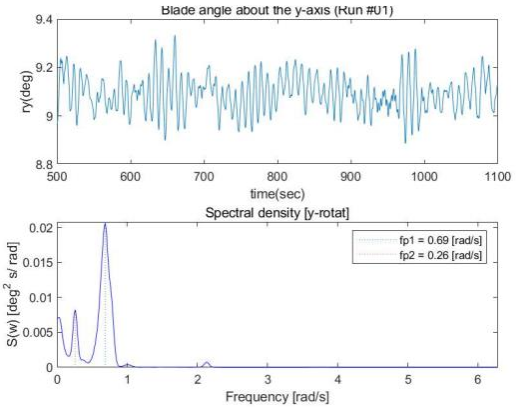

(e) Rotational angle about the y-axis

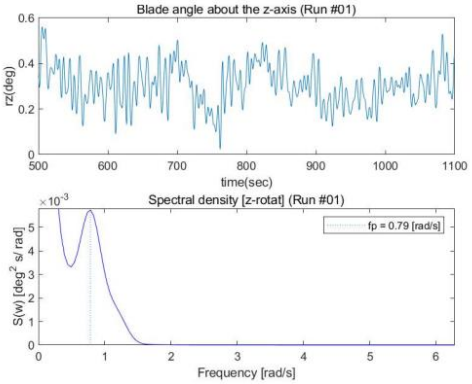

(f) Rotational angle about the z-axis

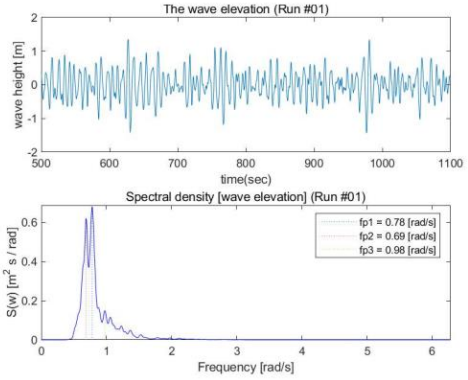

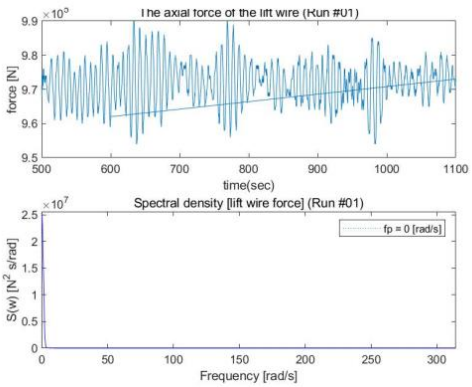

(g) Wave elevation (h) Lift wire axial force

Figure 7. 7: Time series and spectral density plots of wind seed -1261119636, wave seed 201

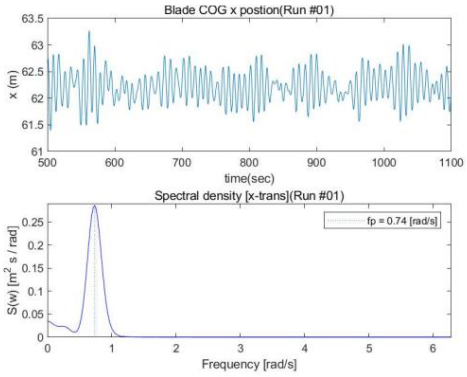

(a) Displacement in the x-direction

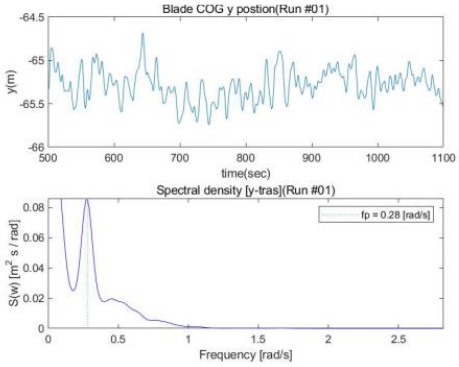

(b) Displacement in the y-direction

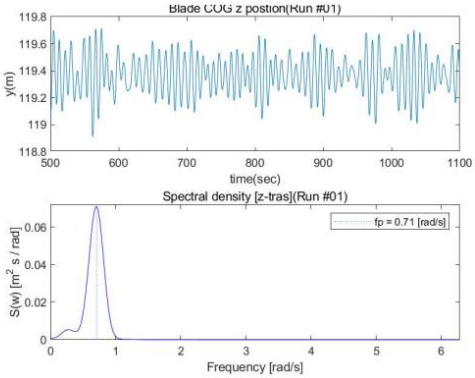

(c) Displacement in the z-direction

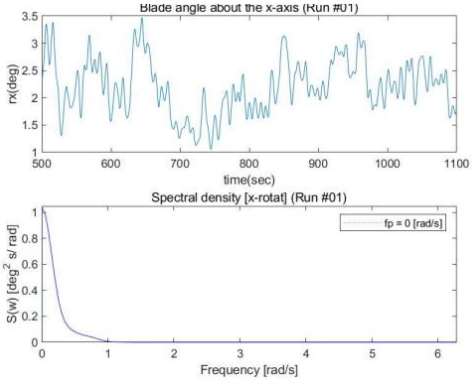

(d) Rotational angle about the x-axis

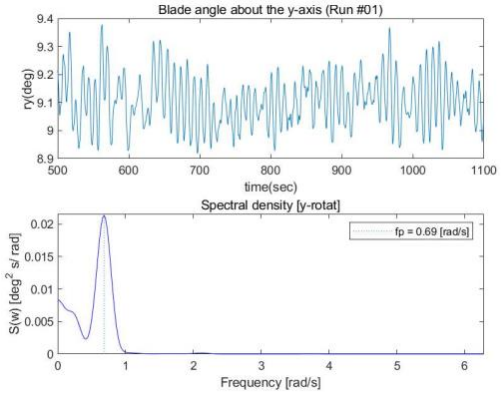

(e) Rotational angle about the y-axis

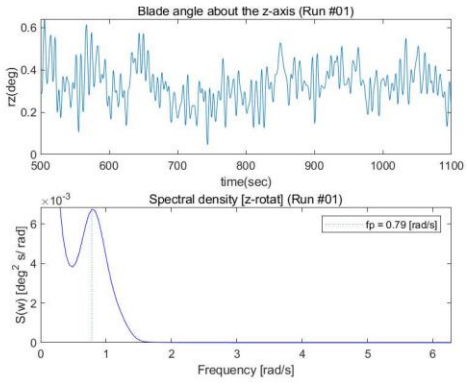

(f) Rotational angle about the z-axis

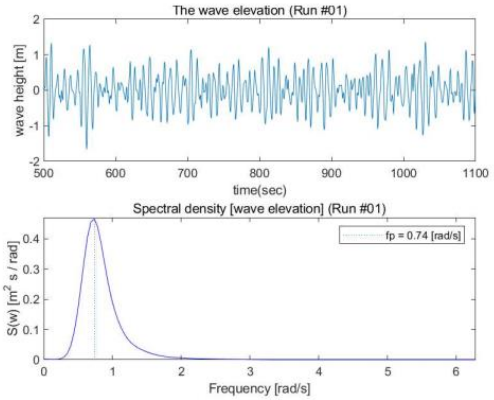

(g) Wave elevation

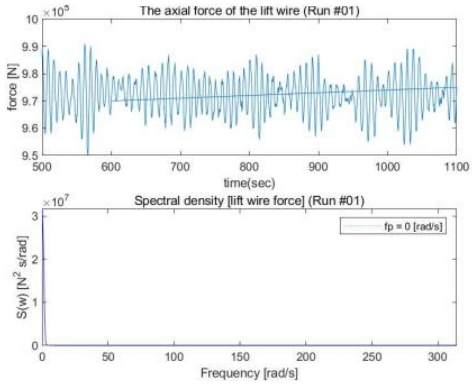

(h) Lift wire axial force

Figure 7. 8: Time series and spectral density plots of wind seed 1899248659, wave seed 202

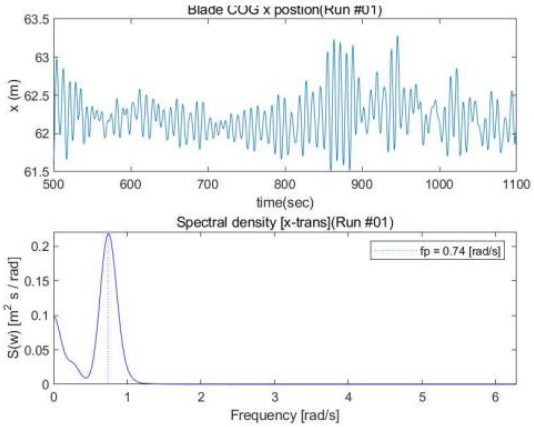

(a) Displacement in the x-direction

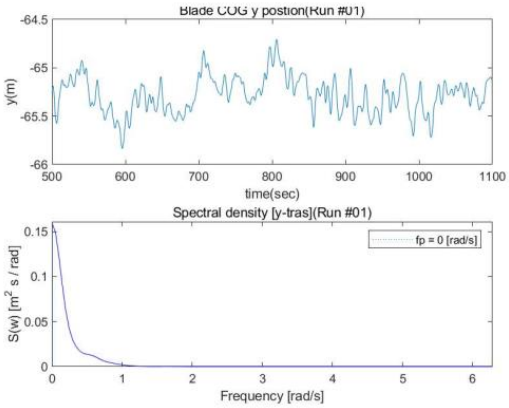

(b) Displacement in the y-direction

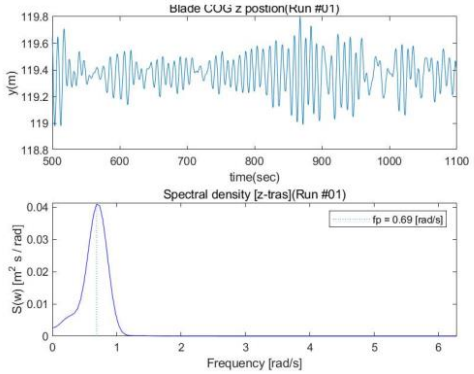

(c) Displacement in the z-direction

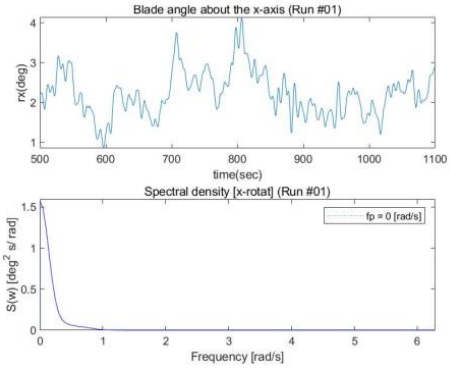

(d) Rotational angle about the x-axis

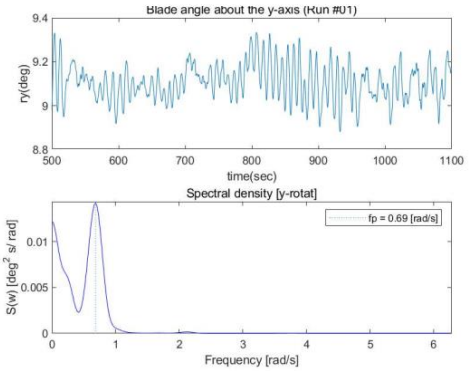

(e) Rotational angle about the y-axis

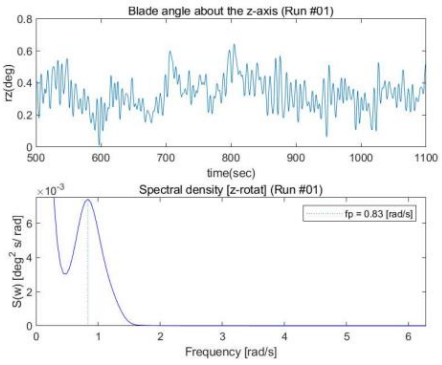

(f) Rotational angle about the z-axis

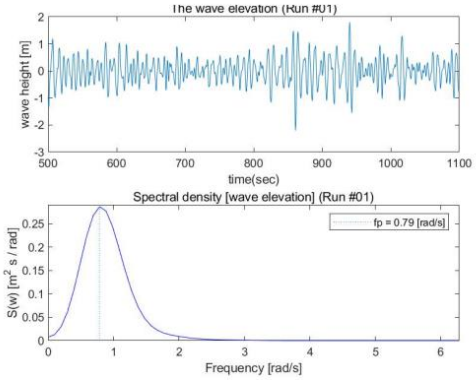

(g) Wave elevation

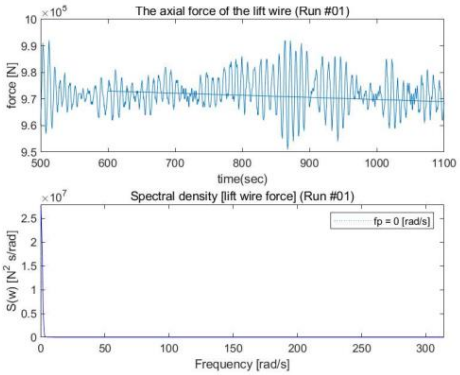

(h) Lift wire axial force

Figure 7. 9: Time series and spectral density plots of wind seed 1899248659, wave seed 203

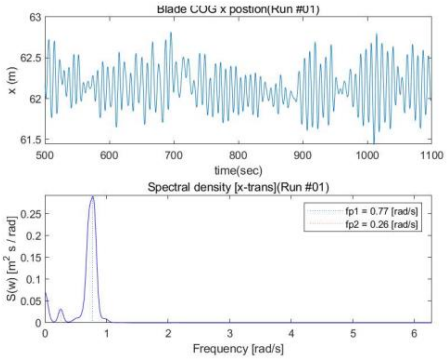

(a) Displacement in the x-direction

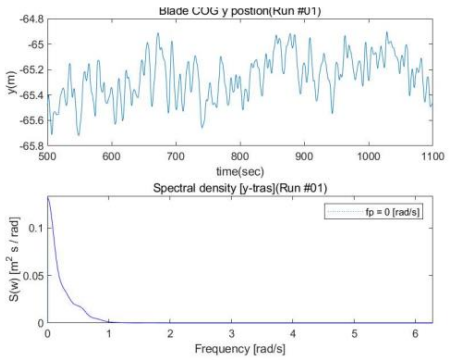

(b) Displacement in the y-direction

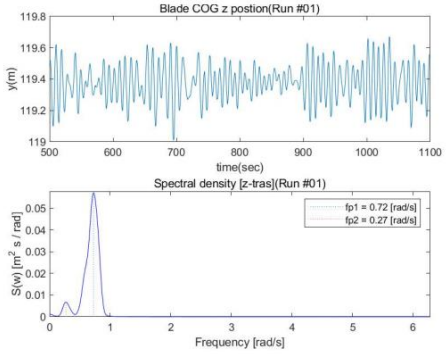

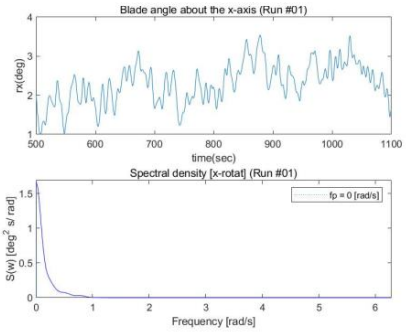

(c) Displacement in the z-direction

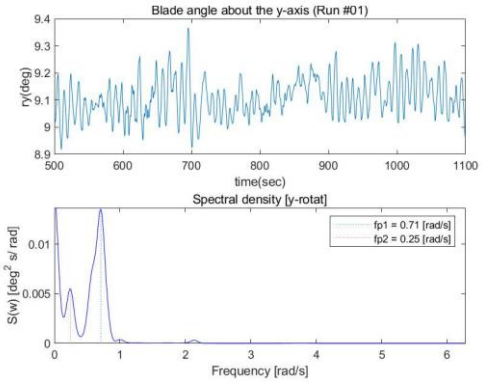

(d) Rotational angle about the x-axis

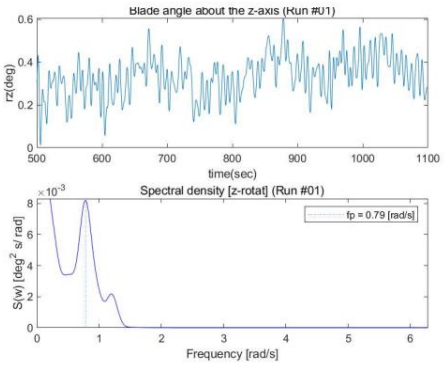

(e) Rotational angle about the y-axis

(f) Rotational angle about the z-axis

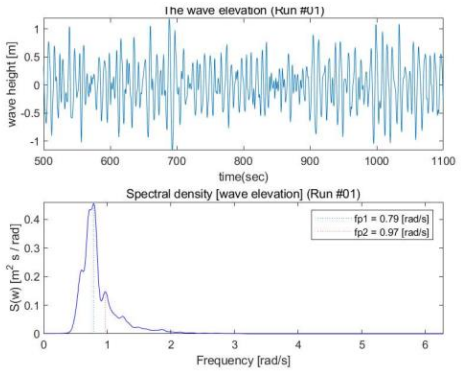

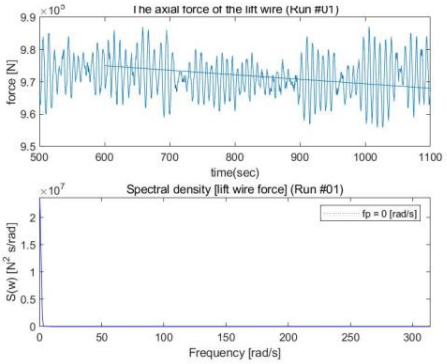

(g) Wave elevation

(h) Lift wire axial force

Figure 7. 10: Time series and spectral density plots of wind seed 1089447476, wave seed 204

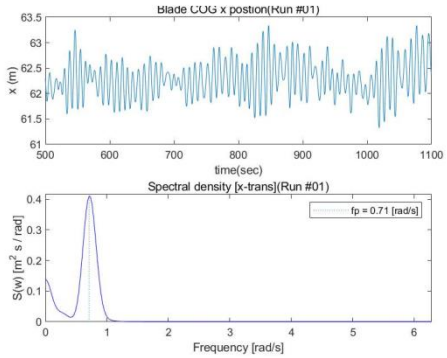

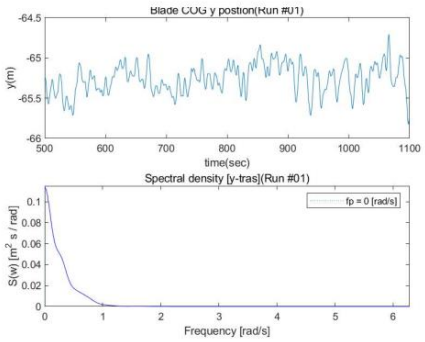

(a) Displacement in the x-direction

(b) Displacement in the y-direction

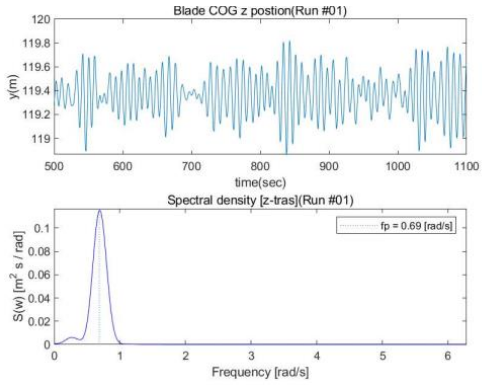

(c) Displacement in the z-direction

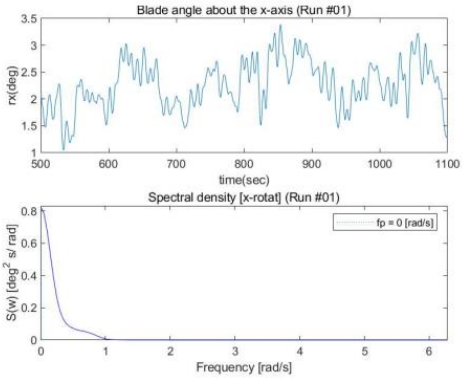

(d) Rotational angle about the x-axis

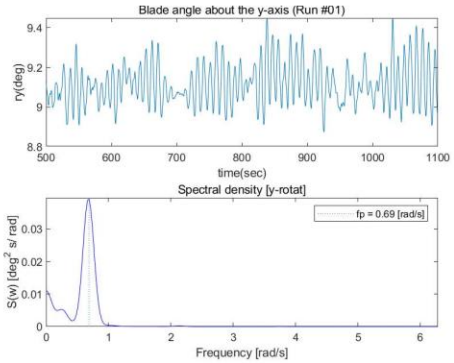

(e) Rotational angle about the y-axis

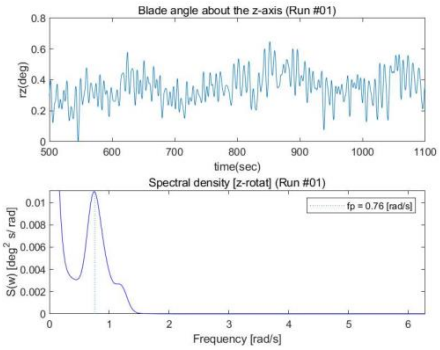

(f) Rotational angle about the z-axis

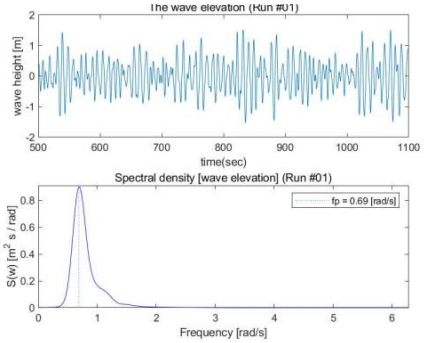

(g) Wave elevation

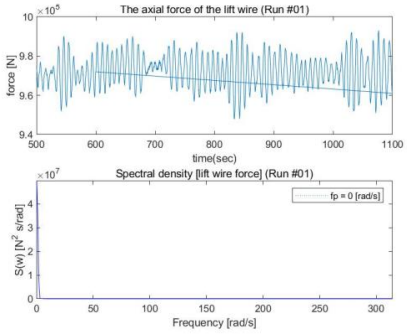

(h) Lift wire axial force

Figure 7. 11: Time series and spectral density plots of wind seed -139118402, wave seed 300

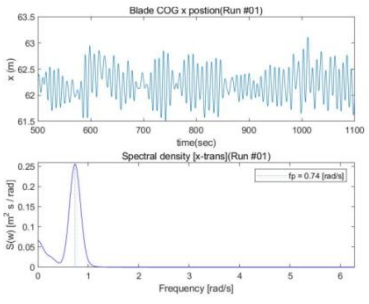

(a) Displacement in the x-direction

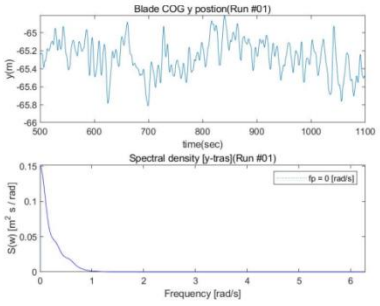

(b) Displacement in the y-direction

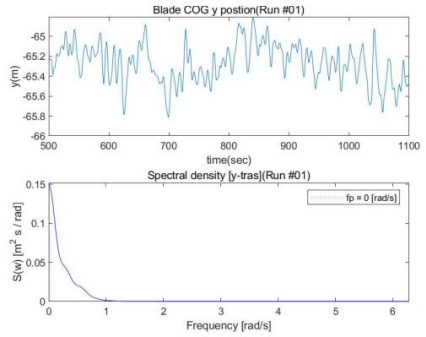

(c) Displacement in the z-direction

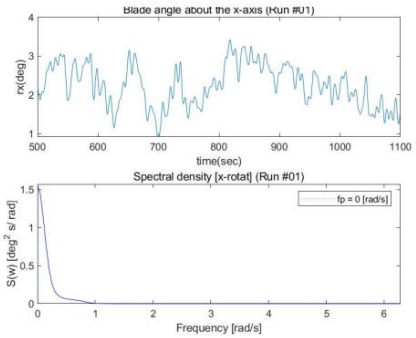

(d) Rotational angle about the x-axis

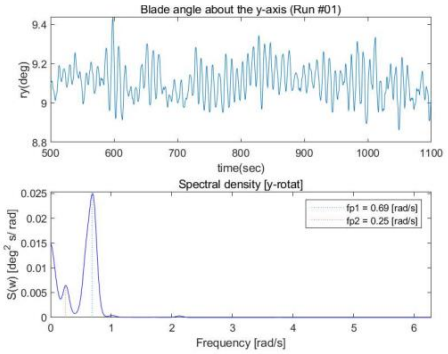

(e) Rotational angle about the y-axis

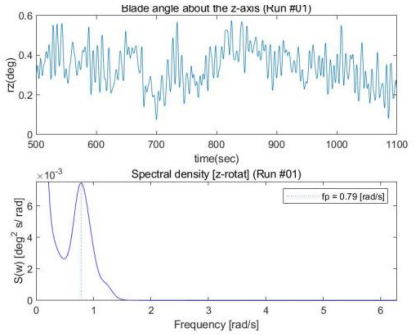

(f) Rotational angle about the z-axis

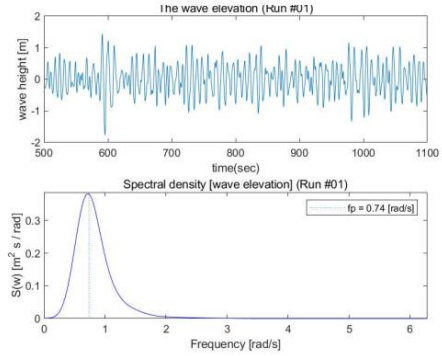

(g) Wave elevation

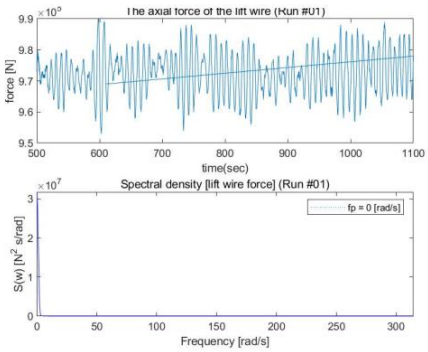

(h) Lift wire axial force

Figure 7. 12: Time series and spectral density plots of wind seed -77431392, wave seed 301

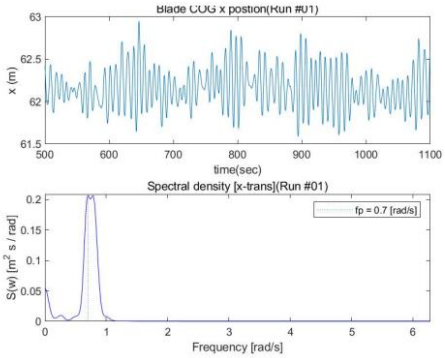

(a) Displacement in the x-direction

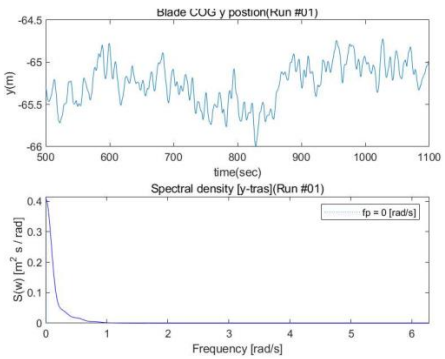

(b) Displacement in the y-direction

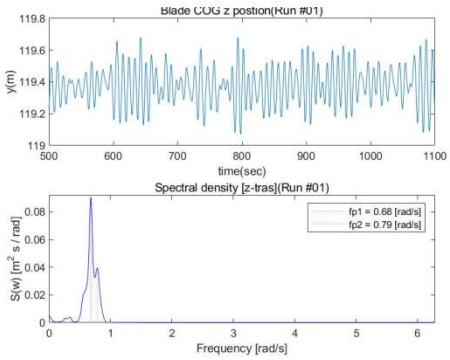

(c) Displacement in the z-direction

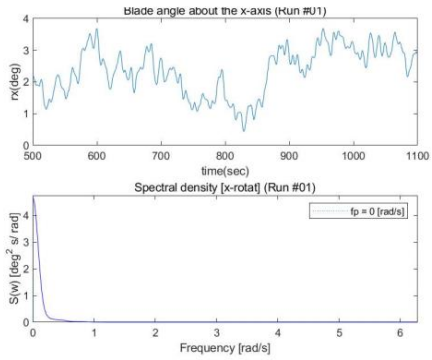

(d) Rotational angle about the x-axis

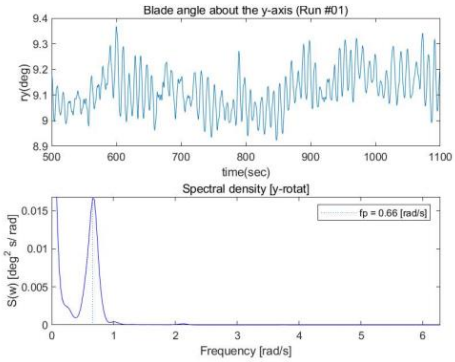

(e) Rotational angle about the y-axis

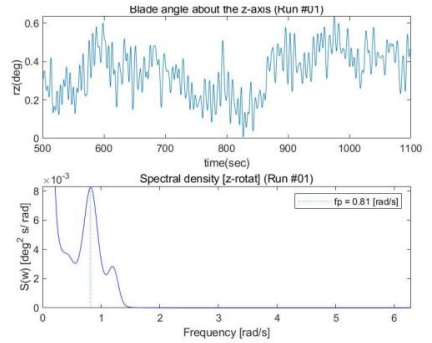

(f) Rotational angle about the z-axis

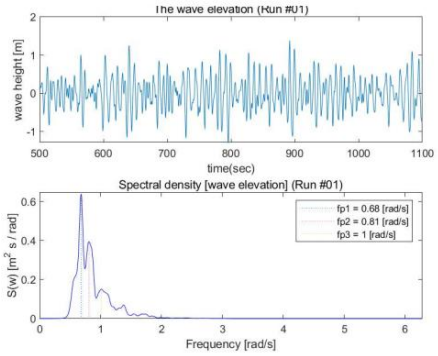

(g) Wave elevation

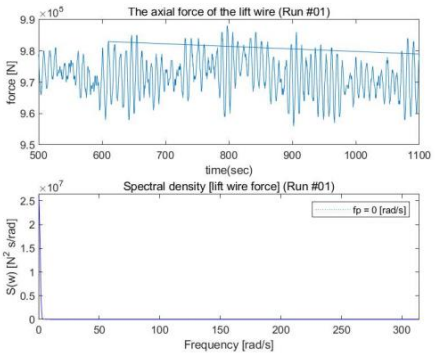

(h) Lift wire axial force

Figure 7. 13: Time series and spectral density plots of wind seed-1035971066, wave seed 302

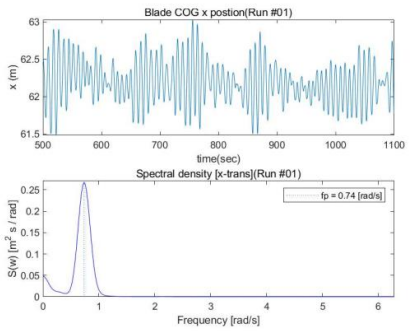

(a) Displacement in the x-direction

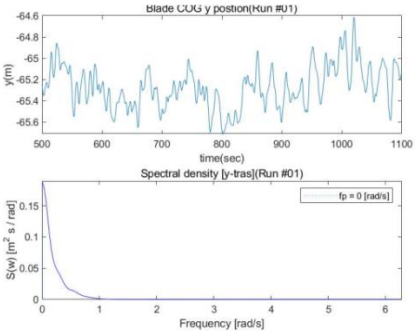

(b) Displacement in the y-direction

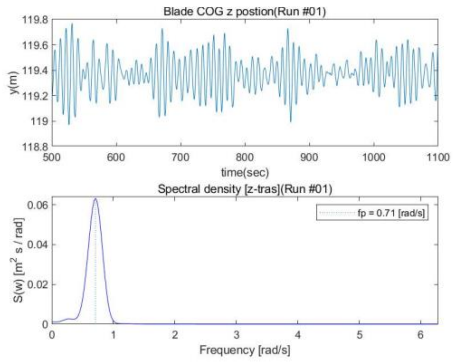

(c) Displacement in the z-direction

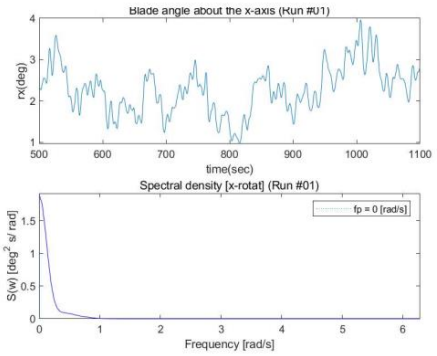

(d) Rotational angle about the x-axis

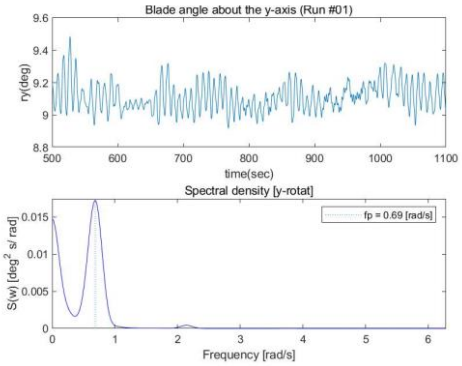

(e) Rotational angle about the y-axis

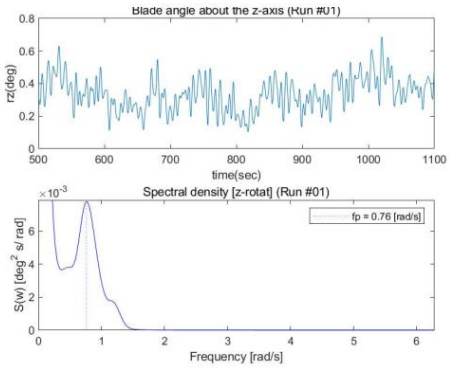

(f) Rotational angle about the z-axis

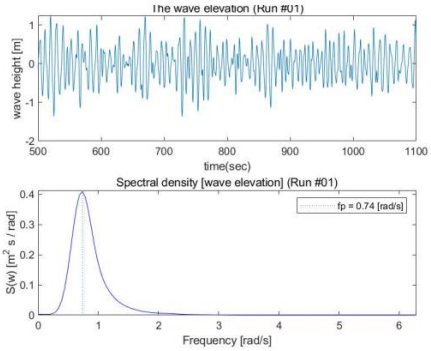

(g) Wave elevation

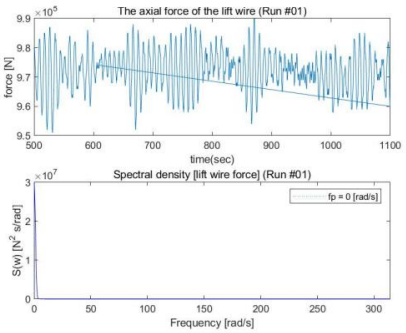

(h) Lift wire axial force

Figure 7. 14: Time series and spectral density plots of wind seed 590771239, wave seed 303

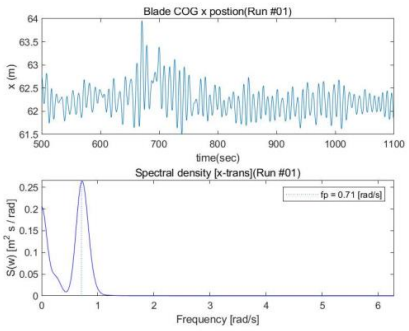

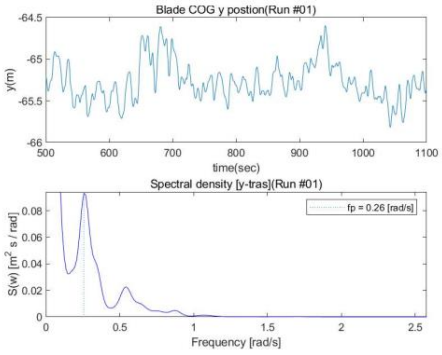

(a) Displacement in the x-direction

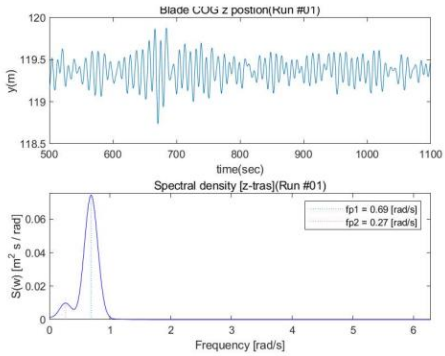

(b) Displacement in the y-direction

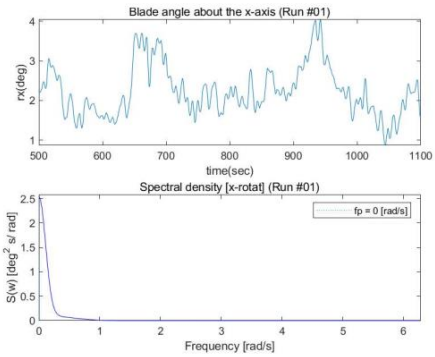

(c) Displacement in the z-direction

(d) Rotational angle about the x-axis

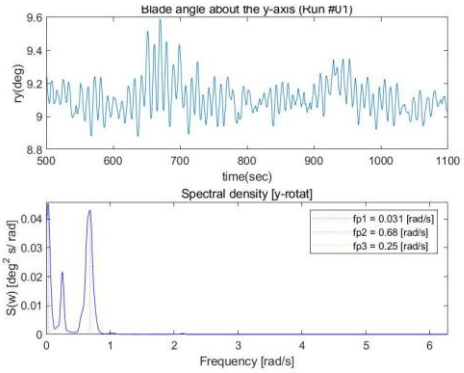

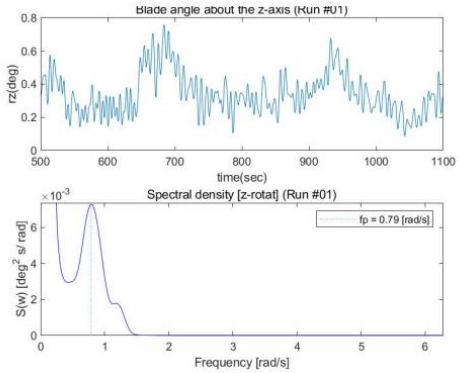

(e) Rotational angle about the y-axis

(f) Rotational angle about the z-axis

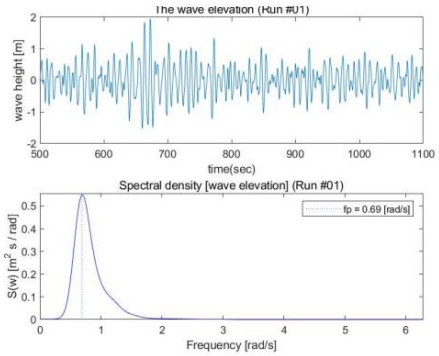

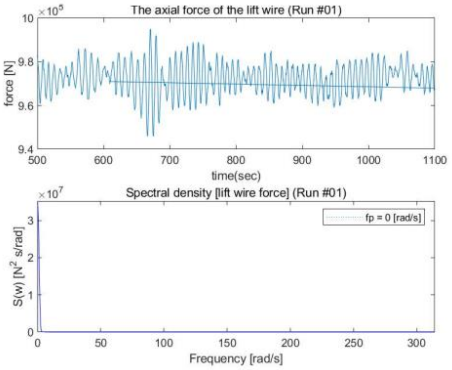

(g) Wave elevation

(h) Lift wire axial force

Figure 7. 15: Time series and spectral density plots of wind seed 132450265, wave seed 304

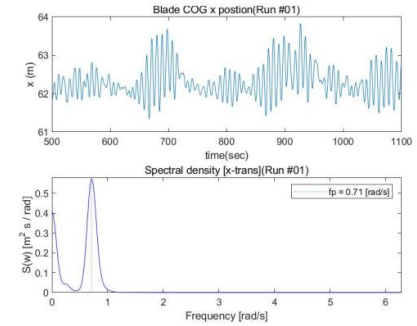

(a) Displacement in the x-direction

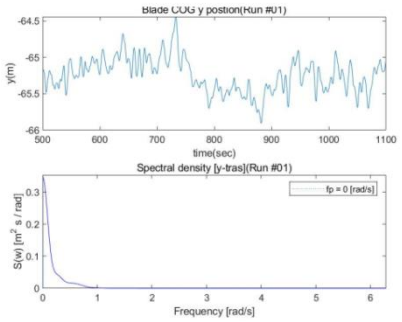

(b) Displacement in the y-direction

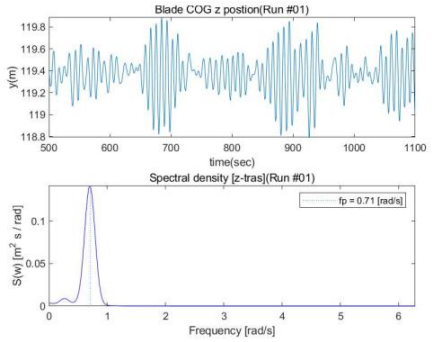

(c) Displacement in the z-direction

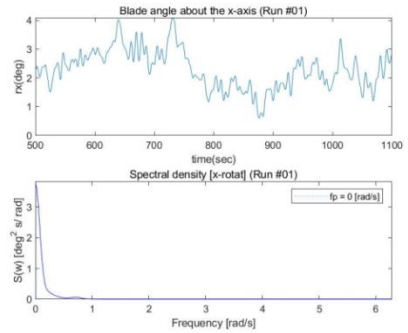

(d) Rotational angle about the x-axis

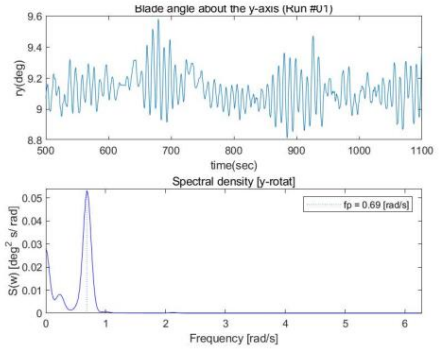

(e) Rotational angle about the y-axis

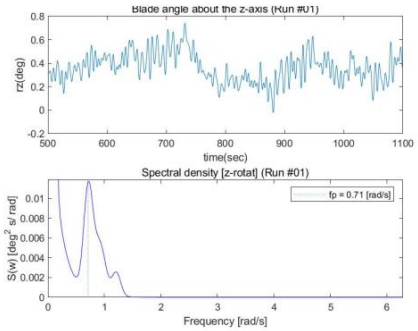

(f) Rotational angle about the z-axis

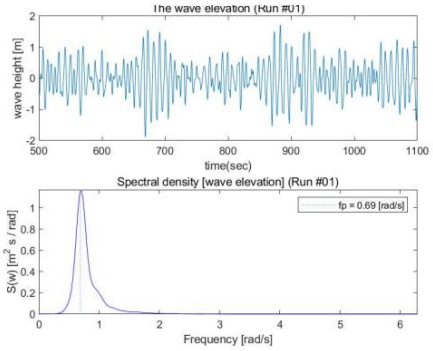

(g) Wave elevation

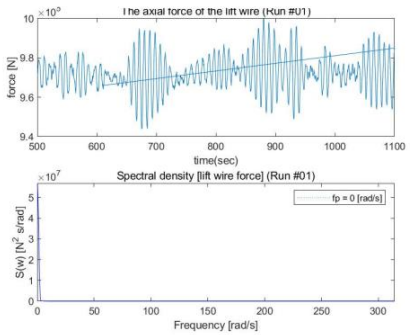

(h) Lift wire axial force

Figure 7. 16: Time series and spectral density plots of wind seed -1220293325, wave seed 400

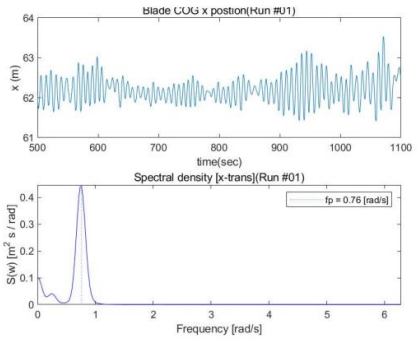

(a) Displacement in the x-direction

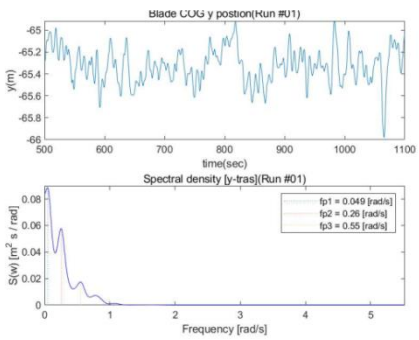

(b) Displacement in the y-direction

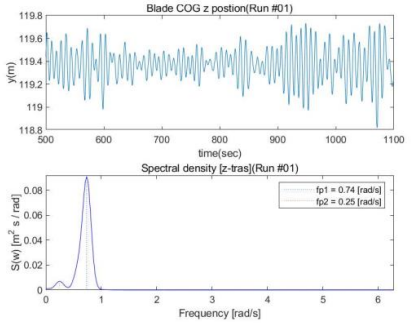

(c) Displacement in the z-direction

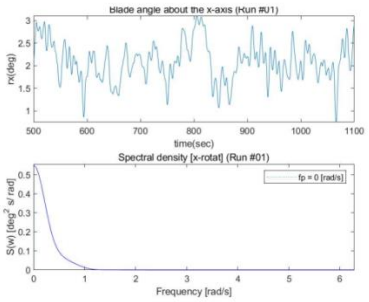

(d) Rotational angle about the x-axis

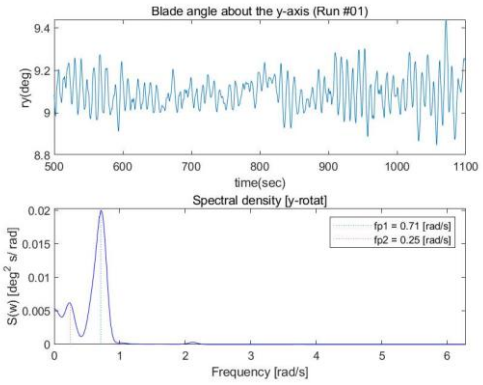

(e) Rotational angle about the y-axis

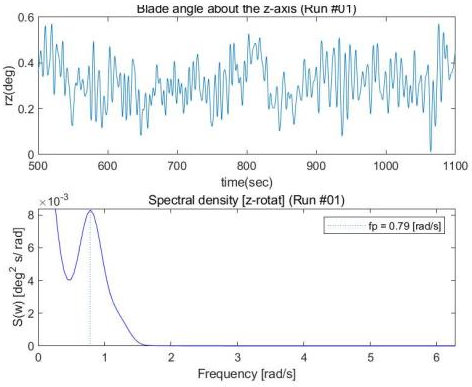

(f) Rotational angle about the z-axis

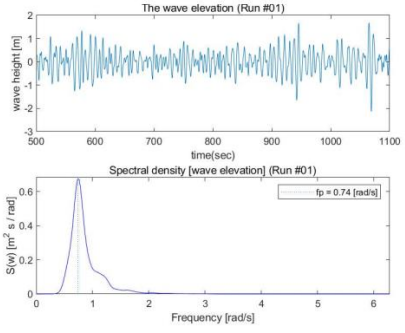

(g) Wave elevation

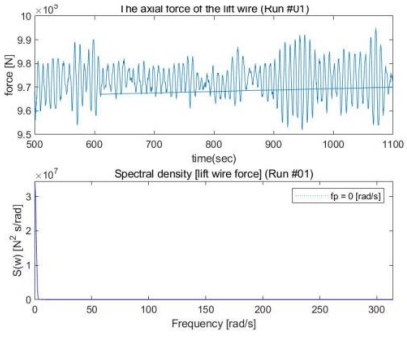

(h) Lift wire axial force

Figure 7. 17: Time series and spectral density plots of wind seed -132430614, wave seed 401

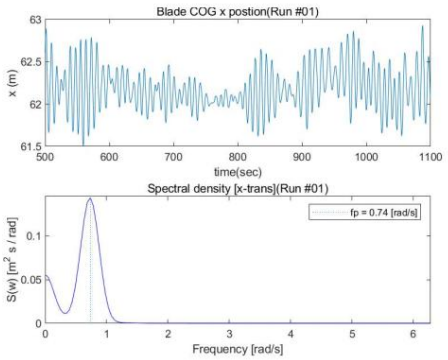

(a) Displacement in the x-direction

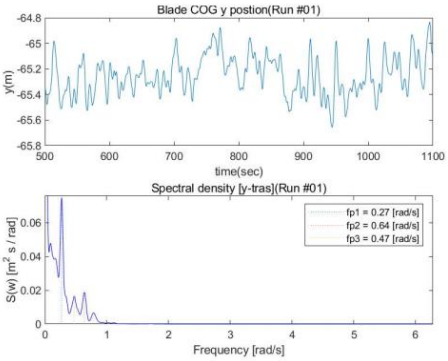

(b) Displacement in the y-direction

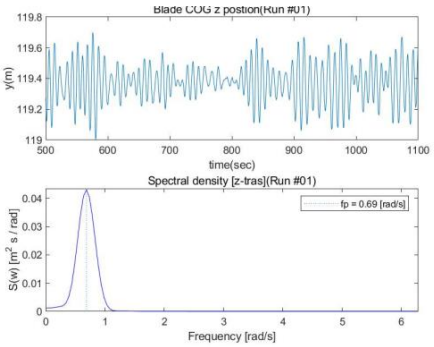

(c) Displacement in the z-direction

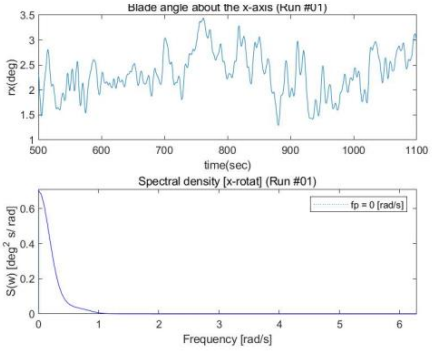

(d) Rotational angle about the x-axis

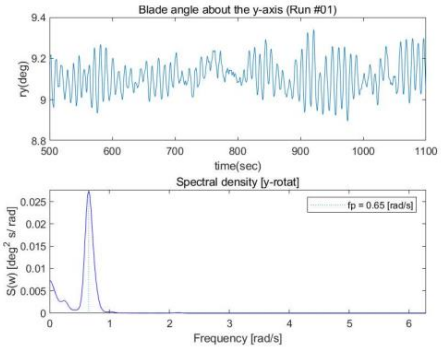

(e) Rotational angle about the y-axis

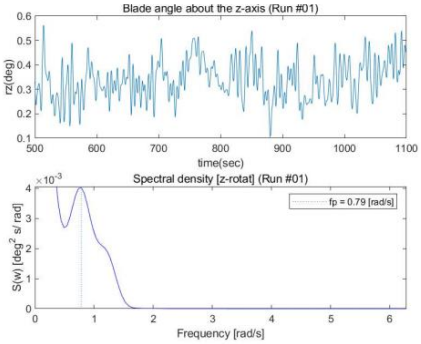

(f) Rotational angle about the z-axis

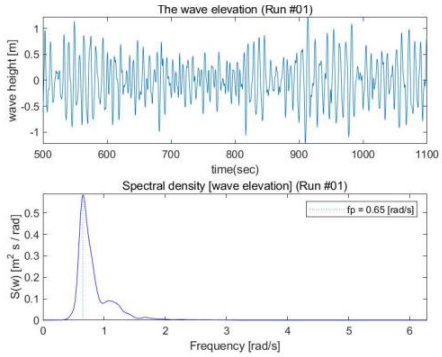

(g) Wave elevation

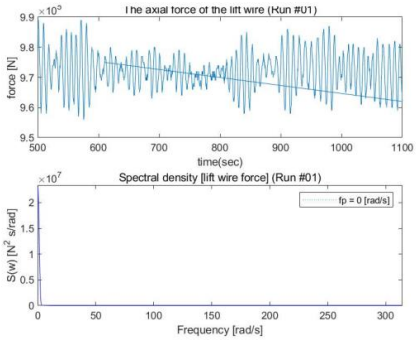

(h) Lift wire axial force

Figure 7. 18: Time series and spectral density plots of wind seed -963395014, wave seed 402

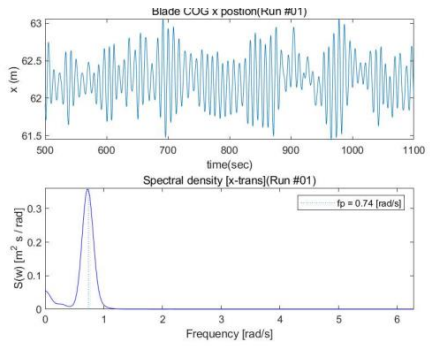

(a) Displacement in the x-direction

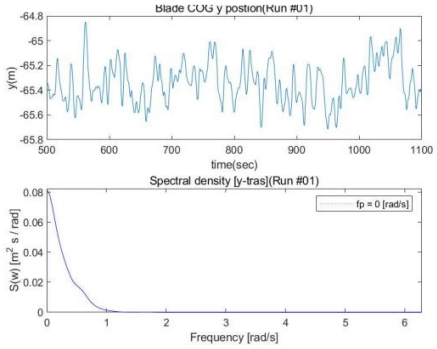

(b) Displacement in the y-direction

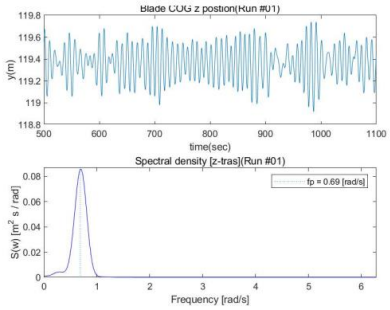

(c) Displacement in the z-direction

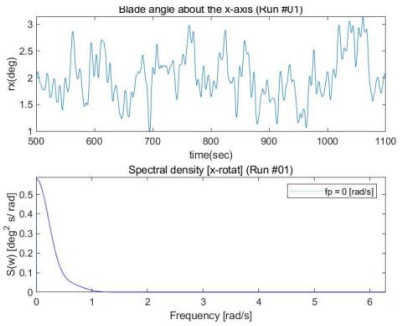

(d) Rotational angle about the x-axis

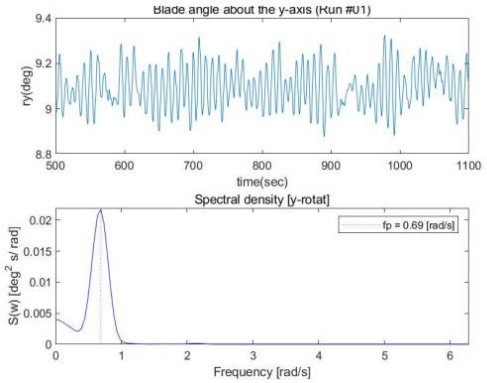

(e) Rotational angle about the y-axis

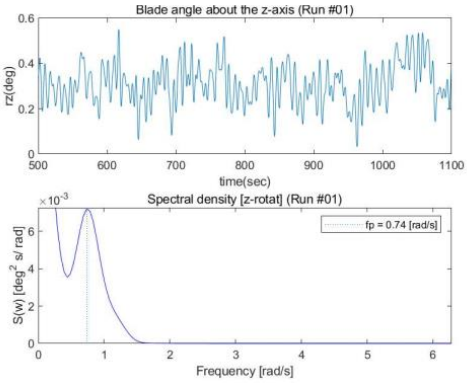

(f) Rotational angle about the z-axis

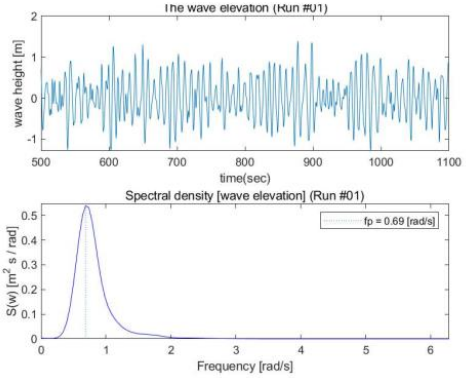

(g) Wave elevation

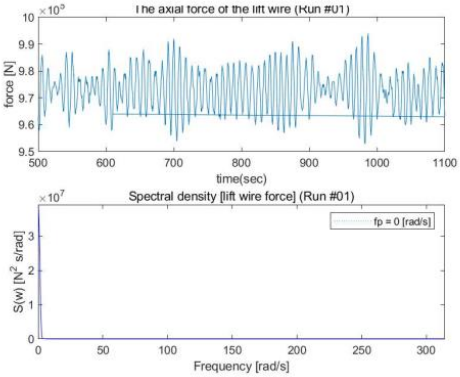

(h) Lift wire axial force

Figure 7. 19: Time series and spectral density plots of wind seed-104419964, wave seed 403

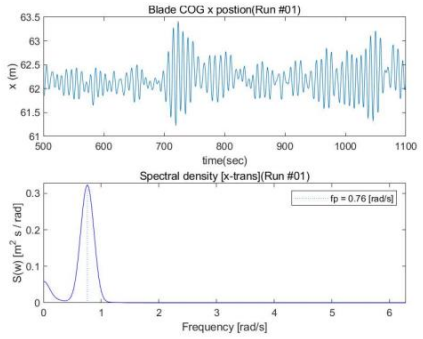

(a) Displacement in the x-direction

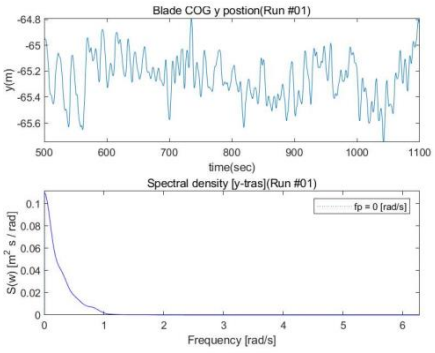

(b) Displacement in the y-direction

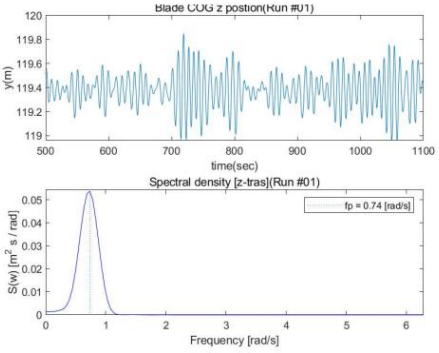

(c) Displacement in the z-direction

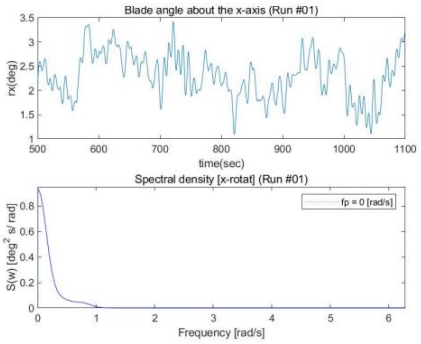

(d) Rotational angle about the x-axis

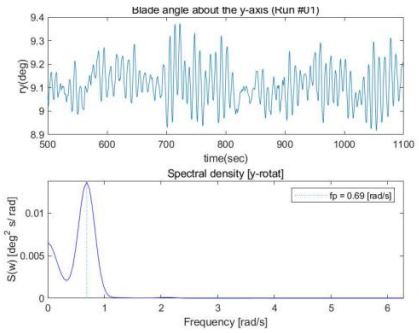

(e) Rotational angle about the y-axis

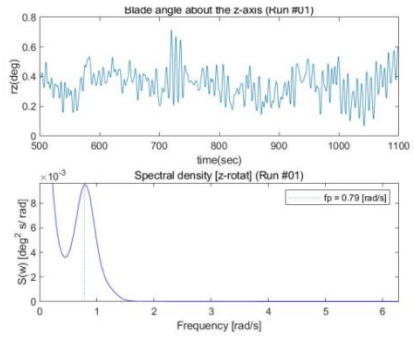

(f) Rotational angle about the z-axis

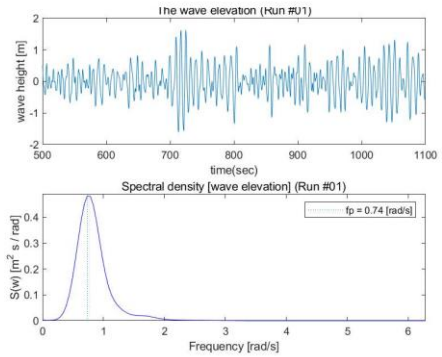

(g) Wave elevation

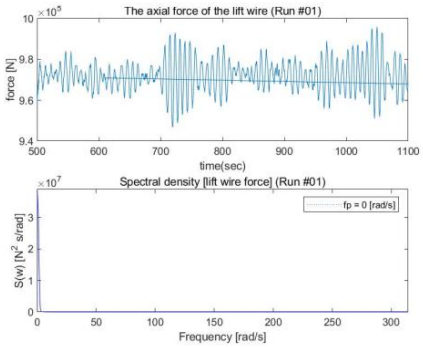

(h) Lift wire axial force

Figure 7. 20: Time series and spectral density plots for wind seed 2088778182 wave seed 404

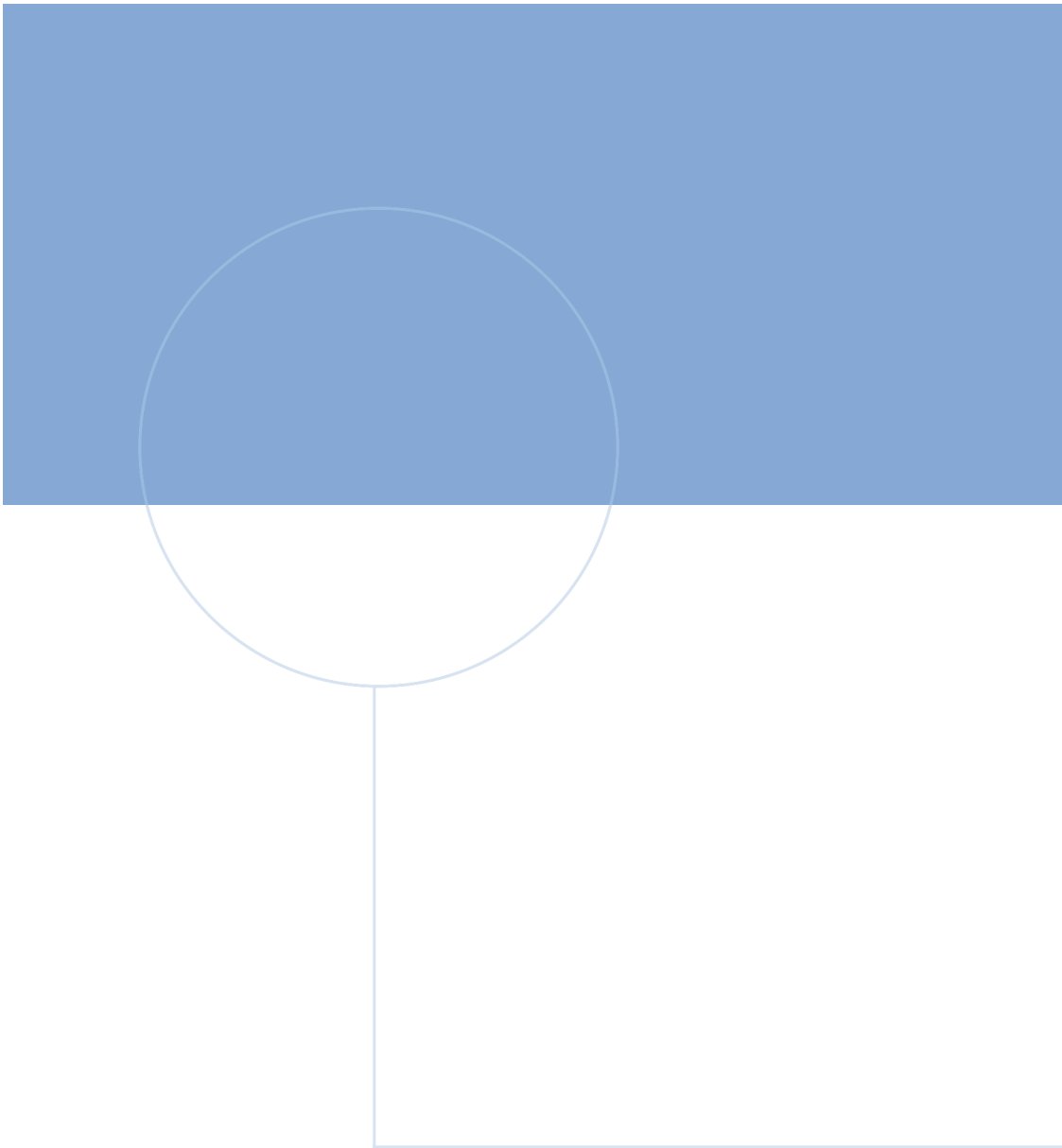

NTNU

Norwegian University of
Science and Technology